8-2023

Non-energy Circular Economy Potential of Rice Husks: A Techno-eco-environmental Assessment

Winfred Oppong Yeboah
University of Arkansas, Fayetteville

Non-energy Circular Economy Potential of Rice Husks: A Techno-eco-environmental Assessment

A thesis submitted in partial fulfillment
of the requirements for the degree of
Master of Science in Biological Engineering

by

Winfred Oppong Yeboah
University of Ghana
Bachelor of Science in Materials Science and Engineering, 2020

August 2023
University of Arkansas

This thesis is approved for recommendation to the Graduate Council.

_____
Dongyi Wang, Ph.D.
Thesis Director

_____
Ebenezer Miezah Kwofie, Ph.D.
Committee Member

_____
Ali Ubeyitogullari, Ph.D.
Committee Member

Abstract

The non-energy circular bioeconomy potential of rice husks was examined via sustainability assessments, namely life cycle assessment (LCA), life cycle impact cost assessment (LCICA), and techno-economic assessment (TEA). The study was conducted with three objectives. The first objective was to review previous studies on the non-energy utilization potential of rice husks by the method of meta-analysis. This review followed a systematic approach where research papers were collected following a defined set of criteria. The study revealed 16 key utilization pathways, all of which showed promising results. However, a comprehensive sustainability assessment was lacking in all of the pathways. The second objective was to examine the circular bioeconomy potential of rice husks as a resource for bioplastic production. This study evaluated the techno-environmental assessment of three bioplastics, namely carboxymethyl cellulose, cellulose acetate, and cellulose nitrate relative to rice husks combustion. This provided information on the environmental impacts and the environmental impact costs of all three bioplastics. The result suggested that carboxymethylcellulose would be the most sustainable pathway, reducing the impact on human health and the cost of open-air combustion by 82% and 74%, respectively. The third objective was to examine the sustainable production of xylo-oligosaccharide from rice husk via a techno-economic and an environmental performance assessment. The study examined two production methods: autohydrolysis and enzymatic hydrolysis, considering a pilot and a large production scale for each. The results revealed that autohydrolysis is the best method to produce xylo-oligosaccharides, considering the damage to the environment and human health, and profitability (net profits of $ 7.1M and $ 42.4M for pilot and large-scale setups) hence, it is viable to thrive in the market.

Acknowledgments

I would, first, thank the Almighty God for His immense grace, mercy, and the gift of strength and life to complete this research.

I would also like to express my sincere appreciation to my academic advisor, Dr. Ebenezer Miezah Kwofie for his guidance and supervision throughout this research. Also, I thank him for making time and getting me every resource that I needed for the research. I really appreciate you, Sir. I also want to acknowledge the support of my supervisor, Dr. Dongyi Wang, and a member of my committee, Dr. Ali Ubeyitogullari. Also, to Dr. Emmanuel Nyankson, I appreciate your advice, guidance and for believing in me from the beginning of my graduate journey.

To every member of the Miezah Lab group, I want to say thank you for your contributions and support throughout this research. A special thank you to Derrick Kpakpo Allotey for making time to help me through some important aspects of my research. I appreciate it. I also thank Linda Pate for her support and help throughout my program.

Finally, I would like to acknowledge with gratitude the love, support, advice, and well-wishes from my family, especially my parents, and the support from my friends. I am grateful to you all.

Dedication

I dedicate this thesis to my parents. I appreciate your love and prayers.

Table of contents

List of Figures

List of Tables

List of Equations

List of Abbreviations

Abbreviation	Meaning
AAS	Atomic Adsorption Spectroscopy
ABS	Atomic Absorption Spectroscopy
ALC	Analytical Liquid Chromatography
ANN	Artificial Neural Network
ANOVA	Analysis of Variance
ASPS	Axis Supra Photoelectron Spectrometry
ATR	Attenuated Toral Reflectance
AVPV	Apparent Volume of Permeable Voids
BET	Brunauer-Emmett-Teller
BJH	Barrett-Joyner-Halenda
BP	Bioactive Peptides
BPARK	Bradford Protein Assay Reagent Kit
BSE	Back-Scattered Electron detection
CA	Cellulose Acetate
CCAK	Commercial Colorimetric Assay Kits
CECAK	Commercial Enzymatic Colorimetric Assay Kits
CHMC	Chloride Migration Coefficient
CHNS	Carbon Hydrogen Nitrogen Sulfur
CMC	Carboxymethyl Cellulose
CN	Cellulose Nitrate
CPT	Chloride ion penetration test
CV	Cyclic Voltammetry
DALY	Disability-Adjusted Life Years
DCB	Dichlorobenzene
DFT	Density Functional Theory
DLSG	Dynamic Light Scattering Granulometry
DMA	Dynamic Mechanical Analysis
DMRT	Duncan's Multiple Range Test
DRIFTS	Diffuse Reflectance Fourier Transform Infrared Spectroscopy
DS	Degree of Substitution
DSC/TGA	Differential Scanning Calorimetry/Thermogravimetry Analysis
DTA	Differential Thermal Analysis
DTG	Derivative Thermogravimetry
DTGS	Deuterated Triglycine Sulphate
EA	Element Analyzer
ECA	Elemental Chemical Analysis
ECL	Enhanced Chemiluminescence
ECLAK	Endpoint Chromogenic LAL Assay Kit
EDAX	Energy Dispersive X-ray Spectroscopy
EIS	Electrochemical Impedance Spectroscopy
EMI	Eco-mechanical Index
ESEM	Environment Scanning Electron Microscopy
FAS	Flame Atomic Spectroscopy
FESEM	Field Emission Scanning Electron Microscope

FRS	Fossil resource scarcity
FTIR	Fourier Transform Infrared
FWE	Freshwater ecotoxicity
GCD	Galvanostatic Charge-Discharge
GC-MS	Gas Chromatography-Mass Spectroscopy
GC-TCD/FID	Gas Chromatography-Thermal Conductivity Detector/Flame Ionization Detector
GWP	Global warming Potential
H2-TPR	H2-programmed-Temperature Reduction
HCT	Human carcinogenic toxicity
HNT	Human non-carcinogenic toxicity
HPLC	High-Performance Liquid Chromatography
HRGC/HRMS	High-Resolution Gas Chromatography/High-Resolution Mass Spectroscopy
HR-SEM	High-Resolution Scanning Electron Microscopy
ICP-MS	Inductive Coupled Plasma-Mass Spectroscopy
ICP-OES	Inductive Coupled Plasma-Optical Emission Spectroscopy
ISO	International Organization for Standardization
KFC	Karl Fischer Coulometry
KFT	Karl -Fischer Titration
LCA	Life Cycle Assessment
LCIA	Life Cycle Impact Assessment
LCICA	Life Cycle Impact Cost Assessment
LHPC	Lignin-derived Hierarchical Porous Carbon
MET	Marine ecotoxicity
MIP	Mercury Intrusion Porosimeter
MJ	Megajoule
MP-XRD	Multi-Purpose X-ray Diffraction
NAMR	Nano Absorbance Microplate Reader
NH3-TPD	NH3-Temperature Programmed Desorption
NIR	Nicolet Infrared
NMR	Nuclear Magnetic Resonance
NMVOC	Non-methane Volatile Organic Compounds
OZH	Ozone formation, Human health
OZT	Ozone formation, Terrestrial ecosystems
PBSA	Polybutylene Succinate Adipate
PCA	Principle Components Analysis
PCL	Polycaprolactone
PDV	Pulse Differential Voltammetry
PES	Photoluminescence Emission Spectra
PHB	Poly(3-hydroxybutyrate)
PIDS	Polarized Intensity Differential Scattering
PM	Particulate Matter
PSD	Particle Size Distribution
PXRD	Powder X-ray Diffraction
RCPT	Rapid Chloride Permeability test
RH	Rice husk

RHA	Rice husk ash
RMSE	Root-mean-squared Error
SAPs	Superabsorbent polymers
SCM	Secondary Cementitious Materials
SDTPS	Silica-doped Tricalcium Phosphate Scaffold
SEM	Scanning Electron Microscopy
SEM-EDS	Scanning Electron Microscopy-X-ray Energy Dispersive
SFRC	Steel Fiber Reinforced Concrete
STS	Split Tensile Strength
SWCNT	Single-Walled Carbon Nanotube
TEC	Terrestrial ecotoxicity
TEM	Transmission Electron Microscopy
TGA	Thermogravimetric Analysis
TOPSIS	Technique for Order Preference by Similarity on an Ideal Solution
TPA	Texture Profile Analysis
TS	Tensile Strength
UPV	Ultrasonic Pulse Velocity
UV-vis DBS	Ultraviolet-visible Dual-Beam Spectrophotometry
UV-vis spec	Ultraviolet-visible spectroscopy
VSM	Vibrating Sample Magnetometry
WD-XRF	Wavelength Dispersive-X-ray Fluorescence
XPS	X-ray Photoelectron spectroscopy
XRD	X-ray Diffraction
XRF	X-ray Fluorescence

1 Chapter One: Introduction

1.1 Background and Justification

The need to find supplements and/or alternatives to natural resources has become a topic of discussion over the past years. This is because of the over-exploitation of these non-renewable natural resources, leading to their drastic depletion (Dixit, 2021). In the quest to curb this problem, research has been geared toward industrial and agricultural by-products, as these materials are abundant and exhibit promising characteristics (Dixit, 2021). Nevertheless, agricultural by-products seem to be more appropriate for this agendum because they are likely to require no extensive pre-treatments before use (Galanakis, 2013; Lai et al., 2017). Among the agricultural by-products, however, rice husks are gaining more attention because they are more common, readily available, and have wide valorization scope (Tan & Norhaizan, 2020). Nonetheless, most studies on rice husks are poised toward energy production, with only a few explorations on the non-energy valorization potentials (Quispe et al., 2017; Lim et al., 2012; Quispe et al., 2017). These energy pathways focus on fuel and electricity generation, but they present us with new problems such as pollution, via the different emissions throughout the process life cycle, making them not entirely sustainable (Kang et al., 2019). An example is the work by Kwofie & Ngadi, (2016), where the potential of rice husk as a substitute fuel for wood for rice parboiling process in West Africa was studied via the processes of direct combustion, briquetting, and gasification. A Green House Gas (GHG) of 8.32, 22.01 and 3.72 tCO_2e/year were recorded for the direct combustion, briquetting, and gasification respectively. Even though the intended purpose of the research, which is to improve fuel situation for the parboiling process was achieved, the values of GHG are high enough to cause problems such as climate changes and health problems. Prasara-A & Grant, (2011) also performed a life cycle assessment on the

utilization of rice husk for energy generation, mainly electricity and cellulosic ethanol. The results showed that such applications will result in high impacts of human toxicity, terrestrial and marine acidification as well as ecotoxicity. Additionally, utilizing rice husks for energy purposes is restricted to small-scale systems, as large-scale applications could cause deforestation and increased rice farming demands. The processes involved in these energy extractions are somewhat complex and require special control systems. Finally, utilizing rice husks for only energy applications is not enough because of the continuous rise in rice production which demands novel means of dealing with associated by-products, such as rice husks, and ensuring sustainability. The need to look at other alternatives by which rice husks can be valorized is thus important. This project is therefore aimed at promoting rice systems' circularity by providing techno-eco-environmental evidence of non-energy utilization pathways of rice husks. The research will be conducted with three objectives; the first objective will review the different non-energy utilization pathways over a 5-year period to understand what has been done and how they could be improved, and the second and third objectives will explore the overall circularity potential of using husks as a resource to produce bioplastics and xylo-oligosaccharides respectively.

1.2 Objectives

1.2.1 Overall Objective

The collective objective of this project is to analyze the circularity potential of rice by evaluating the valorization pathways and developing a decision support system for the non-energy utilization of rice husks. This will be achieved by first reviewing the already existing ways rice husks have been valorized, analyzing the loopholes within those pathways, and finally suggesting ways to improve them. The assessment will include a meta-analysis of the existing studies on rice husks

valorization, an environmental performance analysis by the method of life cycle impact assessment and life cycle cost assessment, and a techno-economic assessment of some selected systems. The assessment is at the farmer/processor level considering selected farmers and processing units and providing inputs for decision-making regarding rice circularity in Arkansas.

1.2.2 Specific objectives

1. Objective 1: A Meta-analysis of the Non-energy Utilization Potential of Rice husks: A Systematic Review
2. Objective 2: Circular Bioeconomy Potential of Rice Husk as a Bioplastic Resource: Techno-environmental Assessment
3. Objective 3: Sustainable Production of Xylo-oligosaccharide from Rice Husk: A Techno-economic and Environmental Performance Assessment

References

Bazargan, A., Bazargan, M., & McKay, G. (2015). Optimization of rice husk pretreatment for energy production. *Renewable Energy*, *77*, 512–520. https://doi.org/10.1016/j.renene.2014.11.072

Dixit, A. (2021). A study on the physical and chemical parameters of industrial by-products ashes useful in making sustainable concrete. *Materials Today: Proceedings*, *43*, 42–50. https://doi.org/10.1016/j.matpr.2020.11.203

Galanakis, C. M. (2013). Emerging technologies for the production of nutraceuticals from agricultural by-products: A viewpoint of opportunities and challenges. *Food and Bioproducts Processing*, *91*(4), 575–579. https://doi.org/10.1016/j.fbp.2013.01.004

Kang, S.-H., Hong, S.-G., & Moon, J. (2019). The use of rice husk ash as reactive filler in ultra-high performance concrete. *Cement and Concrete Research*, *115*, 389–400. https://doi.org/10.1016/j.cemconres.2018.09.004

Kwofie, E. M., & Ngadi, M. (2016). Sustainable energy supply for local rice parboiling in West Africa: The potential of rice husk. *Renewable and Sustainable Energy Reviews*, *56*, 1409–1418. https://doi.org/10.1016/j.rser.2015.12.030

Lai, W. T., Khong, N. M. H., Lim, S. S., Hee, Y. Y., Sim, B. I., Lau, K. Y., & Lai, O. M. (2017). A review: Modified agricultural by-products for the development and fortification of food products and nutraceuticals. *Trends in Food Science & Technology*, *59*, 148–160. https://doi.org/10.1016/j.tifs.2016.11.014

Lim, J. S., Abdul Manan, Z., Wan Alwi, S. R., & Hashim, H. (2012). A review on utilisation of biomass from rice industry as a source of renewable energy. *Renewable and Sustainable Energy Reviews*, *16*(5), 3084–3094. https://doi.org/10.1016/j.rser.2012.02.051

Prasara-A, J., & Grant, T. (2011). Comparative life cycle assessment of uses of rice husk for energy purposes. *The International Journal of Life Cycle Assessment*, *16*(6), 493–502. https://doi.org/10.1007/s11367-011-0293-7

Quispe, I., Navia, R., & Kahhat, R. (2017). Energy potential from rice husk through direct combustion and fast pyrolysis: A review. *Waste Management*, *59*, 200–210. https://doi.org/10.1016/j.wasman.2016.10.001

Tan, B. L., & Norhaizan, M. E. (2020). *Rice By-products: Phytochemicals and Food Products Application*. Springer International Publishing. https://doi.org/10.1007/978-3-030-46153-9

2 Chapter Two: A Meta-analysis of the Non-energy Utilization Potential of Rice Husks: A Systematic Review

Abstract

Rice husk has received enormous attention to be utilized for value-added products over the past years owing to its amazing properties and wide valorization scope. Most studies are, however, centered on energy production, with fuel and electricity being the focus. Utilizing rice husks for energy purposes presents us with new problems such as pollution throughout the process life cycle and increase in rice farming demands due to high volumes of rice husks requirements. Moreover, because of the continuous rise in rice production, only the energy options are not enough. The need to exploit rice by-husks for non-energy purposes is therefore very important. This review therefore aims at presenting a broad overview of the different non-energy utilization pathways of rice husks, identify the current trends and research gaps, and provide insight into the need for further studies in the field. Via a systematic review, a meta-analysis was conducted to assess the different processes and analysis of 105 published studies on the non-energy rice husks utilizations. The analysis revealed 16 utilization pathways, most of which showed positive results in terms of the potential of rice husks. A comprehensive sustainability assessment for these pathways was, however, lacking indicating that further research is required for a good justification of non-energy utilization of rice husks.

2.1 Introduction

Rice is the most common cereal in the world and the staple food of about half the world's population (Chaudhari et al., 2018; B. L. Tan & Norhaizan, 2020). The production of rice has

been maintained and held steady by the rice industry over the past years, such that as of 2020, the annual global rice yield was about 769 million tons (FAO, 2023). This value has been predicted to increase substantially (an estimated value of 3 billion tons of cereal yield), with a corresponding rise in the by-products by the year 2050 (B. L. Tan & Norhaizan, 2020). The by-products of rice are the husk (hull), straw, bran, germ, broken rice, and brewers' rice (Mohd Esa & Ling, 2016; Moraes et al., 2014; B. L. Tan & Norhaizan, 2020). These by-products are obtained via rice milling, a series of mechanisms for processing rice for the market (Figure 2.1). The rice straw is an important by-product of rice, which unlike the rest of the by-products is obtained at harvest. It forms the vegetative part of the rice plant and is typically made of lignocellulosic biomass. Rice straw has the largest mass of all the by-products, about 1.35 tons for every ton of paddy harvested (Kadam et al., 2000; Moraes et al., 2014). Despite its large quantity, rice straw has only a few widespread utilizations, with fuel and non-wood fibers being the major ones (Kadam et al., 2000). Rice husk is the first by-product obtained from the milling process via a mechanism known as dehulling (shelling). It forms the hard outermost layer that makes up about 20% of the rice kernel (0.2 tons for every ton of rice harvested) (Moraes et al., 2014; B. L. Tan & Norhaizan, 2020). It is composed mainly of cellulose (50%), lignin (30%), and inorganic residue (20%) which is mainly made of silica in the amorphous hydrated form (Moraes et al., 2014). Rice husk is palpably the most prominent by-product of rice in terms of valorization potential. This is due to its composition, bulk density (90-150 kgm^{-3}), caloric value (12.3×10^{6}-16.7×10^{6} Jkg^{-1}) and packing density (118.2-122 kgm^{-3}). Following the husk is the rice bran. It forms the fibrous layer after the rice husk and makes up about 10% of the paddy (Moraes et al., 2014; Reaño, 2020). It is composed mainly of lipids, proteins, mineral salts, and vitamins, typically tocotrienols (vitamin E). Notwithstanding its compositions and nature, the

rice bran has not been exploited to its full potential and hence has a very low value in terms of usage. Another by-product that is generated from rice processing is rice germ. This is usually attached to the rice bran after shelling and is considered the most nutritional part of the rice grain (Mohd Esa & Ling, 2016). It makes up about only 2% of the grain yet it is 40 times more concentrated in nutrients than the rest of the rice grain (Reaño, 2020). Just like the bran, the rice germ has had little valorization capacity. Broken rice and brewers' rice are the final by-products after processing. The broken rice is the rice that remains (less than three-fourths of the whole grain) after polishing whereas the brewers' rice is a mixture of the bran, germ, and broken grains that are regarded as waste (Bilo et al., 2018). Seemingly, these by-products possess unique characteristics that can be harnessed to serve as alternatives and/or enhancements for the scarce non-renewable natural resources. Even though over the past years, these by-products were ineffectively utilized and under-exploited causing serious economic and environmental problems, researchers have realized that their unique properties can be harnessed for beneficial purposes (AlBiajawi et al., 2022; Kumar et al., 2017). This has proven to be a step in the right direction as innovative ideas have come up and new materials have been built. However, most studies are poised toward energy production, with fuel and electricity being the focus. These utilization pathways present us with new problems such as pollution (via the different emissions) throughout the process life cycle (Kang et al., 2019). Some examples include the work by Kwofie & Ngadi, (2016), where rice husks were used as a substitute fuel for wood for the rice parboiling process in West Africa, via the processes of direct combustion, briquetting, and gasification. The results from the research recorded a Green House Gas (GHG) of 8.32, 22.01, and 3.72 tCO_2e/year for the direct combustion, briquetting, and gasification respectively. Another study by Prasara-A & Grant, (2011) explored rice husk as a resource for the generation

of electricity and cellulosic ethanol. The results showed that such applications will result in high impacts of climate change (9.53×10^5 kg CO_2 eq), human toxicity (1.61×10^4 kg 1,4-DCB eq), terrestrial acidification (5.83×10^4 kg SO_2 eq), and marine ecotoxicity (1.10×10^2 kg 1,4-DCB eq). These values are high enough to cause significant climate changes and health problems, which are a disadvantage in the long run. Additionally, utilizing rice husks for energy purposes is restricted to small-scale systems, as large-scale applications require large volumes of rice husks for production and this could cause an increase in rice farming demands even though these applications yield low-value products (Stegmann et al., 2020). Moreover, because of the continuous rise in rice production which demands novel means of dealing with associated by-products such as rice husks and ensuring sustainability, only the energy options are not enough. The need to exploit these rice by-products for non-energy purposes is therefore very important. With this idea, the aim of this review is to present a broad overview of the different non-energy utilization pathways of rice husks, identify the current trends and research gaps, and provide insight into the need for further studies in the field.

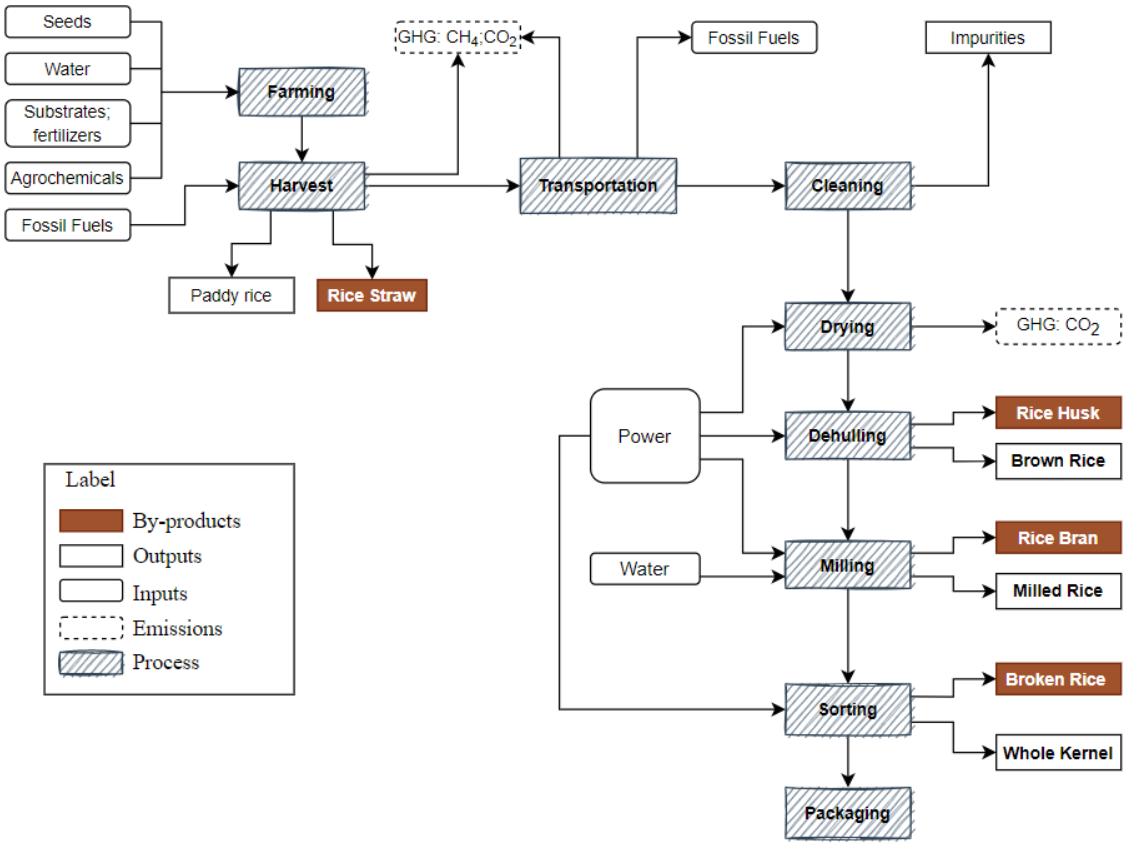

Figure 2.1: The rice processing steps: from harvest to marketing (Moraes et al., 2014)

2.2 Review Methodology

2.2.1 Data Collection

2.2.1.1 Literature search

This review was conducted by following the reporting checklist of the Preferred Reporting Items for Systematic Reviews and Meta-Analysis (PRISMA) (Liberati et al., 2009). A comprehensive search was first undertaken, to gather the different research works that have been done on the utilization of rice husk. Articles were sourced from the Science Direct database following two different search inputs. The searches were focused on papers that fall between the years 2019-2023 (a 5-year span) with “rice AND husks AND valorization” and “rice AND husks AND

utilization" as keywords for the first and second searches, respectively. This means papers that have these terms in either their titles, abstracts, main texts or as part of their keywords should be included as results of the search. The records were next filtered to restrict them to only research articles and Book chapters. 299 and 811 papers were obtained from the first and second search, respectively (Figure 2.2). The last database search was performed on May 10, 2023.

2.2.2 Screening

The authors' name, title, abstract, authors' keywords, index keywords, year of publication, journal name, document type and Digital Object Identifier (DOI) of the identified records were exported to an Excel spreadsheet. The titles and abstracts of the papers were examined, and records that were clearly not related to the topic were discarded. Records that appeared more than once were discarded as well. Finally, review papers that went through the initial filtration in the data search were removed. This left a total of 458 papers, and their full texts were downloaded for subsequent scrutiny.

2.2.3 Eligibility Test

The full texts from the screening process were examined. For the purpose of methodological consistency and to limit biases, the following research questions were formulated to serve as criteria to select the papers for the review.

1. Is the study concerned with a value-added product, process, or service?
2. Does the study have a non-energy application?
3. Are rice husks playing a key role in the study?
4. Are rice husks compensating for the defects of another material to enhance the findings?
5. Does the study solve a problem or help overcome a gap in research?

After careful assessment, 106 papers passed the eligibility test. The study selection is summarized in the flowchart in Figure 2.2. Data from these records were extracted and sampled

based on the publication year, main objectives, methods, and major findings (value-added product, process or service, and application). The review included a general utilization trend, that reveals the frequency and status-quo of non-energy utilization of rice husk. It also highlights the relations and links in the various utilization pathways by means of a bibliometric analysis. Furthermore, an overall analysis of the general overviews of the methods involved in each utilization pathway is performed. Finally, records that perform any form of sustainability assessment were assessed. A table showing the references used for the review can be found in the supplementary document.

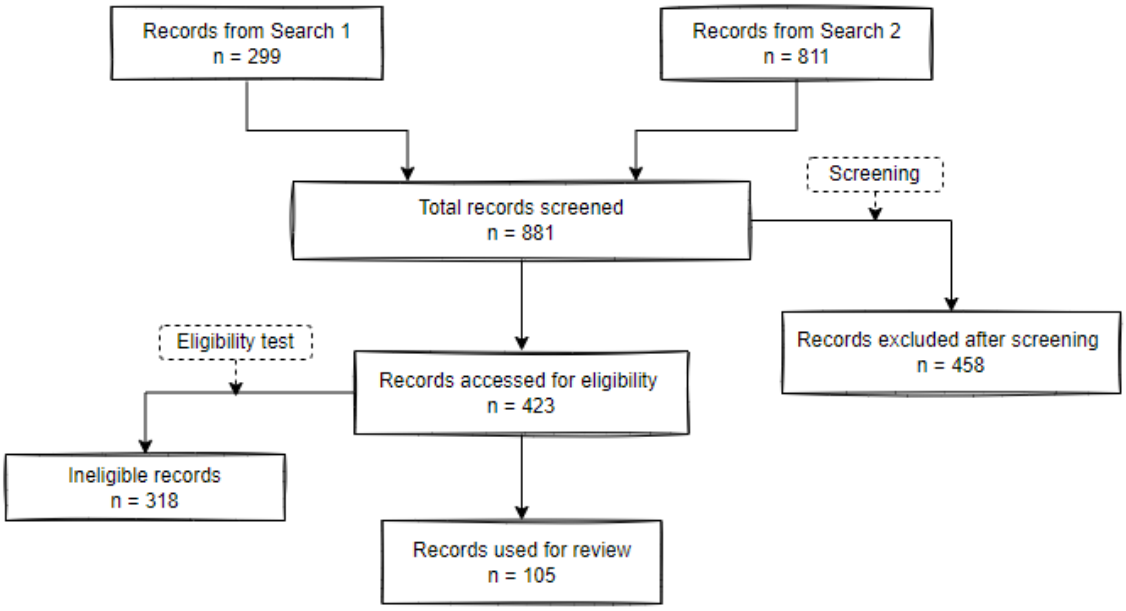

Figure 2.2: Flow diagram of study selection

2.3 Review Discussion

2.3.1 Non-energy Utilization Pathways of Rice Husks

2.3.1.1 Utilization Trend

Figures 2.3(A) and 3(B) show the distribution of the research over the stipulated years (2019-2023) and the frequency of the utilization pathways over these years, respectively. From the graph, it is evident that most studies were conducted in the year 2022, about 47.6% of the total studies (50 studies). This is proceeded by year 2023 (up to May), with 24 studies (22.9%), and then by 2021 (18 studies, 17.1%), 2019 (7 studies, 6.7%) and finally 2020 (6 studies, 5.7%). From this graph, it can be predicted that by the end of the year 2023, there will be more research on the non-energy utilization of rice husks than in any of the previous years. This is because as of only May 2023, the recorded number of research on this topic is half the number recorded for 2022 (highest record). This suggests that the interest in non-energy valorization of rice husks is growing among researchers, especially over the past five years. As shown in Figure 2.3(B), there are 16 different non-energy valorization pathways for rice husks, however, the largest is utilizing them for Secondary Cementitious Materials (SCMs). SCMs make up about 36.2% of the total valorization pathways. Other pathways are biochar (18.1%), biopolymer (11.4%), carbon (10.5%), bio-composites (11.4%), biocatalyst (1.9%), coagulant (1.9%), zeolite (1.9%), aerogel, bioactive peptides (BP), xylo-oligosaccharides (XOS), humic acids, molecular sieve, demulsifier and α amylase.

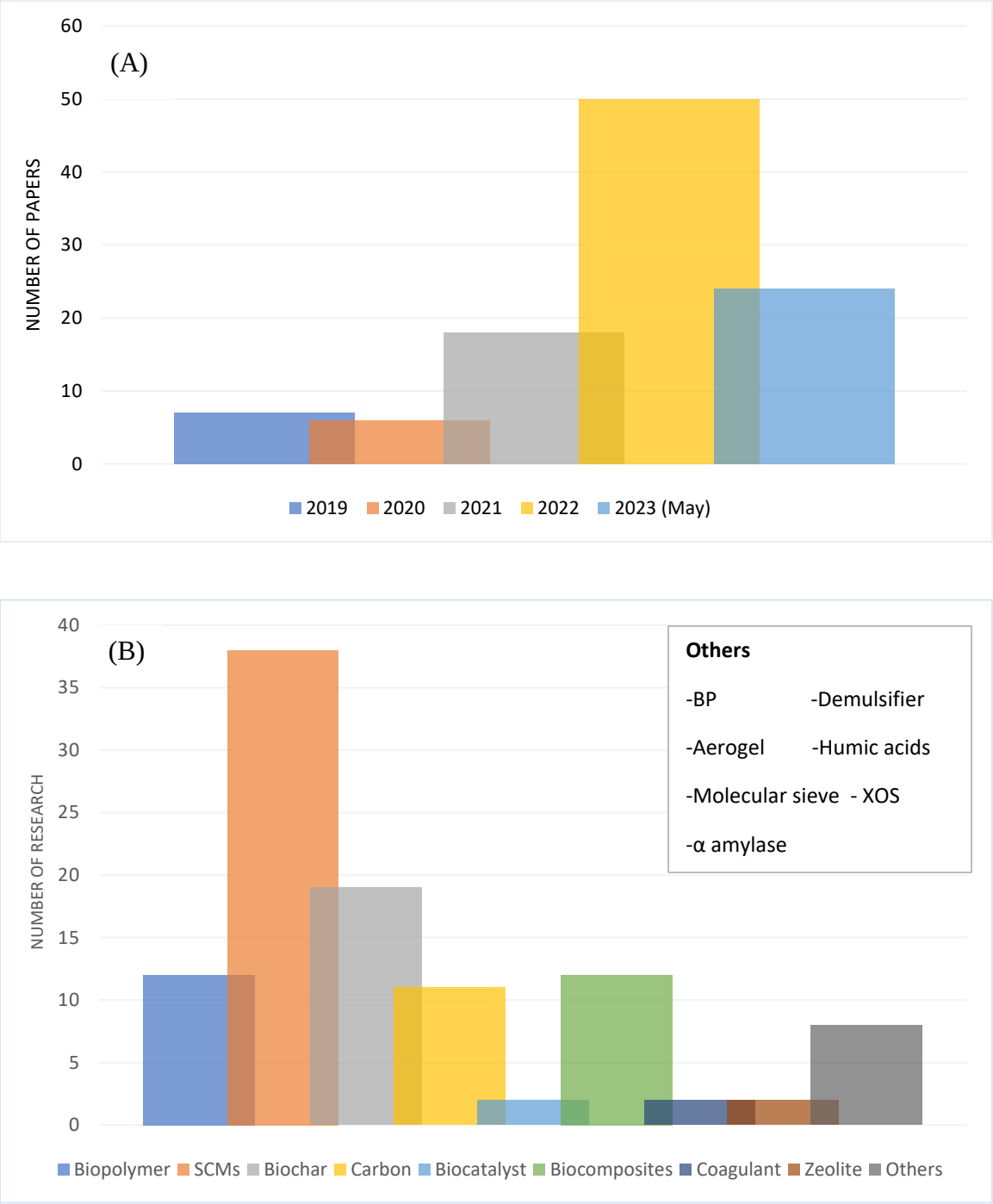

Figure 2.3: (A) Research distribution from 2019 to 2023; (B) Utilization pathway distribution

2.3.1.2 Utilization Specifics

This section details the process/production systems of the various valorization pathways mentioned in the previous section. For each pathway, the process, method, techniques employed and some findings are highlighted.

2.3.1.2.1 Secondary Cementitious Materials (SCMs)

Secondary Cementitious Materials are materials that are used as supplements or alternatives to cement, essentially playing the binder role and in some cases adding new desired properties to the building material. SCMs can however, be refined to serve different purposes other than building materials, such as scaffolds, anticancer drug delivery, acid catalyst and adsorbents (Dhinasekaran et al., 2020; Haider et al., 2022; Mozafari et al., 2022; Yadav et al., 2022). From the papers collected, most studies utilized rice husks as these cementitious materials (38 studies). Table 2.1 shows the different studies on SCMs. From the different studies, the recorded SCMs include cement, silica, geopolymer, concrete, and Ni-phyllosilicate catalyst. Generally, the production of these SCMs precedes with sizing the rice husks into desirable particle sizes to facilitate the subsequent processes within the production system and then subjecting the RH particles to thermochemical processes to finally synthesizing the material. For example, for concrete, cement, geopolymer and bricks, the thermal synthesis involves the calcination (thermal process) of rice husk at a controlled temperature to produce rice husk ash (RHA) and then adding a defined quantity of the RHA to another mixture (Ketov et al., 2021; Muthukrishnan et al., 2019; Nana et al., 2021; Plando et al., 2023). These mixtures vary for each SMC type and even for each study. In the case of geopolymer, examples of mixtures are metakaolin and volcanic (Nana et al., 2021); aluminum anodizing sludge, sodium silicate and sodium hydroxide (da Silva Nuernberg et al., 2021); and ceramic waste powder, waste glass powder, waste brick powder,

waste marble powder, metakaolin, sodium hydroxide, sodium silicate, red mud and superplasticizer (Uysal et al., 2022). For concrete, examples are superplasticizer, alkali solution, water, air-entraining agent, ordinary Portland cement, fine and coarse aggregates (Plando et al., 2023); sand, cement, hollow clay bricks, water, and tire rubber residues (Sampaio et al., 2022); and Portland cement, micro-silica, steel fibers, superplasticizer, water, fine and coarse aggregates (Safdar Raza et al., 2022). Calcium silicate, water, alkali metal aluminosilicate hydrate, metakaolin, sodium hydroxide, and sodium silicate are a typical composition of a mixture for cement (Kamseu et al., 2022). In the synthesis of silica, rice husks are treated with an acid, such as carboxylic acid, gluconic acid, hydrochloric acid, at temperature ranges from 60 – 85 ℃ for about 0.5 – 2 h (Gautam et al., 2021; Nayak et al., 2023; Setiawan & Chiang, 2021). This process is termed acid leaching. This is proceeded by a thorough cleaning of the rice husks with water (de-ionized in some scenarios) to remove excess acid and then dried. The dried husks are afterward calcined at temperatures from 450 – 800 ℃ for 1 – 3 h to produce silica. Silica synthesized via these processes are generally used for constructional purposes, such as scaffolds. For non-constructional purposes such as acid catalyst and anticancer drug delivery, the size of the silica particles required are usually in the nano range hence, the silica produced in the initial processes undergo further treatment. In the work by Dhinasekaran et al., (2020), the silica is dispersed in sodium hydroxide solution and heated at 100 ℃ for an hour while stirring. This process breaks the SiO_2 network and produces a transparent sodium silicate solution. This solution was used to produce silica nanoparticles via the Stöber method. Mozafari et al., (2022) used a similar approach, except that silica is dispersed in sodium hydroxide at room temperature for 24 h. In the synthesis of Ni- phyllosilicate catalyst as described by Y. Chen et al., (2022), silica was first produced following similar approaches described above. It was then dispersed in

a nickel nitrate solution and hydrothermally treated at 220 ℃ for 48 h. The resulting solution was centrifuged, washed, dried, and calcined at 400 ℃ for 2 h to produce Ni-phyllosilicate catalyst. The main application of this SCM was for CO_2 methanation. For each study on SCM, the authors take the materials through some characterization techniques to understand the morphologies, structure, and chemical compositions of the products. Some of these techniques include Scanning Electron Microscopy (SEM), X-ray Diffraction (XRD), Fourier Transform Infrared Spectroscopy (FTIR), Thermogravimetric Analysis (TGA), and X-ray Fluorescence (XRF). Some studies, usually those on cement, concretes, and bricks perform mechanical testing to evaluate the strengths, toughness, hardness, elastic moduli, water absorption capacity, autogenous shrinkage, and load deflection capacity of the materials. Overall, the studies show improvements in these mechanical properties. For example, (Muthukrishnan et al., 2019) recorded an increase of 17% and 23% in compressive strength and water tightness when 20% of RHA was used as cement in mortar. Nikhade & Nag, (2022) also showed that a 10% addition of RHA increased the compressive strength, flexural strength, and tensile strength of the concrete by 27.4%, 29.3% and 34.0% respectively. These indicate that rice husks are good resources for SMCs.

Table 2.1: Different types of SCMs, their application and characterization techniques and analysis used for their evaluation

Reference	SCM	Characterization technique, testing and analysis	Application
(Yadav et al., 2022)	Silica	XRD, SEM, FTIR	SDTPS for tissue engineering
(Muthukrishnan et al., 2019)	Cement	SEM, PIDS, ICP-OES, XRF, XRD, Multipoint N2 adsorption (BET), BJH, MIP	Building
(Setiawan & Chiang, 2021)	Silica	EA, Bomb calorimetry, TGA/DTA, ICP-OES, XRF, XRD, FTIR-DTGS, BET, BJH	N/S
(Taiwo et al., 2022)	Bricks	XRF, FTIR, SEM, Compressive strength test	Building
(Safdar Raza et al., 2022)	SFRC	Compressive strength test, Splitting tensile strength test, Load deflection test, Water absorption, UPV, CHMC	Building
(Nana et al., 2021)	Geopolymer	DLSG, N2 adsorption isotherms (BET), DSC/TGA, XRD, FTIR, Water absorption, Compressive strength test, ESEM	Building
(Plando et al., 2023)	Concrete	XRF, XRD, FTIR, SEM	Building
(Nayak et al., 2023)	Silica	XRD, ANOVA, ANN, TOPSIS, SEM, EDS, FTIR	N/S
(Gautam et al., 2021)	Silica	XRF	N/S
(Kamseu et al., 2022)	Cement	MIP, SEM, Flexural test, Indentation test, XRD, FTIR, Scratch test	Building
(da Silva Nuernberg et al., 2021)	Geopolymer	XRD, FTIR, DSC/TG, XRF, Particle size distribution, Density test (Archimedes principle), Tensile test (diametrical compression test)	N/S
(C. Liu, Zhang, Liu, Lin, et al., 2022)	Cement	XRD, XRF, BET, Particle size analysis, Compressive strength test,	Building
(Fernando et al., 2023)	Concrete	Water absorption analysis, AVPV, Permeability test (air, water, RCPT), Chloride diffusion, Carbonation of concrete, XRD, FTIR, SEM, EDS	Building
(Alkhaly et al., 2022)	Concrete	Compressive strength test, Elastic modulus, Flexural strength test, Tensile strength test, Autogenous shrinkage, Absorption rate test, SEM	Building
(Dhinasekaran et al., 2020)	Silica nanoparticle	TGA-DSC, XRD, FTIR, micro-Raman spectroscopy, SEM, TEM, Zeta potential analysis, UV-Vis spectrophotometry	Anticancer application

(Mozafari et al., 2022)	Nano-silica	FTIR, BET, CHNS analysis, FE-SEM, TEM, VSM, TGA-DTG, EDX, XRD	Acid catalyst
(Nikhade & Nag, 2022)	Concrete	Compressive strength test, flexural test, STS, water penetration test, Chloride penetration resistance test, XRF	Building
(Haider et al., 2022)	Silica	XRD, FTIR, EDS, FESEM, SEM-EDS, XRF, BET, Adsorption capacity analysis, ED-XRF, WD-XRF	Adsorbent for dye removal
(Y. Chen et al., 2022)	Ni-phyllosilicate	XRF, XRD, SEM, TEM, ICP analysis, H2-TPR analysis, DRIFTS	CO2 methanation
(Fernando et al., 2022)	Bricks	LCA, Benefit analysis, leaching analysis, cost analysis	Building
(Sampaio et al., 2022)	Concrete	LCA, Compressive strength test, tensile strength test, flexural test, modulus of elasticity, water absorption analysis, sensitivity analysis	Building
(Xiao et al., 2022)	Cement-stabilized soil	Compressive strength test, STS, SEM	Building
(R. Chen et al., 2022)	Cement	SEM, EDS, XRD, MIP, UCS, BSE, Compressive strength test	Building (road)
(Xia et al., 2023)	Cement	LCA, SEM, MIP, XRD, Compressive strength test, Isothermal calorimetry, TGA	Building
(Manubothula & Gorre, 2022)	Concrete	Compressive strength test,	Building
(Uysal et al., 2022)	Geopolymer	SEM-EDS, XRD, Compressive strength test, water absorption analysis, STS, Flexural test, UPV, abrasion resistance test	N/S
(Kannur & Chore, 2023)	Concrete	Compressive strength test, XRF, XRD, FESEM, Flexural test, STS, RCPT, Water absorption test, water penetration test, EDX	Building (road)
(Nasir Amin et al., 2022)	Concrete	FTIR, XRF, XRD, SEM-EDS, TGA, N2 adsorption isotherm analysis, LCA, Compressive strength test, STS, Apparent porosity analysis, Water absorption analysis,	Building
(Anto et al., 2022)	Cement	UPV, Water absorption test, acid attack test, XRD, Compressive strength test, flexural test,	Building

(Nie et al., 2022)	Magnesium oxychloride cement	Compressive strength test, Water resistance analysis, Water absorption analysis, Volume stability analysis, XRD, TGA, EDS, DSC, Environmental assessment	Building
(Meraz et al., 2023)	Concrete	XRD, XRF, PSD test, EMI, Compressive strength test, flexural test, STS, Modulus of elasticity, structural application assessment, SEM, Chloride ion penetration test, MIP	Building
(Yan et al., 2022)	Cement	Flexural test, Compressive strength test, EDX, XRD, SEM, STS, Shrinkage test, Compression resilience modulus test, Freeze-thaw cycle test	N/S
(C. Liu, Zhang, Liu, Zhu, et al., 2022)	Concrete	SEM, XRD, MIP, STS, Compressive strength test, Environmental Impact Assessment	Building
(Ketov et al., 2021)	Bricks	SEM, DSC, TGA, XRD, Compression test	Building
(Shetye et al., 2023)	Silicate	SEM, EDS, Total organic carbon analysis, turbidity measurement, ANOVA	Oceanic phytoplankton
(Hu et al., 2020)	Cement	Sustainability analysis, Compressive strength test, XRD, XRF, Laser particle size analysis (BJH), Lime-ash test, Isothermal calorimetry, Sulfate resistance analysis, Environmental benefit analysis	Building
(Pimentel Tinoco et al., 2023)	RH particles	XRF, Density measurement (Helium pycnometer), Laser diffraction, SEM, Isothermal calorimetry, Rheological test	3D printable cementitious composites
(Wahab et al., 2022)	Silica	XRD, PES, Electronic densimeter, Color chromaticity, UV-vis spectrometry,	Zinc borosilicate glass

N/S – Not stated

2.3.1.2.2 Biopolymer

Table 2.2 summarizes the different biopolymers from the various studies. From the studies, the different biopolymers produced from rice husks are cellulose, aromatics, Superabsorbent polymers (SAPs) lignin and melamine formaldehyde. Each biopolymer type is produced via a series of thermochemical processes at regulated temperatures and time.

2.3.1.2.2.1 Cellulose and Cellulose-based Polymers

Table 2.3 describes the production of cellulose and cellulose-based biopolymers as illustrated by Hafid et al., (2021), Aboelfetoh et al., (2023), Yeboah et al., (2022), Gupta et al., (2019), Rashid & Dutta, (2021) and Hayatun et al., (2020). The production of cellulose as described by the studies has four main unit procedures, that is pretreatment, milling, alkali treatment, and drying with the only disparities been type of chemical used, temperature values and process times. The first process, pretreatment, usually involves washing and drying of the rice husks to get rid of any inorganic impurities, such as dust that may be part of the husks. However, this process could go beyond washing and drying. For example, in the study by Rashid & Dutta, (2021), the rice husks were dewaxed as part of the pretreatment process. Dewaxing helps remove the extractive substances found in the husks, such as was, fat, fatty acids, terpenes, and steroids that may become impurities in production reactions (Novitasari et al., 2019). Pretreatment is followed by milling, which involves grinding and sieving the rice husks into finer particles to facilitate the subsequent conversion reactions. Following this process is alkali treatment. This process involves treating the husks in an alkali solution at elevated temperatures to remove the silica and some part of lignin and hemicellulose content from the rice husks to obtain cellulose. From the studies, the common alkalis used are sodium hydroxide (NaOH) and potassium hydroxide (KOH). Some studies subjected cellulose to other reactions such as acid hydrolysis, bleaching,

and mercerization for the purpose of obtaining better results. For example, acid hydrolysis is performed to neutralize any excess sodium hydroxide from the alkali treatment step and remove excess lignin and hemicellulose. Some studies perform this process as an environmentally friendly mechanism (Hafid et al., 2021). The process of acid hydrolysis involves heating the alkali-treated husks in acidic solution, such as sulfuric acid and nitric acid. Bleaching involves treating cellulose with bleaching chemicals, such as sodium chlorite ($NaClO_2$) at elevated temperatures to remove the coloring components in the rice husk to obtain white cellulose. Mercerization also involves treating the cellulose with chemicals, usually isopropanol and sodium hydroxide at elevated temperatures to give it a lustrous appearance and increase its strength (Gupta et al., 2019). Cellulose can be further processed to give other forms of biopolymers, such as carboxymethyl cellulose, cellulose acetate, and cellulose nitrate (Gupta et al., 2019; Hayatun et al., 2020; Rashid & Dutta, 2021; Yeboah et al., 2022). The processes involved in each biopolymer type are described in Table 2.3. The production of carboxymethyl cellulose involves treating cellulose in monochloroacetic acid at elevated temperatures, a process termed etherification. This is proceeded by washing the resulting material with ethanol (some studies add hydrochloric acid in this process), filtration and finally drying. Cellulose acetate and cellulose nitrate follow similar routes, except that in their production, the first steps are acetylation and nitration, respectively, rather than etherification. Acetylation involves treating cellulose in acetic anhydride and iodine, whereas nitration involves treating it in a concentrated nitric and sulfuric acid solution (Yeboah et al., 2022). Hayatun et al., (2020) also produced an unknown polymer with the addition of chitosan solution and sorbitol.

Table 2.2: Different types of biopolymers, their application and characterization techniques and analysis used for their evaluation

Reference	Biopolymer	Characterization technique, testing and analysis	Application	Combined resource
(Yeboah et al., 2022)	Carboxymethyl cellulose, cellulose acetate, cellulose nitrate	Uncertainty analysis, Sensitivity analysis, LCA, LCICA	N/S	None
(Zakaria et al., 2020)	Lignin	UV-vis spectroscopy, FTIR, TGA, NMR, FESEM, KFC, GC-MS	N/S	None
(Hafid et al., 2021)	Cellulose	TGA, DTG, FTIR, PCA, XRD, SEM, TEA	N/S	None
(Rashid & Dutta, 2021)	Carboxymethyl cellulose	Degree of substitution (wash method), Rotational viscometry, FTIR, XRD, TGA, TPA, DMRT	Cake additive	None
(Kenawy et al., 2021)	SAPs	FTIR, TGA, SEM, Water absorption capacity test, Pot experiment	Agriculture	None
(Gupta et al., 2019)	Carboxymethyl cellulose	Degree of substitution, FTIR, XRD, Tensile test, Elongation test	Food packaging	None
(Hayatun et al., 2020)	Cellulose-based plastics	FTIR, Tensile test, Elongation test	N/S	None
(Moogi et al., 2022)	Aromatics	N2 physisorption (BET), NH3-TPD, GC-TCD/FID, GC-MS, DTG	N/S	None
(Balasubramanian & Venkatachalam, 2023)	Lignin	Raman Spectrometry, NMR, TGA, FTIR	N/S	Marble waste powders
(Moogi et al., 2021)	Aromatics (benzene, toluene, ethylbenzene, xylene)	N2 physisorption (BET), NH3-TPD, TCD	N/S	None
(Aboelfetoh et al., 2023)	Cellulose	XRD, SEM FTIR, EDX, TEM, VSM, BET, TGA/DTG, Adsorption isotherm study	Wastewater treatment	Iron and Zinc oxide nanoparticles

N/S – Not stated

Table 2.3: Synthesis of cellulose and cellulose-based polymers

Reference	Cellulose production	Cellulose-based polymer production
(Yeboah et al., 2022)	1.Washing RH with distilled water and drying in an oven at 70 ℃ for 16 h 2.Milling to a particel size of 0.177 mm 3.Alkali treatment in sodium hydroxide (5% w/v) in a 1:5 ratio in an autoclave at 120 ℃ for 0.75 h 4.Washing and filtration 5.Acid hydrolysis in nitric acid (10% w/v) at 120 ℃ for 2 h to obtain cellulose 6.Washing with distilled water to remove excess acid 7.Bleaching in sodium chlorite (3% w/v) and acetic acid (25% w/v) at 70 ℃ 8.Mercerization in isopropanol and sodium hydroxide (20% w/v) at 55 ℃ for 3 h	1.Etherification in mono-chloroacetic (20% w/v) acid at 55 ℃ 2.Washing with hydrochloric acid and ethanol 3.Filtration and drying at 60 ℃ to obtain **carboxymethyl cellulose** 1.Acetylation in acetic anhydride and iodine at 80 ℃ for 5 h 2.Cooling and treatment with saturated sodium thiosulphate 3.Ethanol addition and stirring for 1 h 4.Washing with ethanol (75% v/v) and distilled water 5.Drying at 60 ℃ 6.Dissolution in methylene chloride, filtration and evaporation of filtrate 7.Collection of CA residue with ethanol and drying at 60 ℃ for 2 h to obtain **cellulose acetate** 1.Nitration in concentrated nitric and sulfuric acid nitration solution for 1 h 2.Quneching by excess deionized water 3.Filtration of precipitate by vacuum 4.Incubation in boiling water for 5 min

		5.Washing and drying at 60 ℃ to obtain **cellulose nitrate**
(Gupta et al., 2019)	1.Milling to a particle size of 0.25 mm 2.Alkali treatment in potassium hydroxide (6% w/v) at 85 ℃ for 2 h 3.Acid hydrolysis in sulfuric acid (4% w/v) at 85 ℃ for 2-2.5 h 4.Bleaching in sodium chlorite (3% w/v) and acetic acid at 80 ℃ for 4 h 5.Mercerization in isopropanol and sodium hydroxide (20% w/v) at 50-60 ℃ for 2.5-4 h	1.Etherification in 20% chloroacetic acid at 50-60 ℃ for 2.5-4 h 2.Washing and filtration with ethanol and hydrochloric acid 3.Drying at 60 ℃ in oven to obtain **carboxymethyl cellulose**
(Rashid & Dutta, 2021)	1.Milling to a particle size of 0.1-0.25 mm 2.Dewaxing in 1:2 v/v methanol:benzene at 75 ℃ for 9 h 3.Alkali treatment in sodium hydroxide (3% w/v) at 45 ℃ for 8 h 4.Autoclave samples at 121 ℃, 15 psig for 8 h – repeated thrice 5.Bleaching in 6.5:2.0 v/v acetic acid:hydrogen peroxide at 45 ℃ for 7 h 6.Mercerization in isopropanol and sodium hydroxide (40% w/w) for 50 min	1.Etherification in monochloroacetic acid at 55 ℃ for 4 h 2.Washing and filtration with C_2H_5OH 3.Washing with absolute ethanol 4.Drying at 60 ℃ for 9 h to obtain **carboxymethyl cellulose**
(Hayatun et al., 2020)	1.Cleaning and drying RH in sun 2.Milling to a particle size of 0.177 mm 3.Maceration with methanol sovent for 7 dyas 4.Alkali treatment with 5% w/v solution of sodium droxide and sodium carbonate	1.Addition of chitosan solution and mixing homogeneously 2.Additon of sorbitol solution and stirring 3.Printing mixture on glass plate 4.Drying at 60 ℃ to obtain plastic film

	5.Acid hydrolysis with 10% sulfuric acid 6.Drying at 50 ℃ in an oven	
(Aboelfetoh et al., 2023)	1.RH is pulverized and soaked in 0.4 M sulfuric acid for 2 h, while stirring at 90 ℃ 2.Washing of solid residue with distilled water 3.Alkali treatment in 0.9 M sodium hydroxide at 90 ℃ for 2 h 4.Bleaching with 0.33 M sodium chlorite solution and acetic acid at 80 ℃ for 4 h 5.Washing of residue with de-ionized water 6.Drying	None
(Hafid et al., 2021)	1.Alkaline treatment with 5% sodium hydroxide solution in a 1;10 rice husk:liquor ratio at 120 ℃ for 0.75 h 2.Acid hydrolysis with 25 wt% acetic acid, 5 wt% hydrogen peroxide and 5 wt% sulfuric acid or 10 wt% nitric acid 3.Filtration and washing with distilled water – twice 4.Drying at 60 ℃ for 24 h 5.Bleaching with a buffer solution of sodium chlorite, 1.47% acetic acid and distilled water at 70 ℃ 6.Cooling and filtration 7.Drying at 60 ℃ for 24 h	None

2.3.1.2.2.2 Aromatics

Moogi et al., (2021) and Moogi et al., (2022) described the production of another type of aromatics. Aromatics are organic compounds or polymers that emit pleasant smells. Examples are benzene, toluene, ethylbenzene, and xylene. The first step of production involves the synthesis of a catalyst, typically a zeolite-based catalyst, via the incipient wetness impregnation method. The method involves fusing γ-Al_2O_3 with a solution of rare earth metal nitrates, that is $La(NO_3)_3 \cdot 6H_2O$ and $Ce(NO_3)_3 \cdot 6H_2O$ in water and drying it for about 12 h at 110 ℃. This sample is afterward calcined in a nitrogen medium for 5 h at 650 ℃. The resulting material is then impregnated with aqueous nickel nitrate solution, dried at 110 ℃ for 12 h and calcined in a similar nitrogen medium for 5 h at 650 ℃. The catalyst is enhanced by the addition of gallium, typically in the form of $Ga(NO_3) \cdot xH_2O$ aqueous solution, followed by drying, calcination and reduction in hydrogen gas. The catalyst is then passivated at room temperature in nitrogen gas and is used for the aromatic synthesis. The synthesis involves a thermo-catalytic conversion of rice husks in an ex-situ pyrolyzer, consisting of three chambers. The first chamber is filled with methane (40% balanced He, 50 mL/min) and nitrogen gas (50 mL/min) to create the right medium for the production (depending on the stage of production). The second medium is filled with the rice husk feedstock. This is where the production occurs, at a temperature of 650 ℃. The third chamber is filled with the synthesized catalysts and kept at a temperature of 550 ℃. The rice husks in the second chamber are heated to produce biomass vapors, which are quenched at -22.5 ℃ by a chiller system and collected and in the third chamber, where the conversion occurs. Aromatics such as benzene, toluene, ethylbenzene, and xylene are produced in this process, and are used in medicine, plastics and as pesticide components (Moogi et al., 2021).

2.3.1.2.2.3 Superabsorbent polymers (SAPs)

SAPs are hydrophilic homopolymers with lightly crosslinked three-dimensional structure that have high liquid retaining capacities. They are the most successful of the products in the hydrogel family, with applications extending from agriculture to pharmaceuticals (Zohuriaan-Mehr et al., 2010). Their production as described by Kenawy et al., (2021) involves the dissolution of gelatin in distilled water (7-26 wt%) at 50 ℃ while stirring at 750 rpm. RH is then added to the mixture and stirred until homogenization. Acrylic acid (70% neutralized with KOH), acrylamide, methylene bis-acrylamide, tetra methyl ethylene diamine (as catalyst) and potassium persulfate (as initiator) were added, and the entire composition is heated at 70 ℃ for 5-10 minutes. This completely polymerizes the mixture, which is afterward washed with ethanol to remove impurities. The final product is dried in a vacuum oven at 70 ℃ to a constant weight, milled and sieved into powder. The SAP produced was in the form of a composite and was used for water retention purposes in soil.

2.3.1.2.2.4 Lignin

In lignin production, a green solvent termed Deep Eutectic Solvent (DES) is first synthesized by mixing choline chloride and p-toluenesulfonic acid monohydrate in a 1:0.5 ratio at 50 ℃. A slurry of RH (5-30 wt%) is added to the solvent and reacted at 70 ℃ for an hour. The mixture is then centrifuged, and the cellulose-rich residue is filtered out. The filtrate is washed with distilled water to remove any excess DES, and then dried at 50 ℃. The remaining content was treated with 1 wt% sulfuric acid to obtain a liquified fraction, containing solubilized lignin. Lignin is precipitated by adding deionized water as an antisolvent and allowing the solution to sit for 24 h at room temperature. After precipitation, lignin is washed with deionized water and dried at room temperature (Balasubramanian & Venkatachalam, 2023).

2.3.1.2.2.5 Melamine formaldehyde

The production involves washing rice husks with distilled water and drying them in an oven at 100 ℃. The dried RH are milled to submicron sizes and treated with sodium hydroxide at 100 ℃ for 12 h. Alkali-treated RH are washed to remove any excess sodium hydroxide and then treated with sodium periodate ($NaIO_4$) aqueous solution for 5 h at 60 ℃. Sodium periodate-treated RH and melamine were added to dimethylsulfoxide and heated for 6 h in dry air atmosphere at 120 ℃, followed by a refluxed at 180 ℃ for 2 days. The sample is filtered to obtain melamine formaldehyde (R. Chen et al., 2023). The authors utilized this as an adsorbent to remove bisphenol A, bisphenol B and some other micropollutant (dye). The results showed that there was a rapid mass transport and a good adsorption performance towards phenolic and other antibiotic pollutants.

These biopolymers after production were characterized to study their thermal, physical, and chemical properties. Techniques such as FTIR, TGA, SEM, XRD, UV-vis spectroscopy and viscometry were employed. Some authors also studied their sustainability, including Life Cycle Assessment (LCA) and Techno-economic Assessment (TEA).

2.3.1.2.3 Bio-composites

Rice husks have been combined with other distinct materials to form new materials via different methods such as extruding, stir casting, . Table 2.4 summarizes some different bio-composites, the method used for their production and their applications. MP-XRD, HR-SEM, TEM, FTIR, XPS, EDAX, ICP-OES, TGA, DSC, mechanical testing (tensile, flexural, and dynamic mechanical analysis), and 3D surface characterization were some characterization techniques employed for the study. Other bio-composites produced includes Co_3O_4-RH, AlN-epoxy-RH, novolac-epoxy-RH, MCM-41-RH, protein isolate-RH, epoxy-RH, and SiC/C (Alshahrani &

Arun Prakash, 2022; Balaji et al., 2022; Di et al., 2021; Kavitha et al., 2021; Mortada et al., 2022; Wu et al., 2022; Zuwanna et al., 2023).

Table 2.4: Different types of bio-composites, their production and application

Reference	Bio-composite	Production	Application
(Hidalgo-Salazar & Salinas, 2019)	Polypropylene-RH (PP-RH)	1.RH is milled (0.42 mm) 2.Polypropylene and RH are fed into a corotating twin screw extruder separately at 165-185 ℃ and 50 rpm 3.PP-RH are cooled in water bath 4.PP-RH are cut into pellets and dried at 60 ℃	Reusable spoons
(Kamran et al., 2023)	Nickel-doped TiO_2-RH	1.RH is washed with distilled water and dried at 95 ℃ for 48 h 2.Dried RH is pyrolyzed at 600 ℃ for 3 h in nitrogen to obtain biochar 3.Na-TiO_2 nanoparticles is synthesized by dissolving p25-TiO_2 powder in 10 M NaOH for 2 h, followed by hydrothermal processing at 130 ℃ for 63 h, filtration and washing 4.Biochar is dissolved to distilled water to form a solution via ultrasonication 5.Na-TiO_2 is dissolved in $Ni(CH_3CO_2)\cdot 4H_2O$ via ultrasonication 6.Both solutions are mixed and autoclaved at 120 ℃ for 15 h 7.Obtained precipitates (bio-composite) are filtered, washed, dried, and heated at 350 ℃ for 8 h	Wastewater treatment (Pb(II) ions removal)
(Dada et al., 2022)	RH-ZnO	1.RH is washed and dried at 110 ℃ for 3 h 2.RH is treated with 1 M nitric acid and then 1 M NaOH 3.RH is carbonized at 400 ℃ for 1 h in 1 M phosphoric acid and dried at 105 ℃ to obtain RH activated carbon (RHAC)	Wastewater treatment

		4.RHAC is dissolved in 1.5 M $(NH_4)_2CO_3$ and 1 M $Zn(NO_3)_2$ is added 5.Bio-composite begin to precipitate after 3 h 6.Bio-composite is filtered, washed with water and ethanol, annealed, ground, and calcined at 550 ℃ for 4 h	
(Udoye et al., 2021)	AA6061-RH	1.RHA is milled to 75 microns 2.AA6061 is melted in a graphite crucible at 750 ℃ 3.Magnesium and wetting agent were added to the melt to reduce casting fluidity and surface tension 4.RHA powder is heated at 200 ℃ for 1h 5.RHA powder is heated at 600 ℃ and added to the melt to obtain bio-composite	N/S
(Arumugam et al., 2021)	RH-SD-Bio-benzoxazine	1.RH and SD are treated in sodium hydroxide solution at 80 ℃ for 3h 2.The fibers are washed and dried at 60 ℃ for 24 h 3.Alkali-treated RH and SD were soaked separately into DGEBA-isophorone diamine blend 4.The blends are poured into a mold and cured overnight at room temperature under mild pressure 5.The bio-composites are post cured at 100 ℃ for 3 h	Acoustic adsorption

DGEBA – bisphenol-A epoxy; AAA6061 – Aluminum Alloy 6061; SD – Saw dust

2.3.1.2.4 Biocatalysts

Wang et al., (2023) and Unglaube et al., (2022) produced catalysts from rice husks. The processes described by each study were different and as a result, different outcomes were observed. Wang et al., (2023) synthesized the catalysts via the incipient wetness impregnation method. The process involves extracting silica from rice husks by pretreating (washing with deionized water and drying at 60 ℃ for 24 h), treating dried RH in sulfuric acid (0.5 mol/L) at 60 ℃ for 0.5 h, filtration, washing, drying acid-treated RH at 60 ℃ for 24 h, and finally calcining RH at 600 ℃ for 6 h. Silica from RH is added to a solution of dichloromethane and Co(II) acetylacetone while stirring. The mixture is allowed to sit for half an hour at a temperature of 30 ℃, and afterward dried at 60 ℃ for 12 h. The sample is milled into fine powder and calcined at 450 ℃ for 3 h to obtain the catalysts. The study by Wang et al., (2023) utilized the RH-based catalyst in the selective synthesis of a large diameter single-walled carbon nanotube. Raman spectroscopy, UV-vis-NIR spectroscopy, TEM, SEM, TGA, FTIR, XRD, UV-vis-DRS spectroscopy and XPS were used in the study. Unglaube et al., (2022) on the other hand dissolved rice husk in a solution of $Co(II)Cl_2 \cdot 6H_2O$, ethanol and phthalocyanine at 21 ℃ while stirring for 24 h. The solvent is evaporated in a vacuum and the treated RH is pyrolyzed under a nitrogen atmosphere at 600 ℃ in an alumina pot inside a quartz tube furnace (which is flushed out after pyrolysis) to obtain the catalyst. SEM, XRD, BET, XPS, IR, and ICP-OES were employed in the study. For both studies however, the catalysts showed amazing stability and ease in usage and reusability.

2.3.1.2.5 Coagulants

K. L. Tan et al., (2022) and Dadebo et al., (2023) derived coagulants from rice husks and used them for wastewater treatment. In the study by K. L. Tan et al., (2022), RH is first washed with

distilled water to remove soil particles, dirt and other surface impurities, and milled to a particle size in 50-100 microns range. RH powder is treated with 0.1 M sodium hydroxide solution while stirring at 300 rpm for 0.5 h. The solution is centrifuged at 5000 rpm for 5 minutes to obtain an aqueous suspension of RH. The suspension is filtered, and the filtrate is used as coagulant to treat urban and agricultural runoffs. The results showed that RH-based coagulant exhibited a good performance with optimized removal rates of 85.9-95.2%, 85.1-89.8% , and 68.5-74.2% for turbidity, total suspended solids, and chemical oxygen demand, respectively. FTIR, EDX and SEM were employed in this study for surface functionalities, morphological characteristics, and elemental composition. Dadebo et al., (2023) used a different approach. Firstly, RHA was produced by calcining pretreated RH (double washed with distilled water and dried at 105 ℃ for 24 h) at 700 ℃ for 2 h. RHA is sieved to obtain a particle size of 0.2-0.3 mm and is used as coagulant to remove surfactant-laden wastewater. The results showed that RHA can removed surfactant by 42.3% at a 3.79 g/L RHA dosage. SEM, EDX, FTIR and XRD were used in the characterization analysis. TEA for the design process was also studied.

2.3.1.2.6 Zeolite

Zeolite (beta) was produced by Phouthavong et al., (2023) via the dry-gel conversion method. The process involves extracting rice husk ash from rice husks by alkaline extraction, followed by acid precipitation to produce silica needed for the production. RHA is dissolved in 20 wt% sodium hydroxide solution and 10 wt% tetraethyl ammonium hydroxide solution and stirred for half an hour. Further dissolution was achieved by using ultrasonication for 2 h. $Al_2(SO_4)_3 \cdot 16H_2O$ is then added and mixed via ultrasonication for an hour. The mixture is stirred for 16 h, followed by heating at 80 ℃. The solution is stirred for another 8 h and iron oxide (Fe_3O_4) is added. The solution is allowed to sit until a dry gel is formed. The gel is collected, crushed, and put in an

autoclave at 180 ℃ for 12 h in a convection oven. The product is collected and calcined at 450 ℃ for 12 h to obtain zeolite. The zeolite produced was utilized as an adsorbent to remove paraquat herbicide from an aqueous solution. The results showed that the zeolite had a high adsorption rate, quick magnetic separability, and excellent reusability up to about five cycles. XRD, UV-vis spectrophotometry, FE-SEM and EDS were used in the study for property analysis, such as crystallinity and morphology. Na Chat et al., (2022) also produced zeolite (X) for adsorbent purposes, specifically propionic acid adsorption. The production involves washing and drying of RH overnight to remove any inorganic impurity. Dried RH is dissolved in 1 M hydrochloric acid at 90 ℃ for 2 h, after which they are filtered, washed with distilled water, and dried. The acid-treated RH are calcined at 750 ℃ for 4 h to obtain RHA (silica source). Zeolite X is produced afterward following another authors' work, but with sodium aluminate as alumina source and sodium silicate as extra silica source. XRF, XRD, SEM, and nitrogen adsorption/ desorption test were utilized in the study to characterize the zeolite adsorbent. The results showed that the highest propionic acid adsorbed by the zeolite was 516 mg/g for 0.5 h equilibrium time.

2.3.1.2.7 Bioactive Peptides (BP)

The production begins with extracting protein hydrolysates from rice husks. This is done by putting rice husks into an extraction vessel containing pressurized hot water at a pressure of 5 bar for 45 minutes. The temperature, pH, water flow rates were varied to evaluate the best parameters for optimum protein yield. From the experiment, the optimum parameters were found to be 60 ℃ , pH 10.0 and 2.0 mL/min flow rate. The process hydrolyzed rice husks to give protein hydrolysate (bioactive peptides). The authors studied the anticancer activities of free bioactive peptides and chitosan-encapsulated bioactive peptides (synthesized using ionic gelation

method) using the Hoechst 33,342 staining fluorescent dye (apoptosis process). Analysis such as UV-vis spectrophotometry, fluorescence microscopy, and Box-Behnken response surface design (based on ANOVA) were also performed.

2.3.1.2.8 Xylo-oligosaccharides (XOS)

XOS are prebiotics which serve the purpose of feeding beneficial bacteria within the digestive tract of organisms, specifically humans. Their production as described by Khat-udomkiri et al., (2020) involves treating RH in 12% sodium hydroxide solution in a 1:10 ratio at 120 ℃ for 0.75 h. The liquid from the alkali treatment is acidified afterward with glacial acetic acid. Three volumes of ice-cold ethanol are added to precipitate xylan from the liquid and is dried in hot air oven. The precipitated xylan is dissolved in a 50 Mm of citric acid-Na_2PO_4 buffer and incubated with commercial xylanase at 120 rpm and 50 ℃ for 2 h. After this time, the extract is boiled for 5 minutes in a boiling water bath to terminate the reaction. XOS slurry is filtered and dried to obtain XOS powder. The authors further studied antihyperglycemic effect and putative mechanisms of XOS using a diabetic rat model, using biochemical analysis, in vivo intestinal permeability analysis (Fluorescein isothiocyanate-dextran), q-PCR and some statistical studies, specifically ANOVA. The results showed that XOS can be used to treat diabetes.

2.3.1.2.9 Humic Acid

The production of humic acid from rice husks follows a bio-fermentation approach, as described by Zhao et al., (2023). RH is dried in the sun and then milled to about 10 mm. Urea is added to the crushed RH, followed by water (60% water content). Active bio-enzymes are then inoculated into the system and left for 7 days to cause fermentation, and the subsequent production of humic acid. Humic acid has different benefits such as improving soil properties and enhancing plant growth, but in this study, it was used as an adsorbent to remove lead contaminants (Pb(II)). Also,

some characterization techniques, such as XRD, elemental analysis, hexamine cobalt (III) chloride extraction spectrophotometry, BET, EDS, and XPS were employed for property analysis.

2.3.1.2.10 Molecular Sieve

Molecular sieves are three-dimensional crystalline metal aluminosilicates that are usually used for drying fluids and for separating molecules based on their size and shape. Their production as described by Mahdavi Fard et al., (2022) washing RH and drying them at 110 ℃ for 12 h. The dried RH is burnt at 700 ℃ for 5 h to obtain RHA, which is treated with hydrochloric acid in a 1:10 ratio at 80 ℃ for 3.5 h. The treated-RH (purified) is filtered and washed with distilled water until a pH of about 7 is reached. The RHA is dried at 120 ℃ for 16 h afterwards. Aluminum isopropoxide, tetraethyl ammonium hydroxide, morpholine and water are mixed for 2 h until homogenization to obtain a white color gel. Phosphoric acid is added dropwise to the gel and mixed for 1 h forming $AlPO_4$ structures. RHA is finally added to the solution and mixed for 24 h at room temperature. The mixture is autoclaved at 200 ℃ to obtain a solid and liquid phase, which is then centrifuged at 5700 rpm to separate the phases. The solid matter is filtered, washed with deionized water and ethanol, and dried at 110 ℃ for 14 h. The dried sample is calcined at 550 ℃ for 6 h to obtain molecular sieve. The authors further studied the properties of the molecular sieve by employing XRD, SEM, BET and EDX. The molecular sieve was also used by the authors as catalyst in the synthesis of olefin from methanol.

2.3.1.2.11 Demulsifier

Yuan et al., (2022) described the production of demulsifier from rice husks using a one-step hydrothermal approach. The process involves adding rice husks, distilled water and sulfuric acid into an autoclave and stirring at 180 ℃ for 12 h, after which the mixture was cooled. The

mixture is washed with distilled water to remove any excess sulfuric acid and then dried in a vacuum freeze dryer to obtain the demulsifier. This was used to study the separation of crude oil and distilled water. FTIR, zeta potential, EDS, and XPS were employed to study the properties of the demulsifier.

2.3.1.2.12 Aerogel

The production of aerogel as described by De Oliveira et al., (2019) begins with the extraction of cellulose nanocrystals (method is described by (García-González et al., 2011)). Cellulose nanocrystals are dispersed in water (2% w/v) and stirred at 35 ℃ for an hour. Poly (vinyl alcohol) is dispersed in water (21% w/v) and stirred at 90 ℃ for an hour. The two dispersions were mixed until homogenization to obtain aerogel. The morphology, crystallinity, thermal stability, and suspension ability were analyzed by means of SEM, XRD, TGA, and zeta potential, respectively. The water absorption potential and of the aerogel was also measured and the aerogel was applied in food packaging.

2.3.1.2.13 Biochar

Biochar is basically charcoal produced from plant matter mainly for carbon dioxide removal from the soil. The production of biochar from rice husks is similar for all the studies that worked on this valorization pathway, with the only difference being the method of pretreating rice husks prior to the conversion process. Biochar is produced from rice husks by the process of pyrolysis, however, treating rice husks in certain chemicals increases the yield of biochar and enhances some properties as well (Bian et al., 2022; Khan et al., 2020; Pham et al., 2022). Some pretreatment processes include alkali treatment, addition of other biomasses, and acid treatment (Phan et al., 2022; Shi et al., 2019; Tabassam et al., 2022). Certain conditions such as pyrolyzing RH in the presence of nitrogen gas and pyrolyzing temperature have proved to influence some

properties such as adsorption efficiency within the biochar (Khan et al., 2020; Shi et al., 2019). The authors studied these properties using techniques such as XRD, Catio Exchange Capacity analysis, BET, UV-vis spectroscopy, and SEM-EDS.

2.3.1.2.14 Carbon/Activated carbon

The production of carbon and activated carbon from rice husks follow similar processes, involving rice husks pretreatment and carbonization. The rice husks pretreatment generally involves washing, drying, and treating the rice husks in an acidic and/or an alkali solution at elevated temperatures. In the pretreatment process by Tagne et al., (2021), rice husks are washed with tap and distilled water and dried in the sun for 72 h. Dried rice husks are treated in 1 M phosphoric acid for 0.5 h and afterwards dried at 105 ℃ for 24 h. In the experiment by Leal Da Silva et al., (2021), rice husks are cleaned, treated in 1 mol/L nitric acid for 24 h, washed, and dried at 105 ℃ for 24 h. The dried rice husks are treated in sodium hydroxide with the same concentration as the acid for 24 h before carbonization. Some studies such as Y. Liu, Tan, Tan, & Cheng, (2022) washed RH with reverse osmosis water and dried them at 105 ℃ overnight as pretreatment process. The idea behind pretreating RH prior to carbonization is to remove the organic contents, such as lignin and hemicellulose and some inorganic contents, such as silica from the rice husks before carbonization (Leal Da Silva et al., 2021). The process of carbonization generally involves pyrolyzing rice husks in an inert condition, such as nitrogen gas and argon gas environments at temperatures typically around 450-900 ℃. The carbon/activated carbons produced are usually used for wastewater treatment and supercapacitors (Arkhipova et al., 2022; Gaikwad & Balomajumder, 2023; Xue et al., 2022).

2.3.1.2.15 α-amylase

α-amylase is a hydrolytic endoenzyme that is used in the production of short-chain oligosaccharides such as maltose and maltotriose. Its production from rice husks, as described by Rathi et al., (2022) involves autoclaving an RH substrate which is made of RH and distilled water in a 1:10 ratio at 15 psi and 121 ℃ for 20 minutes. Sub-cultured bacterial strains (Staphylococcus aureus MTCC and Bacillus subtilis MB6) were inoculated into the substrate T 37 ℃ for 48 h in an incubator. The substrate hydrolysate is then centrifuged at 10000 rpm and 4 ℃ for 20 minutes. The supernatant collected is α-amylase. UV-vis spectroscopy was employed to study the protein concentrations in the enzyme.

2.3.2 Sustainability assessment (SA)

The idea behind utilizing rice husks for non-energy applications is to reduce the impacts the energy applications have on the environment, humans and resources. To justify this, some form of assessments are required to put metrices on the impacts of the various non-energy valorization pathways. Sustainability assessment presents these metrices via techniques such as Life Cycle Assessment (LCA), Life Cycle Costing (LCC), and Social Life Cycle Assessment (SLCA) (Allotey et al., 2023; Sala et al., 2015). This section therefore describes the methodologies and results of the sustainability assessments for the studies. Out of the 105 studies, only 10 studies performed at least one of the sustainability assessments (Table 2.5). From the table, 7 studies performed only LCA, 1 study performed only LCC, two studies performed both LCA and LCC, and none of the studies performed SLCA.

Table 2.5: Sustainability assessment studies

Reference	Product	SA techniques		
		LCA	LCC	SLCA
(Yeboah et al., 2022)	Biopolymer	✓	✓	×
(Setiawan & Chiang, 2021)	Silica	✓	×	×
(Hafid et al., 2021)	Biopolymer	×	✓	×
(Fernando et al., 2022)	Bricks	✓	✓	×
(Sampaio et al., 2022)	Concrete	✓	×	×
(Xia et al., 2023)	Cement	✓	×	×
(Nasir Amin et al., 2022)	Concrete	✓	×	×
(Nie et al., 2022)	Cement	✓	×	×
(C. Liu, Zhang, Liu, Zhu, et al., 2022)	Concrete	✓	×	×
(Hu et al., 2020)	Cement	✓	×	×

2.3.2.1 Life Cycle Assessment (LCA)

LCA is the part of sustainability assessment that deals with measuring the potential environmental impacts associated with a process, product, or service throughout its life, usually from raw material acquisition to use and disposal (termed cradle-to-grave) (Arvanitoyannis, 2008). According to the International Standards Organization (ISO 14040), LCA is performed following 4 main phases: goal and scope definition, inventory analysis, impact assessment, and interpretation (Figure 4) (ISO, 2006). For the goal and scope phase, the goal section involves defining the reasons for carrying out the assessment, the intended application, and the intended audience for the study. ISO requires that the goal should be stated without any ambiguity. The scope section involves describing the product system in question, the areas of the system to be considered in the study (system boundaries), the functions of the system, the unit measurement the impacts are going to be scaled to (functional unit), the impact method used for the study, data

requirements (sources of data, geographical coverage, time, technology, and uncertainties), assumptions, and limitations. These are defined to ensure that the goal of the study is met. The second phase, inventory analysis involves collecting data (both qualitative and quantitative) and performing some calculations to get relevant inputs and outputs, such as resources, energy, and emissions for the study. In the impact assessment phase, the potential environmental impacts are evaluated using results from the inventory analysis and methods defined by the goal and scope phase. The final phase, interpretation is where the results from the inventory and the impact assessment phases are clarified in the form of conclusions and recommendations, usually to decision-makers for the direct applications. LCA is an iterative process hence, all phases are connected (Figure 4). Even though the ISO 14040 is the global standard of performing LCA, there are a wide range of pathways LCA can be made (Cellura et al., 2022). Table 2.6 summarizes the different approaches LCA was performed by the different studies. From the table, all except two clearly stated the goal of their study. Their goals mainly focus on evaluating the environmental impacts associated with their production system, however, some studies also focused on comparing impacts between different pathways within the same system or other systems. An example is the study by Yeboah et al., (2022) where the impacts between biopolymer production from RH were compared to that for RH combustion. Setiawang & Chang, (2021) also compared the impacts of two different pretreatment methods for producing silica. Some studies also focused on evaluating only the impacts associated with their system by a single impact indicator, for example, global warming potential (Nasir Amin et al., 2022). Most studies used a similar framework for their system boundaries, that is, a cradle-to-gate system that includes raw material extraction, transportation, and process/production. Some studies extended their system boundaries to distribution, usage, and end-of-life (Fernando et al., 2022). The major

types of data used in most studies were secondary, usually from literature or LCA databases, such as Ecoinvent, Agribalyse, and European Life Cycle Database (ELCD). In addition to these sources, some studies performed mass and energy balance calculations to generate other inputs for the study (Setiawan & Chiang, 2021; Yeboah et al., 2022). Overall, data availability was not an issue for the studies hence, performing the LCA was not very challenging. The common impact assessment used in the studies was the ReCiPe 2016. However, most studies did not state the type of impact assessment method used in the LCA, and some adopted equations from literature to compute the impacts (Hu et al., 2020). The TRACI was also employed by one of the studies (Setiawan & Chiang, 2021). SimaPro and OpenLCA were the predominant software used for the assessment. Nevertheless, one study used the GreenConcrete LCA tool for the assessment (Nasir Amin et al., 2022). Overall, the results obtained by the studies showed positive environmental performances of RH utilization, highlighting different impact indicators with their respective refernce units. However, the common impact indicator was global warming potential (climate change), with CO_2 as refernce unit. From Table 2.6, SCMs are showing the highest CO_2 emissions, compared to biopolymers, with cement having the highest of all SCMs (182-630 kg) (Hu et al., 2020; Nie et al., 2022); Xia et al., 2023). Even though this value is high, it is a "mitigated result" due to the addition of RH. The original CO_2 emission was around 273-660 kg.

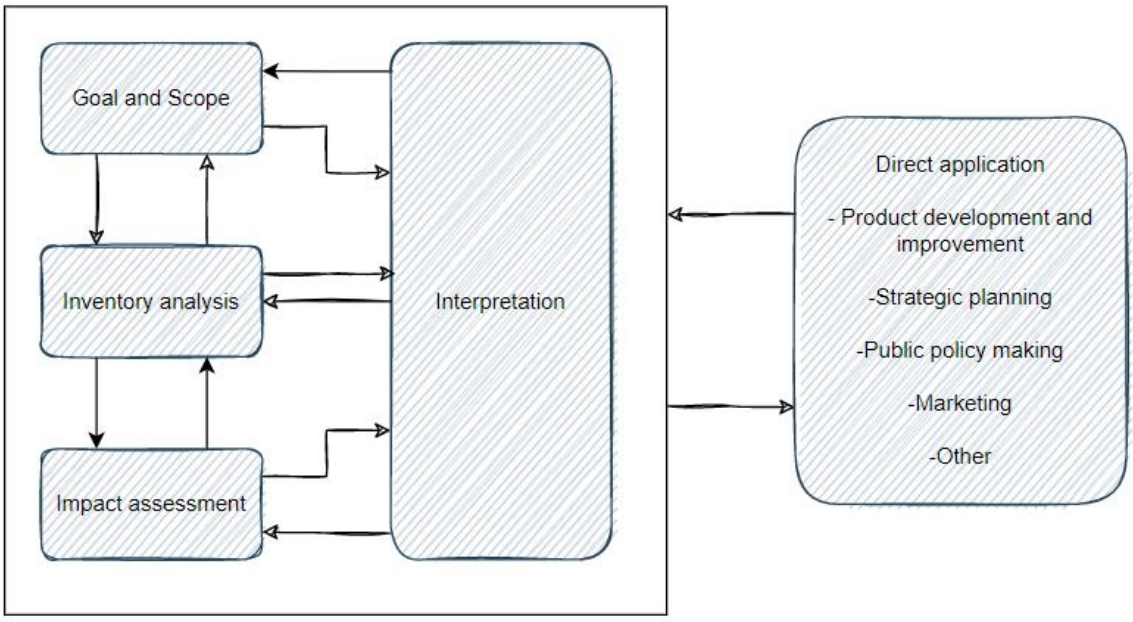

Figure 2.4: Phases of Life Cycle Assessment (ISO, 1997)

Table 2.6: Summary of LCA studies showing their methodologies and results

Reference	Methodology					
	Goal	**Inventory source**	**Impact method**	**Functional unit**	**System boundaries**	**Software**
(Yeboah et al., 2022)	Compare impacts between biopolymer production from RH and RH combustion	• Literature • M/E (SuperPro Designer) • Ecoinvent database	ReCiPe 2016 (M) and (E)	• 1 kg of biopolymer produced • 10 kg of RH combusted	Cellulose extraction, biopolymer production	OpenLCA
(Setiawan & Chiang, 2021)	Compare impacts of silica production between two pretreatment methods	• M/E • Agribalyse v3.0.1 • ELCD v3.2	TRACI v2.1	1 kg of RH used	Silica production	OpenLCA
(Fernando et al., 2022)	Compare the impacts of producing bricks from RH and fly ash versus Portland cement	• Literature • Ecoinvent database	ReCiPe (M) (H)	1 m^2 of brick wall	Raw materials extraction, transportation, brick production, distribution, usage, end of life	SimaPro
(Sampaio et al., 2022)	Analyze the impacts of producing concrete from RH and tire rubber residue (TRR)	• Literature • Ecoinvent database	ReCiPe 2016 (M)	1 lab-scale floor slab (that supports 720 kg load and manages 2.81 kg TRR and 1.38 kg RH)	Raw materials production, transportation, slab assembly, waste management	SimaPro
(Xia et al., 2023)	Investigate the impacts of producing cement from co-	• Literature • Ecoinvent database	N/S	N/S	Raw material production, transportation, cement production	SimaPro

	combustion RH and sewage sludge					
(Nasir Amin et al., 2022)	Estimate the global warming potential of unit, binary and ternary concrete mixes	Literature	N/S	1 unit volume concrete	Raw materials production, transportation	GreenConcrete LCA tool
(Nie et al., 2022)	N/S	Literature	N/S	1 m^3 of cement	N/S	N/S
(C. Liu, Zhang, Liu, Zhu, et al., 2022)	N/S	Literature	N/S	1 m^3 of concrete mixture	Raw material extraction, cement production	N/S
(Hu et al., 2020)	Evaluate the impacts of RH in cement production	Literature	N/S	1 metric ton of RH	Raw material extraction, transportation, cement production	N/S (Equations from literature were used)

Reference	**Results**	
	Impacts of RH utilization	**Conclusion**
(Yeboah et al., 2022)	Global warming potential: 0.0404 – 0.0408 kg CO_2 eq Fine particulate matter formation: 0.0002 – 0.0005 kg PM2.5 eq Terrestrial acidification: 0.0005 – 0.0008 kg SO_2 eq Human health damage: 0.0731 – 0.0745 DALY Ecosystem damage: 0.00000765 – 0.00000774 species.yr	Utilizing RH to produce biopolymers is environmentally sound than combusting it. However, CMC gives the best results compared to the other biopolymers (CN and CA)
(Setiawan & Chiang, 2021)	Eutrophication: 0.02 kg N eq Global warming potential: 3.57 kg CO_2 eq Smog formation: 0.1 kg O_3 Acidification: 0.02 kg SO_2 Respiratory effects: 0.002 kg PM2.5 eq	Producing silica from RH is environmentally sound however, using gluconic acid as pretreatment agent instead of carboxylic acid gives better results

(Fernando et al., 2022)	Global warming potential: 36.9 kg CO_2 eq Particulate matter formation: 0.0553 kg PM2.5 eq Human toxicity: 1.22 kg 1,4 DBC eq	Bricks produced with RH addition shows overall benefit of 1.77 kg 1,4 DBC eq/m^2 in terms of human toxicity impact compared to those with only Portland cement
(Sampaio et al., 2022)	Climate change: ~36 kg CO_2 eq Fine particulate matter: ~0.035 PM2.5 eq Ozone formation: ~0.072 kg NO_x eq Terrestrial acidification: ~0.0765 kg SO_2 eq	Utilizing RH for concrete production reduces its environmental impacts
(Xia et al., 2023)	Acidification potential: ~0.06 kg SO_2 eq Photochemical ozone creation potential: ~0.007 kg C_2H_4 eq Global warming potential: ~182 kg CO_2 eq Fossil fuel depletion: ~800 MJ eq	RH reduces the overall environmental impact when used in cement production. The best outcome is using 50 wt% RHA replacement
(Nasir Amin et al., 2022)	Global warming potential: 293 kg CO_2 /m^3	Utilizing RH and other SCMs as cement is a safe practice and results in the production of green concretes with low GWP and uncompromised strengths
(Nie et al., 2022)	Embodied CO_2 index: ~575 – 630 kg CO_2	RH has high environmental benefits
(C. Liu, Zhang, Liu, Zhu, et al., 2022)	Global warming potential: 282.64 – 427.09 kg CO_2 eq	RH reduces the carbon emissions in concrete and overall improves environmental benefits
(Hu et al., 2020)	CO_2 emission: 317.21 – 346.22 kg CO_2 eq Energy consumption: 1127.46 – 1278.83 MJ eq	RH reduces CO_2 emission and energy consumption in cement production

2.3.2.2 Life Cycle Costing (LCC)

Life Cycle Costing is a technique of sustainability assessment that evaluates all the costs associated with the life cycle (production, use, and end of life) of a product, process, or service (Korpi & Ala-Risku, 2008). LCC can be performed at two levels: internal and external assessments. The internal assessment deals with the costs associated with the technological aspect of the production system, typically by method of a Techno-economic Assessment (TEA) whereas the external assessment deals with the costs associated with the effects the production system has on the environment, typically by method of an Environmental Impact Cost Assessment (EICA). TEA is performed in two parts: a technical analysis that involves the process design, modeling and simulation, and an overall process optimization, and an economic analysis that estimates the production cost and profitability of the production (Allotey et al., 2023). EICA estimates the costs associated with the environmental impacts of the production system by transforming those impacts into monetary units (Yeboah et al., 2022). From the studies reviewed, three performed LCC: Yeboah et al., (2022) performed an environmental impact cost assessment, and Hafid et al., (2021) and Fernando et al., (2022) performed techno-economic assessment. In the environmental impact cost assessment by Yeboah et al., (2022), the environmental impacts of each production system (carboxymethyl cellulose, cellulose acetate, cellulose nitrate, and combustion) was transformed into monetary units using weighting factors from the EcoValue14 impact monetization method. The transformation involved multiplying the impacts by the factors, which are originally in Euros (€) and later converted to US Dollars ($). The weighting factors provided were for nine midpoint impact categories including abiotic resources (€ 0.01136/MJ), global warming potential (€ 0.3315/kg CO_2-eq), photochemical oxidation (€ 2.06/kg NMVOC-eq)), acidification (€ 3.76/kg SO_2-eq), marine eutrophication (€

11.45/kg N), freshwater eutrophication (€ 84.7/kg P), human toxicity (€ 0.3555/kg 1,4 DCB-eq), marine toxicity (€ 1.15/kg 1,4 DCB-eq), and particulate matter formation (€ 34.3/kg PM). The costs were computed in reference to 1 kg of rice husks used and based on the different impacts associated with the production systems, however, the weighting factors for some of these impacts were missing, blurring the actual results. Overall, the costs associated with the biopolymers were significantly smaller than that for combustion. Carboxymethyl cellulose, nevertheless had the lowest cost of approximately $ 0.72 among the all the biopolymers. Fernando et al., (2022) performed a cost analysis on brick production, scoping from raw materials manufacturing, raw material transportation to brick production for two different systems; RH-brick and Portland cement (PC) brick. The analysis was mainly focused on determining the costs involved in the production, without any profitability assessments.The conventional TEA was used to estimate the costs for the various unit processes for both systems, and it was found that producing RH-bricks will have an overall cost of $ 0.22 per brick produced, with the highest contributor being the raw material manufacturing stage, specifically, sodium silicate manufacturing ($ 30.36/m^3) . A cost of $ 0.16 was recorded for a single PC brick produced (27% reduction in cost). Hafid et al., (2021) perfomed a similar analysis on cellulose production from rice husks via two methods (chlorine and nitric acid exctarction methods) using SuperPro Designer software. The analysis was on an annual basis, focuisng on fixed and general equipment, utilities, maintenance, labor, raw materials, and consumables. The analysis revealed a capital investment cost of $ 1.309 million and $ 3.191 million for chlroine and nitric acid extraction method, respectively, and total production cost of $ 13.316 million/year at a plant capacity of 13,190 tons/year, and $34.285 million/year at a capacity of 26,380 tons/year for chlroine and nitric acid extraction method, respectively. Hafid et al., (2021) further perfomed a

profitability assessment at a selling price of $ 5500/ton of cellulose and project lifetime of 15 years. Overall, a higher revenue was generated for the chlorine method, with a Net Present Value (NPV), return on investment and payback time of $ 21.13 million (at a 7% rate of interest), 240.64% and 0.42 years, respectively.

2.3.2.3 Social Life Cycle Assessment (SLCA)

Social life cycle assessment is the branch of sustainability assessment that evaluates the sociological impacts of a product, process, or a service. It follows a similar approach to the conventional life cycle assessment, except that the functional units and impact indicators are different. The functional units used in SLCA are not directly expressed in terms of processing units (Allotey et al., 2023). The common impact indicators used in SLCA are human rights, working conditions, health and safety, cultural heritage, governance, and socio-economic repercussions, and these are generally linked to five main stakeholders, namely worker, consumer, local community, society, and value chain actors (UNEP/SETAC, 2013). Social life cycle assessment is under gradual development yet, a very important assessment of sustainability assessment, mainly because it helps recognize damages that may occur to businesses when they do not meet stakeholder demands (reputational risks) and alleviate them. Nevertheless, none of the studies performed SLCA.

2.4 Conclusion and Recommendations

This study reviews the different non-energy utilization pathways of rice husks by analyzing the different processes involved in each production system and assessing their sustainability, in terms of life cycle assessment, life cycle costing, and social life cycle assessment. The review showed that rice husks have high non-energy utilization potential and have been used in different fields and for different applications including medicine (xylo-oligosaccharide, scaffolds,

bioactive peptides, nano silica), construction (cement, concrete, bricks, silica), food (biopolymers, aerogel), wastewater treatment (adsorbents, coagulant, demulsifier, bio-composites, zeolite), electronics (capacitors, carbon nanotubes, sensors), agriculture (biochar, fertilizer, humic acid) and biochemical industry (biocatalysts, molecular sieve, α-amylase). Overall, the authors recorded positive results in terms of improvements in their products, reduction in production costs, and ease of production. However, there were limited studies on the sustainability of the various utilization pathways. Less than 10% of the total articles reviewed conducted a sustainability assessment, with no study on social life cycle assessment. Moreover, the few studies on the sustainability assessments (LCA and LCC) were incomprehensive, as only limited relationships between the two assessments were established. To justify the use of rice husks for non-energy applications, more studies should be conducted on the sustainability of the production systems for the said applications.

References

Aboelfetoh, E. F., Zain Elabedien, M. E., & Ebeid, E.-Z. M. (2023). In situ anchoring of iron and zinc oxides nanoparticles onto rice husk cellulose for efficient wastewater remediation. *International Journal of Biological Macromolecules*, *233*, 123562. https://doi.org/10.1016/j.ijbiomac.2023.123562

AlBiajawi, M. I., Embong, R., & Muthusamy, K. (2022). An overview of the utilization and method for improving pozzolanic performance of agricultural and industrial wastes in concrete. *Materials Today: Proceedings*, *48*, 778–783. https://doi.org/10.1016/j.matpr.2021.02.260

Alkhaly, Y. R., Abdullah, Husaini, & Hasan, M. (2022). Characteristics of reactive powder concrete comprising synthesized rice husk ash and quartzite powder. *Journal of Cleaner Production*, *375*, 134154. https://doi.org/10.1016/j.jclepro.2022.134154

Allotey, D. K., Kwofie, E. M., Adewale, P., Lam, E., & Ngadi, M. (2023). Life cycle sustainability assessment outlook of plant-based protein processing and product formulations. *Sustainable Production and Consumption*, *36*, 108–125. https://doi.org/10.1016/j.spc.2022.12.021

Alshahrani, H., & Arun Prakash, V. R. (2022). Thermal, mechanical and barrier properties of rice husk ash biosilica toughened epoxy biocomposite coating for structural application. *Progress in Organic Coatings*, *172*, 107080. https://doi.org/10.1016/j.porgcoat.2022.107080

Anto, G., Athira, K., Nair, N. A., Sai, T. Y., Yadav, A. L., & Sairam, V. (2022). Mechanical properties and durability of ternary blended cement paste containing rice husk ash and nano silica. *Construction and Building Materials*, *342*, 127732. https://doi.org/10.1016/j.conbuildmat.2022.127732

Arkhipova, E. A., Novotortsev, R. Yu., Ivanov, A. S., Maslakov, K. I., & Savilov, S. V. (2022). Rice husk-derived activated carbon electrode in redox-active electrolyte – New approach for enhancing supercapacitor performance. *Journal of Energy Storage*, *55*, 105699. https://doi.org/10.1016/j.est.2022.105699

Arumugam, H., Krishnasamy, B., Perumal, G., A, A. D., Abdul Aleem, M. I., & Muthukaruppan, A. (2021). Bio-composites of rice husk and saw dust reinforced bio-benzoxazine/epoxy hybridized matrices: Thermal, mechanical, electrical resistance and acoustic absorption properties. *Construction and Building Materials*, *312*, 125381. https://doi.org/10.1016/j.conbuildmat.2021.125381

Arvanitoyannis, I. S. (Ed.). (2008). *Waste management for the food industries*. Elsevier Acad. Press.

Balaji, J., Nataraja, M. M., & Rajesh, A. (2022). Experimental investigation on mechanical properties of polymer composites reinforced with aluminium nitride & rice husk. *Materials Today: Proceedings*, *52*, 1781–1787. https://doi.org/10.1016/j.matpr.2021.11.445

Balasubramanian, S., & Venkatachalam, P. (2023). Valorization of rice husk agricultural waste through lignin extraction using acidic deep eutectic solvent. *Biomass and Bioenergy*, *173*, 106776. https://doi.org/10.1016/j.biombioe.2023.106776

Bian, R., Shi, W., Luo, J., Li, W., Wang, Y., Joseph, S., Gould, H., Zheng, J., Zhang, X., Liu, X., Wang, Y., Liu, X., Shan, S., Li, L., & Pan, G. (2022). Copyrolysis of food waste and rice husk to biochar to create a sustainable resource for soil amendment: A pilot-scale case study in Jinhua, China. *Journal of Cleaner Production*, *347*, 131269. https://doi.org/10.1016/j.jclepro.2022.131269

Bilo, F., Pandini, S., Sartore, L., Depero, L. E., Gargiulo, G., Bonassi, A., Federici, S., & Bontempi, E. (2018). A sustainable bioplastic obtained from rice straw. *Journal of Cleaner Production*, *200*, 357–368. https://doi.org/10.1016/j.jclepro.2018.07.252

Cellura, M., Cusenza, M. A., Longo, S., Luu, L. Q., & Skurk, T. (2022). Life Cycle Environmental Impacts and Health Effects of Protein-Rich Food as Meat Alternatives: A Review. *Sustainability*, *14*(2), 979. https://doi.org/10.3390/su14020979

Chaudhari, P. R., Tamrakar, N., Singh, L., Tandon, A., & Sharma, D. (2018). *Rice nutritional and medicinal properties: A review article*. 7.

Chen, R., Cai, G., Dong, X., Pu, S., Dai, X., & Duan, W. (2022). Green utilization of modified biomass by-product rice husk ash: A novel eco-friendly binder for stabilizing waste clay as road material. *Journal of Cleaner Production*, *376*, 134303. https://doi.org/10.1016/j.jclepro.2022.134303

Chen, R., Liu, Y., Weng, J., Huang, H., Gao, X., Wang, Z., & Liu, J. (2023). Microporous melamine-formaldehyde networks loaded on rice husks for dynamic removal of organic micropollutants. *Environmental Pollution*, *322*, 121200. https://doi.org/10.1016/j.envpol.2023.121200

Chen, Y., Li, H., Liu, J., Liu, N., Yang, J., Zhang, Y., Guo, Q., Wang, F., & Liu, Q. (2022). Efficient utilization of silanol group in rice husk to promote the synthesis of Ni-

phyllosilicate for CO2 methanation. *International Journal of Hydrogen Energy*, *47*(49), 21173–21181. https://doi.org/10.1016/j.ijhydene.2022.04.249

da Silva Nuernberg, N. B., Niero, D. F., & Bernardin, A. M. (2021). Valorization of rice husk ash and aluminum anodizing sludge as precursors for the synthesis of geopolymers. *Journal of Cleaner Production*, *298*, 126770. https://doi.org/10.1016/j.jclepro.2021.126770

Dada, A. O., Inyinbor, A. A., Tokula, B. E., Bello, O. S., & Pal, U. (2022). Preparation and characterization of rice husk activated carbon-supported zinc oxide nanocomposite (RHAC-ZnO-NC). *Heliyon*, *8*(8), e10167. https://doi.org/10.1016/j.heliyon.2022.e10167

Dadebo, D., Ibrahim, M. G., Fujii, M., & Nasr, M. (2023). Sequential treatment of surfactant-laden wastewater using low-cost rice husk ash coagulant and activated carbon: Modeling, optimization, characterization, and techno-economic analysis. *Bioresource Technology Reports*, *22*, 101464. https://doi.org/10.1016/j.biteb.2023.101464

De Oliveira, J. P., Bruni, G. P., El Halal, S. L. M., Bertoldi, F. C., Dias, A. R. G., & Zavareze, E. D. R. (2019). Cellulose nanocrystals from rice and oat husks and their application in aerogels for food packaging. *International Journal of Biological Macromolecules*, *124*, 175–184. https://doi.org/10.1016/j.ijbiomac.2018.11.205

Dhinasekaran, D., Raj, R., Rajendran, A. R., Purushothaman, B., Subramanian, B., Prakasarao, A., & Singaravelu, G. (2020). Chitosan mediated 5-Fluorouracil functionalized silica nanoparticle from rice husk for anticancer activity. *International Journal of Biological Macromolecules*, *156*, 969–980. https://doi.org/10.1016/j.ijbiomac.2020.04.098

Di, J., Jamakanga, R., Chen, Q., Li, J., Gai, X., Li, Y., Yang, R., & Ma, Q. (2021). Degradation of Rhodamine B by activation of peroxymonosulfate using Co3O4-rice husk ash composites. *Science of The Total Environment*, *784*, 147258. https://doi.org/10.1016/j.scitotenv.2021.147258

Dixit, A. (2021). A study on the physical and chemical parameters of industrial by-products ashes useful in making sustainable concrete. *Materials Today: Proceedings*, *43*, 42–50. https://doi.org/10.1016/j.matpr.2020.11.203

Food and Agriculture Organization of the United Nations. (1997). FAOSTAT statistical database. Retrieved March 19, 2023, from https://www.fao.org/faostat/en/#data/QCL

Fernando, S., Gunasekara, C., Law, D. W., Nasvi, M. C. M., Setunge, S., & Dissanayake, R. (2023). Assessment of long term durability properties of blended fly ash-Rice husk ash

alkali activated concrete. *Construction and Building Materials*, *369*, 130449. https://doi.org/10.1016/j.conbuildmat.2023.130449

Fernando, S., Gunasekara, C., Law, D. W., Nasvi, M. C. M., Setunge, S., Dissanayake, R., & Robert, D. (2022). Environmental evaluation and economic analysis of fly ash-rice husk ash blended alkali-activated bricks. *Environmental Impact Assessment Review*, *95*, 106784. https://doi.org/10.1016/j.eiar.2022.106784

Gaikwad, M. S., & Balomajumder, C. (2023). Multicomponent isotherm modeling of hexavalent chromium and fluoride ions simultaneous removal using rice husk derived activated carbon (RHDAC) electrode. *Journal of the Indian Chemical Society*, *100*(2), 100900. https://doi.org/10.1016/j.jics.2023.100900

García-González, C. A., Alnaief, M., & Smirnova, I. (2011). Polysaccharide-based aerogels—Promising biodegradable carriers for drug delivery systems. *Carbohydrate Polymers*, *86*(4), 1425–1438. https://doi.org/10.1016/j.carbpol.2011.06.066

Gautam, N., Kate, G., & Chaurasia, A. (2021). Upgrading of rice husk char obtained by pyrolysis process to amorphous silica and activated carbon. *Materials Today: Proceedings*, *39*, 1382–1385. https://doi.org/10.1016/j.matpr.2020.04.859

Gupta, H., Kumar, H., Kumar, M., Gehlaut, A. K., Gaur, A., Sachan, S., & Park, J.-W. (2019). Synthesis of biodegradable films obtained from rice husk and sugarcane bagasse to be used as food packaging material. *Environmental Engineering Research*, *25*(4), 506–514. https://doi.org/10.4491/eer.2019.191

Hafid, H. S., Omar, F. N., Zhu, J., & Wakisaka, M. (2021). Enhanced crystallinity and thermal properties of cellulose from rice husk using acid hydrolysis treatment. *Carbohydrate Polymers*, *260*, 117789. https://doi.org/10.1016/j.carbpol.2021.117789

Haider, J. B., Haque, Md. I., Hoque, M., Hossen, Md. M., Mottakin, M., Khaleque, Md. A., Johir, M. A. H., Zhou, J. L., Ahmed, M. B., & Zargar, M. (2022). Efficient extraction of silica from openly burned rice husk ash as adsorbent for dye removal. *Journal of Cleaner Production*, *380*, 135121. https://doi.org/10.1016/j.jclepro.2022.135121

Hayatun, A., Jannah, M., Ahmad, A., & Taba, P. (2020). Synthetic Bioplastic Film from Rice Husk Cellulose. *Journal of Physics: Conference Series*, *1463*, 012009. https://doi.org/10.1088/1742-6596/1463/1/012009

Hidalgo-Salazar, M. A., & Salinas, E. (2019). Mechanical, thermal, viscoelastic performance and product application of PP- rice husk Colombian biocomposites. *Composites Part B: Engineering*, *176*, 107135. https://doi.org/10.1016/j.compositesb.2019.107135

Hu, L., He, Z., & Zhang, S. (2020). Sustainable use of rice husk ash in cement-based materials: Environmental evaluation and performance improvement. *Journal of Cleaner Production*, *264*, 121744. https://doi.org/10.1016/j.jclepro.2020.121744

ISO, 2006. Environmental management — Life Cycle Assessment — Requirements and Guidelines. International Standard, Switzerland, p. 54

Kadam, K. L., Forrest, L. H., & Jacobson, W. A. (2000). Rice straw as a lignocellulosic resource: Collection, processing, transportation, and environmental aspects. *Biomass and Bioenergy*, 21.

Kamran, U., Lee, S.-Y., Rhee, K. Y., & Park, S.-J. (2023). Rice husk valorization into sustainable Ni@TiO2/biochar nanocomposite for highly selective Pb (II) ions removal from an aqueous media. *Chemosphere*, *323*, 138210. https://doi.org/10.1016/j.chemosphere.2023.138210

Kamseu, E., Akono, A.-T., Rosa, R., Mariani, A., & Leonelli, C. (2022). Valorization of marble powder wastes using rice husk ash to yield enhanced-performance inorganic polymer cements: Phase evolution, microstructure, and micromechanics analyses. *Cleaner Engineering and Technology*, *8*, 100461. https://doi.org/10.1016/j.clet.2022.100461

Kang, S.-H., Kwon, Y.-H., Hong, S.-G., Chun, S., & Moon, J. (2019). Hydrated lime activation on byproducts for eco-friendly production of structural mortars. *Journal of Cleaner Production*, *231*, 1389–1398. https://doi.org/10.1016/j.jclepro.2019.05.313

Kannur, B., & Chore, H. S. (2023). Low-fines self-consolidating concrete using rice husk ash for road pavement: An environment-friendly and sustainable approach. *Construction and Building Materials*, *365*, 130036. https://doi.org/10.1016/j.conbuildmat.2022.130036

Kavitha, D., Chandrasekaran Murugavel, S., & Thenmozhi, S. (2021). Flame retarding cardanol based novolac-epoxy/rice husk composites. *Materials Chemistry and Physics*, *263*, 124225. https://doi.org/10.1016/j.matchemphys.2021.124225

Kenawy, E.-R., Seggiani, M., Hosny, A., Rashad, M., Cinelli, P., Saad-Allah, K. M., El-Sharnouby, M., Shendy, S., & Azaam, M. M. (2021). Superabsorbent composites based on rice husk for agricultural applications: Swelling behavior, biodegradability in soil and drought alleviation. *Journal of Saudi Chemical Society*, *25*(6), 101254. https://doi.org/10.1016/j.jscs.2021.101254

Ketov, A., Rudakova, L., Vaisman, I., Ketov, I., Haritonovs, V., & Sahmenko, G. (2021). Recycling of rice husks ash for the preparation of resistant, lightweight and environment-

friendly fired bricks. *Construction and Building Materials*, *302*, 124385. https://doi.org/10.1016/j.conbuildmat.2021.124385

Khan, N., Chowdhary, P., Ahmad, A., Shekher Giri, B., & Chaturvedi, P. (2020). Hydrothermal liquefaction of rice husk and cow dung in Mixed-Bed-Rotating Pyrolyzer and application of biochar for dye removal. *Bioresource Technology*, *309*, 123294. https://doi.org/10.1016/j.biortech.2020.123294

Khat-udomkiri, N., Toejing, P., Sirilun, S., Chaiyasut, C., & Lailerd, N. (2020). Antihyperglycemic effect of rice husk derived xylooligosaccharides in high-fat diet and low-dose streptozotocin-induced type 2 diabetic rat model. *Food Science & Nutrition*, *8*(1), 428–444. https://doi.org/10.1002/fsn3.1327

Korpi, E., & Ala-Risku, T. (2008). Life cycle costing: A review of published case studies. *Managerial Auditing Journal*, *23*(3), 240–261. https://doi.org/10.1108/02686900810857703

Kumar, A., Roy, A., Priyadarshinee, R., Sengupta, B., Malaviya, A., Dasguptamandal, D., & Mandal, T. (2017). Economic and sustainable management of wastes from rice industry: Combating the potential threats. *Environmental Science and Pollution Research*, *24*(34), 26279–26296. https://doi.org/10.1007/s11356-017-0293-7

Leal Da Silva, E., Torres, M., Portugau, P., & Cuña, A. (2021). High surface activated carbon obtained from Uruguayan rice husk wastes for supercapacitor electrode applications: Correlation between physicochemical and electrochemical properties. *Journal of Energy Storage*, *44*, 103494. https://doi.org/10.1016/j.est.2021.103494

Liberati, A., Altman, D. G., Tetzlaff, J., Mulrow, C., Gotzsche, P. C., Ioannidis, J. P. A., Clarke, M., Devereaux, P. J., Kleijnen, J., & Moher, D. (2009). The PRISMA statement for reporting systematic reviews and meta-analyses of studies that evaluate healthcare interventions: Explanation and elaboration. *BMJ*, *339*(jul21 1), b2700–b2700. https://doi.org/10.1136/bmj.b2700

Liu, C., Zhang, W., Liu, H., Lin, X., & Zhang, R. (2022). A compressive strength prediction model based on the hydration reaction of cement paste by rice husk ash. *Construction and Building Materials*, *340*, 127841. https://doi.org/10.1016/j.conbuildmat.2022.127841

Liu, C., Zhang, W., Liu, H., Zhu, C., Wu, Y., He, C., & Wang, Z. (2022). Recycled aggregate concrete with the incorporation of rice husk ash: Mechanical properties and microstructure. *Construction and Building Materials*, *351*, 128934. https://doi.org/10.1016/j.conbuildmat.2022.128934

Liu, Y., Tan, H., Tan, Z., & Cheng, X. (2022). Rice husk derived capacitive carbon prepared by one-step molten salt carbonization for supercapacitors. *Journal of Energy Storage*, *55*, 105437. https://doi.org/10.1016/j.est.2022.105437

Mahdavi Fard, A., Askari, S., Afshar Ebrahimi, A., & Heydarinasab, A. (2022). Green synthesis of SAPO-34 molecular sieve using rice husk ash as a silica source: Evaluation of synthesis and catalytic performance parameters in methanol-to-olefin reaction. *Microporous and Mesoporous Materials*, *341*, 112037. https://doi.org/10.1016/j.micromeso.2022.112037

Manubothula, S., & Gorre, M. (2022). Influence of rice husk ash on compressive strength of an aerated concrete. *Materials Today: Proceedings*, *65*, 1982–1986. https://doi.org/10.1016/j.matpr.2022.05.320

Meraz, M. M., Mim, N. J., Mehedi, Md. T., Noroozinejad Farsangi, E., Arafin, Sk. A. K., Shrestha, R. K., & Hussain, Md. S. (2023). On the utilization of rice husk ash in high-performance fiber reinforced concrete (HPFRC) to reduce silica fume content. *Construction and Building Materials*, *369*, 130576. https://doi.org/10.1016/j.conbuildmat.2023.130576

Mohd Esa, N., & Ling, T. B. (2016). By-products of Rice Processing: An Overview of Health Benefits and Applications. *Rice Research: Open Access*, *4*(1). https://doi.org/10.4172/jrr.1000107

Moogi, S., Lee, J., Jae, J., Sonne, C., Rinklebe, J., Heui Kim, D., Shiung Lam, S., Loke Show, P., & Park, Y.-K. (2021). Valorization of rice husk to aromatics via thermocatalytic conversion in the presence of decomposed methane. *Chemical Engineering Journal*, *417*, 129264. https://doi.org/10.1016/j.cej.2021.129264

Moogi, S., Lee, J., Rhee, G. H., Jae, J., Kim, D. H., Jung, S.-C., Chen, W.-H., & Park, Y.-K. (2022). The effect of NaOH treatment of rice husk on its catalytic fast pyrolysis under decomposed methane for the production of aromatics. *Catalysis Today*, *397–399*, 272–277. https://doi.org/10.1016/j.cattod.2021.09.014

Moraes, C. A., Fernandes, I. J., Calheiro, D., Kieling, A. G., Brehm, F. A., Rigon, M. R., Berwanger Filho, J. A., Schneider, I. A., & Osorio, E. (2014). Review of the rice production cycle: By-products and the main applications focusing on rice husk combustion and ash recycling. *Waste Management & Research: The Journal for a Sustainable Circular Economy*, *32*(11), 1034–1048. https://doi.org/10.1177/0734242X14557379

Mortada, W. I., Nabieh, K. A., Helmy, T. E., & Abou El-Reash, Y. G. (2022). Microwave-assisted synthesis of MCM-41 composite with rice husk and its functionalization by

dithizone for preconcentration of some metal ions from water and food samples. *Journal of Food Composition and Analysis*, *106*, 104352. https://doi.org/10.1016/j.jfca.2021.104352

Mozafari, R., Gheisvandi, Z., & Ghadermazi, M. (2022). Covalently bonded sulfonic acid onto the surface of magnetic nanosilica obtained from rice husk: CoFe2O4@RH-Pr-SO3H as novel acid catalyst for synthesis of octahydroquinazolinone and 3,4-dihydropyrimidinone. *Journal of Molecular Structure*, *1265*, 133421. https://doi.org/10.1016/j.molstruc.2022.133421

Muthukrishnan, S., Gupta, S., & Kua, H. W. (2019). Application of rice husk biochar and thermally treated low silica rice husk ash to improve physical properties of cement mortar. *Theoretical and Applied Fracture Mechanics*, *104*, 102376. https://doi.org/10.1016/j.tafmec.2019.102376

Na Chat, N., Sangsuradet, S., Tobarameekul, P., & Worathanakul, P. (2022). Modified hierarchical zeolite X derived from riceberry rice husk for propionic acid adsorption. *Materials Chemistry and Physics*, *282*, 125933. https://doi.org/10.1016/j.matchemphys.2022.125933

Nana, A., Epey, N., Rodrique, K. C., Deutou, J. G. N., Djobo, J. N. Y., Tomé, S., Alomayri, T. S., Ngouné, J., Kamseu, E., & Leonelli, C. (2021). Mechanical strength and microstructure of metakaolin/volcanic ash-based geopolymer composites reinforced with reactive silica from rice husk ash (RHA). *Materialia*, *16*, 101083. https://doi.org/10.1016/j.mtla.2021.101083

Nasir Amin, M., Ur Rehman, K., Shahzada, K., Khan, K., Wahab, N., & Abdulalim Alabdullah, A. (2022). Mechanical and microstructure performance and global warming potential of blended concrete containing rice husk ash and silica fume. *Construction and Building Materials*, *346*, 128470. https://doi.org/10.1016/j.conbuildmat.2022.128470

Nayak, P. P., Nandi, S., Bhunia, K., & Datta, A. K. (2023). Modelling the extraction process parameters of amorphous silica-rich rice husk ash using hybrid RSM−BPANN−MOGA optimization technique. *Materials Chemistry and Physics*, *293*, 126944. https://doi.org/10.1016/j.matchemphys.2022.126944

Nie, Y., Lu, J., Liu, Z., Meng, D., He, Z., & Shi, J. (2022). Mechanical, water resistance and environmental benefits of magnesium oxychloride cement incorporating rice husk ash. *Science of The Total Environment*, *849*, 157871. https://doi.org/10.1016/j.scitotenv.2022.157871

Nikhade, A., & Nag, A. (2022). Effective utilization of sugarcane bagasse Ash, rice husk Ash& Metakaolin in concrete. *Materials Today: Proceedings*, *62*, 3658–3664. https://doi.org/10.1016/j.matpr.2022.04.422

Novitasari, I., Rahayu, D. U. C., & Krisnandi, Y. K. (2019). Effect of rice husk pretreatment on the conversion of cellulose to levulinic acid over the Mn_3O_4/ZSM-5 catalyst. *IOP Conference Series: Materials Science and Engineering*, *496*, 012014. https://doi.org/10.1088/1757-899X/496/1/012014

Pham, T. H., Chu, T. T. H., Nguyen, D. K., Le, T. K. O., Obaid, S. A., Alharbi, S. A., Kim, J., & Nguyen, M. V. (2022). Alginate-modified biochar derived from rice husk waste for improvement uptake performance of lead in wastewater. *Chemosphere*, *307*, 135956. https://doi.org/10.1016/j.chemosphere.2022.135956

Phan, K. A., Phihusut, D., & Tuntiwiwattanapun, N. (2022). Preparation of rice husk hydrochar as an atrazine adsorbent: Optimization, characterization, and adsorption mechanisms. *Journal of Environmental Chemical Engineering*, *10*(3), 107575. https://doi.org/10.1016/j.jece.2022.107575

Phouthavong, V., Hagio, T., Park, J.-H., Nijpanich, S., Srihirunthanon, T., Chantanurak, N., Duangkhai, K., Rujiravanit, R., Chounlamany, V., Phomkeona, K., Kong, L., Li, L., & Ichino, R. (2023). Utilization of agricultural waste to herbicide removal: Magnetic BEA zeolite adsorbents prepared by dry-gel conversion using rice husk ash–derived SiO2 for paraquat removal. *Arabian Journal of Chemistry*, *16*(8), 104959. https://doi.org/10.1016/j.arabjc.2023.104959

Pimentel Tinoco, M., Gouvêa, L., De Cássia Magalhães Martins, K., Dias Toledo Filho, R., & Aurelio Mendoza Reales, O. (2023). The use of rice husk particles to adjust the rheological properties of 3D printable cementitious composites through water sorption. *Construction and Building Materials*, *365*, 130046. https://doi.org/10.1016/j.conbuildmat.2022.130046

Plando, F. R. P., Gili, M. B. Z., & Maquiling, J. T. (2023). Microstructural characterizations and radiation shielding quantities of rice husk ash-based self-compacting concrete and its precursors. *Radiation Physics and Chemistry*, *208*, 110916. https://doi.org/10.1016/j.radphyschem.2023.110916

Rashid, S., & Dutta, H. (2021). Physicochemical characterization of carboxymethyl cellulose from differently sized rice husks and application as cake additive. *LWT*, 112630. https://doi.org/10.1016/j.lwt.2021.112630

Rathi, A., Gupta, N., Dhruw, V., Beliya, E., Tiwari, S., Paul, J. S., & Jadhav, S. K. (2022). Valorization of rice milled by-products (rice husk and de-oiled rice bran) into α-amylase

with its process optimization, partial purification and kinetic study. *Process Biochemistry*, *120*, 101–113. https://doi.org/10.1016/j.procbio.2022.06.006

Reaño, R. L. (2020). Assessment of environmental impact and energy performance of rice husk utilization in various biohydrogen production pathways. *Bioresource Technology*, *299*, 122590. https://doi.org/10.1016/j.biortech.2019.122590

Safdar Raza, S., Ali, B., Noman, M., Fahad, M., & Mohamed Elhadi, K. (2022). Mechanical properties, flexural behavior, and chloride permeability of high-performance steel fiber-reinforced concrete (SFRC) modified with rice husk ash and micro-silica. *Construction and Building Materials*, *359*, 129520. https://doi.org/10.1016/j.conbuildmat.2022.129520

Sala, S., Ciuffo, B., & Nijkamp, P. (2015). A systemic framework for sustainability assessment. *Ecological Economics*, *119*, 314–325. https://doi.org/10.1016/j.ecolecon.2015.09.015

Sampaio, D. O. A., Tashima, M. M., Costa, D., Quinteiro, P., Dias, A. C., & Akasaki, J. L. (2022). Evaluation of the environmental performance of rice husk ash and tire rubber residues incorporated in concrete slabs. *Construction and Building Materials*, *357*, 129332. https://doi.org/10.1016/j.conbuildmat.2022.129332

Setiawan, W. K., & Chiang, K.-Y. (2021). Eco-friendly rice husk pre-treatment for preparing biogenic silica: Gluconic acid and citric acid comparative study. *Chemosphere*, *279*, 130541. https://doi.org/10.1016/j.chemosphere.2021.130541

Shetye, S., Pratihary, A., Shenoy, D., Kurian, S., Gauns, M., Uskaikar, H., Naik, B., Nandakumar, K., & Borker, S. (2023). Rice husk as a potential source of silicate to oceanic phytoplankton. *Science of The Total Environment*, *879*, 162941. https://doi.org/10.1016/j.scitotenv.2023.162941

Shi, J., Fan, X., Tsang, D. C. W., Wang, F., Shen, Z., Hou, D., & Alessi, D. S. (2019). Removal of lead by rice husk biochars produced at different temperatures and implications for their environmental utilizations. *Chemosphere*, *235*, 825–831. https://doi.org/10.1016/j.chemosphere.2019.06.237

Tabassam, N., Mutahir, S., Khan, M. A., Khan, I. U., Habiba, U., & Refat, M. S. (2022). Facile synthesis of cinnamic acid sensitized rice husk biochar for removal of organic dyes from wastewaters: Batch experimental and theoretical studies. *Materials Chemistry and Physics*, *288*, 126327. https://doi.org/10.1016/j.matchemphys.2022.126327

Tagne, R. F. T., Ndifor-Angwagor, N. G., Temgoua, R. C. T., Tchuifon, D. R. T., Vintila, T., Ngueabouo, A. S., & Anagho, S. G. (2021). Development of an electroanalytical method

using activated rice husk-derived carbon for the detection of a paraquat herbicide. *Carbon Trends*, *4*, 100060. https://doi.org/10.1016/j.cartre.2021.100060

Taiwo, L. A., Obianyo, I. I., Omoniyi, A. O., Onwualu, A. P., Soboyejo, A. B. O., & Amu, O. O. (2022). Mechanical behaviour of composite produced with quarry dust and rice husk ash for sustainable building applications. *Case Studies in Construction Materials*, *17*, e01157. https://doi.org/10.1016/j.cscm.2022.e01157

Tan, B. L., & Norhaizan, M. E. (2020). *Rice By-products: Phytochemicals and Food Products Application*. Springer International Publishing. https://doi.org/10.1007/978-3-030-46153-9

Tan, K. L., Lim, K. Y., Chow, Y. N., Foo, K. Y., Liew, Y. S., Desa, S. M., Yahaya, N. K. E. M., & Noh, M. N. M. (2022). Facile preparation of rice husk-derived green coagulant via water-based heatless and salt-free technique for the effective treatment of urban and agricultural runoffs. *Industrial Crops and Products*, *178*, 114547. https://doi.org/10.1016/j.indcrop.2022.114547

Udoye, N. E., Nnamba, O. J., Fayomi, O. S. I., Inegbenebor, A. O., & Jolayemi, K. J. (2021). Analysis on mechanical properties of AA6061/Rice husk ash composites produced through stir casting technique. *Materials Today: Proceedings*, *43*, 1415–1420. https://doi.org/10.1016/j.matpr.2020.09.178

UNEP/SETAC, 2013. In: Initiative, L.C. (Ed.), The Methodological Sheets for Subcategories in Social Life Cycle Assessment (S-LCA). UNEP and SETAC, Sweden, p. 150

Unglaube, F., Schlapp, J., Quade, A., Schäfer, J., & Mejía, E. (2022). Highly active heterogeneous hydrogenation catalysts prepared from cobalt complexes and rice husk waste. *Catalysis Science & Technology*, *12*(10), 3123–3136. https://doi.org/10.1039/D2CY00005A

Uysal, M., Aygörmez, Y., Canpolat, O., Cosgun, T., & Faruk Kuranlı, Ö. (2022). Investigation of using waste marble powder, brick powder, ceramic powder, glass powder, and rice husk ash as eco-friendly aggregate in sustainable red mud-metakaolin based geopolymer composites. *Construction and Building Materials*, *361*, 129718. https://doi.org/10.1016/j.conbuildmat.2022.129718

Wahab, R. A. A., Zaid, M. H. M., Matori, K. A., Kamari, H. M., Sarmani, A. R., Loh, Z. W., Cheong, W. M., Honda, S., & Iwamoto, Y. (2022). Tunable white emission from scintillated zinc borosilicate doped with dysprosium oxide and incorporated with bio-silica from rice husk. *Optik*, *270*, 170082. https://doi.org/10.1016/j.ijleo.2022.170082

Wang, H., Zhu, S., Dai, Z., Li, X., & Zhou, T. (2023). Selective synthesis of large diameter single-walled carbon nanotubes on rice husk-derived catalysts. *Journal of Environmental Chemical Engineering*, *11*(2), 109261. https://doi.org/10.1016/j.jece.2022.109261

Wu, Z., Guo, X., Meng, Z., Yao, C., Deng, Y., Zhou, H., & Wang, Y. (2022). Nickel/porous carbon derived from rice husk with high microwave absorption performance. *Journal of Alloys and Compounds*, *925*, 166732. https://doi.org/10.1016/j.jallcom.2022.166732

Xia, Y., Liu, M., Zhao, Y., Guo, J., Chi, X., Du, J., Du, D., & Shi, D. (2023). Hydration mechanism and environmental impacts of blended cements containing co-combustion ash of sewage sludge and rice husk: Compared with blended cements containing sewage sludge ash. *Science of The Total Environment*, *864*, 161116. https://doi.org/10.1016/j.scitotenv.2022.161116

Xiao, Y., Tong, L., Che, H., Guo, Q., & Pan, H. (2022). Experimental studies on compressive and tensile strength of cement-stabilized soil reinforced with rice husks and polypropylene fibers. *Construction and Building Materials*, *344*, 128242. https://doi.org/10.1016/j.conbuildmat.2022.128242

Xue, L., Chen, N., Zhao, J., Yang, C., & Feng, C. (2022). Rice husk-intensified cathode driving bioelectrochemical reactor for remediating nitrate-contaminated groundwater. *Science of The Total Environment*, *837*, 155917. https://doi.org/10.1016/j.scitotenv.2022.155917

Yadav, M. K., Pandey, V., Mohanta, K., & Singh, V. K. (2022). A low-cost approach to develop silica doped Tricalcium Phosphate (TCP) scaffold by valorizing animal bone waste and rice husk for tissue engineering applications. *Ceramics International*, *48*(17), 25335–25345. https://doi.org/10.1016/j.ceramint.2022.05.207

Yan, K., Lan, H., Li, Q., Ge, D., & Li, Y. (2022). Optimum utilization of recycled aggregate and rice husk ash stabilized base material. *Construction and Building Materials*, *348*, 128627. https://doi.org/10.1016/j.conbuildmat.2022.128627

Yeboah, W. O., Kwofie, E. M., & Wang, D. (2022). Circular bioeconomy potential of rice husk as a bioplastic resource: Techno-environmental assessment. *Bioresource Technology Reports*, *20*, 101248. https://doi.org/10.1016/j.biteb.2022.101248

Yuan, H., Ye, F., Ai, G., Zeng, G., Chen, L., Shen, L., Yang, Y., Feng, X., Zhang, Z., & Mi, Y. (2022). Preparation of an environmentally friendly demulsifier using waste rice husk as raw materials for oil–water emulsion separation. *Journal of Molecular Liquids*, *367*, 120497. https://doi.org/10.1016/j.molliq.2022.120497

Zakaria, S. M., Idris, A., Chandrasekaram, K., & Alias, Y. (2020). Efficiency of bronsted acidic ionic liquids in the dissolution and depolymerization of lignin from rice husk into high value-added products. *Industrial Crops and Products, 157*, 112885. https://doi.org/10.1016/j.indcrop.2020.112885

Zhao, P., Huang, Z., Wang, P., & Wang, A. (2023). Comparative study on high-efficiency Pb(II) removal from aqueous solutions using coal and rice husk based humic acids. *Journal of Molecular Liquids*, *369*, 120875. https://doi.org/10.1016/j.molliq.2022.120875

Zohuriaan-Mehr, M. J., Omidian, H., Doroudiani, S., & Kabiri, K. (2010). Advances in non-hygienic applications of superabsorbent hydrogel materials. *Journal of Materials Science, 45*(21), 5711–5735. https://doi.org/10.1007/s10853-010-4780-1

Zuwanna, I., Riza, M., Aprilia, S., Syamsuddin, Y., & Dewi, R. (2023). Preparation and characterization of silica from rice husk ash as a reinforcing agent in whey protein isolate biocomposites film. *South African Journal of Chemical Engineering*, *44*, 337–343. https://doi.org/10.1016/j.sajce.2023.03.005

3 Chapter Three: Circularity Potential of Rice Husk as a Bioplastic Resource: Techno-environmental Assessment

Abstract

Rice is the most common cereal and staple food to about half the world's population, with high annual production. The effective utilization and exploitation of rice husk, a significant by-product of rice, has been challenging. The negative environmental consequences of current practices, primarily caused by open-air combustion, have led to several other utilization options being explored for more sustainable use. Therefore, in this study, we examine the techno-environment potential of rice husks as a resource for bioplastic production relative to open-air combustion. Specifically, we explore three technologies and their environmental implications for biodegradable bioplastics production pathways: carboxymethylcellulose, cellulose acetate, and cellulose nitrate. Using life cycle assessment (LCA), we examine the environmental impact and associated environmental cost for bioplastic transformation relative to open-air combustion. The result suggests that carboxymethylcellulose would be the most sustainable pathway, reducing the impact on human health and the cost of open-air combustion by 82% and 74%, respectively.

3.1 Introduction

Rice is the staple food for about half the world's population, and its production has continued to rise for the past decade (Tan & Norhaizan, 2020). With the development of new technologies and tools, the production rate is estimated to boost (a value of about 3 billion tons of total cereal yield) in 2050 (Tan & Norhaizan, 2020). This rise will call for the need to deal with its associated by-products, specifically rice husk, along the rice value chain. Figure 3.1A shows rice

husk yield for the top three rice-producing countries in the world (China, India, and Indonesia) and USA for 57 years. Rice husk (RH) makes up about 20% of the total rice paddy and is composed of 28-50% cellulose, 25-30% lignin, 15-20% silica, and 8.68-10.44% moisture (Korotkova et al., 2016; Tan & Norhaizan, 2020). Until recently, the effective utilization and exploitation of rice husk has been difficult (Goodman, 2020). It was usually used for animal bedding, mulch, or burnt in open fields, which are unsustainable (Battegazzore et al., 2014; Tan & Norhaizan, 2020). With the realization of its organic compositions, the continuous rise in its yield, and other important mechanical properties such as bulk density (90 – 150 kg/m^3), high calorific value (12.3×10^6 – 16.7×10^6 J/kg) (Awulu et al., 2018), packing density (118.2 – 122 kg/m^3) and a characteristic dimension of 8-10 mm long, 2-3 mm wide, and 0.2 mm thick (Bajo Jr & Acda, 2017), rice husk has gained the attention of researchers and other stakeholders, particularly towards circular explorations (Singh, 2018; Zou & Yang, 2019). These explorations include fuel production, building materials, insulation materials, bioplastics, and fertilizer production (Mistry, 2016; Moayedi et al., 2019; Moraes et al., 2014). Figure 3.1B shows some research on valorization pathways of rice husks from 2010 to 2021. Among these, research on bioplastics production is gradually getting massive attention due to the need to replace synthetic plastics and utilize agricultural wastes such as rice husk for non-energy applications (Hayatun et al., 2020; R. G. de Azevedo et al., 2022). This is because synthetic plastics have shown huge production growth, as millions of tons are being produced annually worldwide with huge environmental problems throughout their life cycle, from monomer synthesis to disposal or recycling, due to their non-biodegradable nature (Appendix A) (Gökçe, 2018; Heredia-Guerrero et al., 2019; Khazaei et al., 2014; Okunola A et al., 2019). As of 2015, about 322 million tons of synthetic plastics have been produced (Gupta et al., 2019). This value surged to about 380

million in 2018, and is predicted to increase in the coming years, mainly due to the inexpensive cost of production (Okunola A et al., 2019). Also, the high cellulose content makes rice husk a good fit for bioplastic production (Singh, 2018). While most research focuses on bioplastics to reduce the negative implications associated with the production and use of synthetic plastics, there is little data on the environmental performance of their production (Life Cycle Assessment (LCA), eco-efficiency) (Wang et al., 2019). Thus, a thorough knowledge of the environmental impacts associated with the processes as well as their variations involved in the production, is essential (Di Maria et al., 2020). This will provide insight into the selection of the most appropriate technology to use for optimal environmental benefits and will also serve as preliminary data for future projects. As highlighted by Aidoo et al., (2022), the utilization of co-products and byproducts from the agri-food sector to achieve a circular bioeconomy is the critical pathway to achieving a meaningful food system sustainability. This study therefore aims to provide comprehensive techno-environmental data on rice husk conversion to bioplastics across multiple process options and provide data quality analysis in terms of uncertainty analysis. Specifically, we are exploring the technological and environmental trade-offs of the production of three different biodegradable bioplastics: carboxymethylcellulose (CMC), cellulose acetate (CA), and cellulose nitrate (CN), from rice husk and compare their overall sustainability to open-air combustion (a current practice of disposing rice husks).

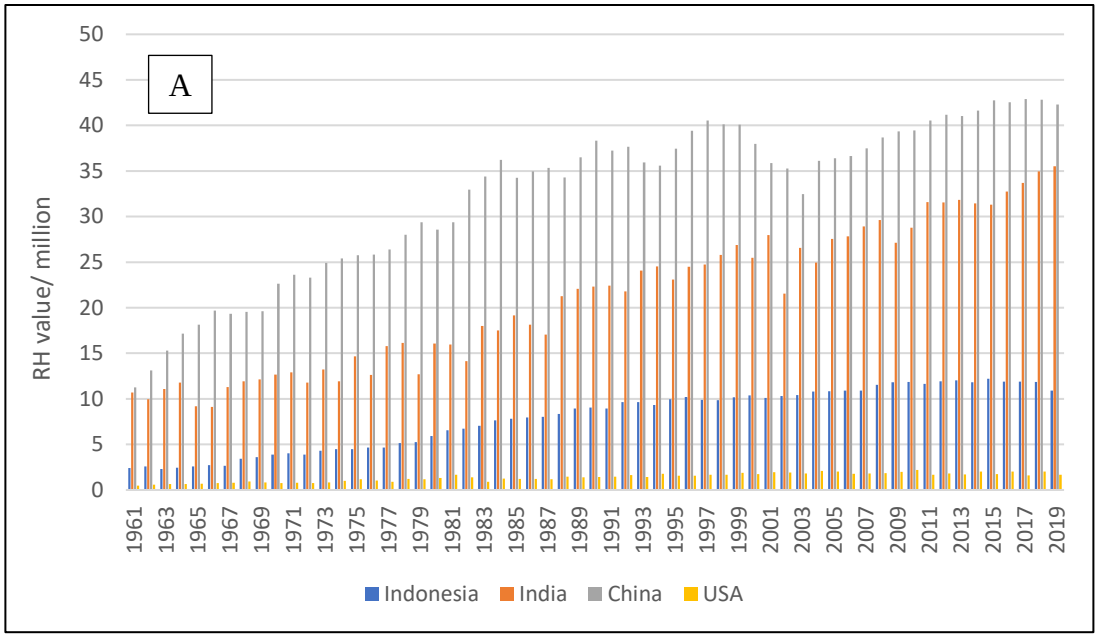

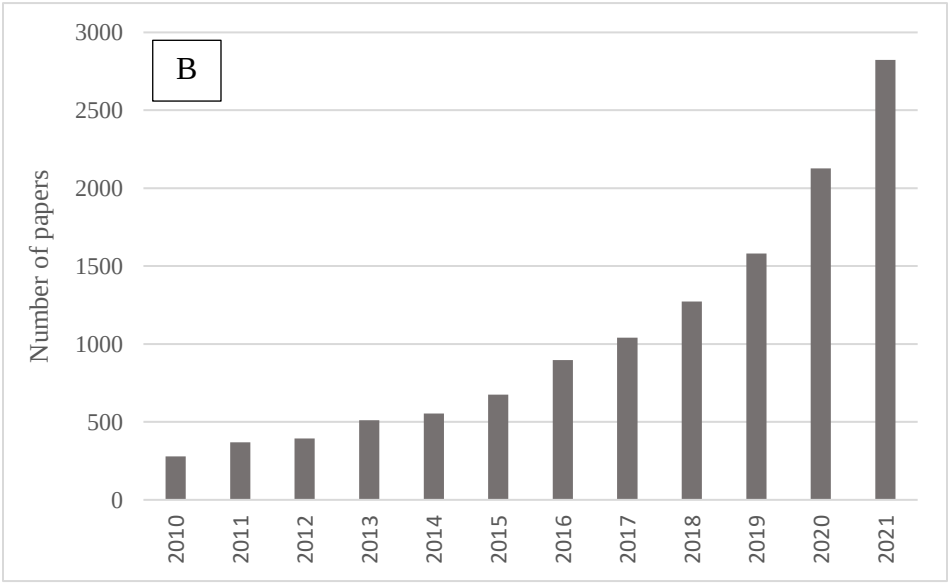

Figure 3.1: (A) Rice husk yield from 1961 to 2019 for China, India, Indonesia, and USA; (B) Trend in rice husk utilization

3.2 Methodology

3.2.1 Process Description and Design

3.2.1.1 Overview of Conversion of Rice Husks into Cellulose-based Biopolymer

The first production step for all cellulose-based bioplastics from rice husk involves the extraction of cellulose. The cellulose is then set to undergo some series of processes and reactions to produce the final bioplastic. This series of processes and reactions determine the form of bioplastic made (Cao et al., 2009; Das et al., 2014; Gupta et al., 2019; Jamal et al., 2020). For the three bioplastics of interest, the determining processes are etherification, acetylation and nitration for CMC, CA, and CN, respectively. Generally, for the first part of the conversion (cellulose extraction), the rice husk undergoes pretreatment (washing and drying) to remove any impurities and then ground and sieved to obtain finer particles. The husk powder is afterward subjected to alkali treatment and heated to remove the silica content and some parts of lignin and hemicellulose (Gupta et al., 2019; Hafid et al., 2021). This is followed by removing the amorphous regions present in the cellulose fibers by adding acid at a suitable concentration to the rice husk and heating the resulting matter. The acid also neutralizes any left-over alkali after the alkali treatment. This process is termed acid hydrolysis. The final step in the cellulose extraction is bleaching, where the coloring components in the rice husk are removed to obtain white cellulose. This process involves the addition of a bleaching agent to the colored cellulose and subjecting the resulting matter to heat.

3.2.1.2 Process and Product Characteristics

In this section, details of the production of each bioplastic from rice husk, as well as the characteristics of the bioplastic produced were examined. The results of this analysis are presented

in Table 3.1. From literature, only works on carboxymethyl cellulose and cellulose acetate were found, no research work was found on the conversion of rice husk to cellulose nitrate.

Table 3.1: Review of the processes involved in the synthesis of CMC and CA from rice husk

Bioplastic		Cellulose Extraction	Bioplastic formation	Bioplastic Characteristics		
				DS	Mechanical Properties	
					TS (MPa)	Elongation (%)
CMC	REFERENCE (Gupta et al., 2019)	1.Milling (0.25 mm) 2.Alkali treatment (6% w/v KOH) at 85 ℃ for 2 h 3.Acid hydrolysis (4% w/v H_2SO_4) at 85 ℃ for 2-2.5h 4.Bleaching (3% w/v $NaClO_2$) and CH_3COOH (to maintain a pH of 3-4) at 80 ℃ for 4 h	1.Mercerization (20% w/v NaOH in 100 mL C_3H_8O) at 50-60 ℃ for 2.5-4h 2.Etherification (100 mL of 20% $C_2H_3ClO_2$) at 50-60 ℃ for 2.5-4h 3.Washing and filtration with C_2H_5OH and HCl 4.Drying at 60 ℃ in oven	0.53	12.72	12.69
	REFERENCE (Jarmkom et al., 2021)	1.Milling (0.297 mm) 2.Acid hydrolysis (39 g H_2SO_4 in 1000 g water) at 90 ℃ for 2 h 3.Alkali treatment (50 g KOH in 1000 g water) at 90 ℃ for 2 h 4.Bleaching (30 g NaClO in 1000 g water) at 80 ℃ for 2 h 5.Neutralization to a pH of 4.5 with glacial acetic acid	1.Mercerization (30 % w/v NaOH in an unknown amount of C_3H_8O) at room temperature for 0.5 h 2.Etherification (10 g of $C_2H_3ClO_2$) at 55 ℃ for 3 h 3.Suspension of sedimentary phase in 70% CH_3OH solution and neutralization with glacial CH_3COOH 4.Washing and filtration with 70% C_2H_5OH	0.78	N/S	N/S

			5.Washing with absolute CH_3OH solution 6.Drying at 55 ℃ in oven			
	(Rashid & Dutta, 2021)	1.Milling (0.1-0.25 mm) 2.Dewaxing (1:2 v/v CH_3OH:C_6H_6) at 75 ℃ for 9 h 3.Alkali treatment (3% w/v NaOH) at 45 ℃ for 8 h 4.Autoclave samples at 121 ℃, 15 psig for 8 h – repeated thrice 5.Bleaching (6.5:2.0 CH_3COOH:H_2O_2, v/v) at 45 ℃ for 7 h	5.Mercerization (100 mL C_3H_8O and 40% w/w, 14.15 g NaOH) for 50 min 6.Addition of 150 mL C_3H_8O and 40% NaOH under agitation for 0.5 h after filtration 7.Etherification (7 g $C_2H_3ClO_2$) at 55 ℃ for 4 h 8.Washing and filtration with C_2H_5OH (concentration unknown) 9.Washing with absolute C_2H_5OH 10.Drying at 60 ℃ for 9 h	0.87	N/S	N/S
CA	(Das et al., 2014)	1.Milling (1-2 mm) 2.Dewaxing (2:1 v/v C_6H_{14}:CH_3OH) for 10 h 3.Alkali treatment (5 wt% NaOH-Na_2CO_3) at 80 ℃ for 5 h 4.Acid hydrolysis (10% H_2SO_4) at 50 ℃	1.Acetylation (10 mL $C_4H_6O_3$ and 0.3 g iodine) at 80 ℃ for 5h 2.Mixing with 5 mL saturated solution of $Na_2S_2O_3$ 3.Mixing with 30 mL C_2H_5OH for 1 h	2.91	N/S	N/S

	5.Bleaching (2% H_2O_2, pH of 9) at room temperature for 5 h	4.Filtration and washing with 75% C_2H_5OH 5.Dissolution in methylene chloride 6. Washing with C_2H_5OH 7.Drying at 60 ℃ for 24 h			
(Biswas et al., 2014)	1.Milling (1.27 mm) 2.Acid hydrolysis (1% v/v H_2SO_4) at 121 ℃ for 24 h 3.Alkali treatment (10 M NaOH)	1.Mixing with 0.5 g acetic acid, 5.0 g acetic anhydride, 30 mL methylene chloride, and 0.04 g H_2SO_4 at 80 ℃ for 4 h 2.Addition of 60 mL chloroform for 0.5 h at room temperature 3.Evaporation of filtrate to dryness 4.Washing with ethanol 5.Drying at 80 ℃ in a vacuum oven overnight	2.8	N/S	N/S

DS – Degree of Substitution; TS – Tensile Strength; N/S – Not Stated

3.2.1.3 Process Design Simulations

Based on the above processes, a comprehensive method of converting the rice husk to bioplastic was designed for each bioplastic type. Each system was modeled and simulated with the SuperPro Designer; version 9.0 Build commercial software (Intelligen, Scotch Plains, NJ, United States of America). The model included a flowchart design with the various unit processes and streams. The simulations included a materials and stream evaluation (mass and energy balances). The simulation was run based on a small-scale experimental input, assuming that the rice processing mill is 20 km away from the processing plant for each method. Because of limited industrial-scale feed rate information, a presumptive value of 10 tons RH/batch with an estimated total batch number of 990 per year (3 batches per day for 330 days) was used for the mass balance calculation. This simulation generated some preliminary results that was used together with data from literature to estimate the amount of rice husk needed to achieve the functional unit of the various pathways in the LCA.

3.2.1.3.1 Cellulose extraction

For the first significant part of the process, the rice husk is first pretreated by washing it with distilled water and subsequently drying it in an oven at 70 ℃ for 16 hours (Gupta et al., 2019). This will eliminate any form of impurities and water content in the husk. The dried husk is ground and sieved to an average particle size of 0.177 mm (80 mesh size) (Jannah et al., 2019). This particle size is selected to give the husk a more extensive surface distribution to ensure optimum reaction. In the alkali treatment process, 10 tons of the powdered husk is homogeneously mixed with sodium hydroxide (NaOH, 5% w/v) in a 1:5 ratio in an autoclave at 120 ℃ for 45 minutes (Hafid et al., 2021). Sodium hydroxide was used in this process instead of potassium hydroxide (KOH) because NaOH is less expensive (87% less expensive, according to

Sigma-Aldrich; https://www.sigmaaldrich.com/US/en) and will achieve the same objective as KOH. The macerated powder is then washed and filtered with distilled water until the alkali solution is completely removed. In the acid hydrolysis process, 10% w/v HNO_3, was heated with the cellulose fibers at 120 ℃ for two h. The cellulose obtained was then washed with distilled water to remove the excess acid. This was proceeded by bleaching, with the addition of 3% w/v $NaClO_2$ and 25% w/v CH_3COOH at 70 ℃. The final process involved the formation of the bioplastic where the cellulose was mixed with isopropanol and 20% w/v NaOH and stirred for about 3 hours at 55 ℃, a process termed mercerization. Subsequently, the sample was washed and dried at 70 ℃.

3.2.1.3.2 Cellulose Acetate Production

In this process, the white cellulose is reacted with acetic anhydride and iodine at a temperature of 80 ℃ for about 5 hours. The mixture is allowed to cool and then treated with a saturated sodium thiosulphate ($Na_2S_2O_3$) solution. Ethanol is added and stirred for about an hour to the resulting material. The product is filtered, and the residue is washed with 75 % v/v ethanol and distilled water. This removes any unreacted acetic acid and other by-products in the medium. The solid material left is dried at a temperature of about 60 ℃. The dried sample is dissolved afterward in methylene chloride and filtered. The filtrate is subjected to evaporation, and cellulose acetate is formed as a residue. Cellulose acetate is collected using ethanol addition and dried for 24 hours at 60 ℃.

3.2.1.3.3 Carboxymethyl Cellulose production

For this process, 20% w/v mono-chloroacetic acid solution was reacted with the white cellulose at 55 ℃. The resulting material was washed and filtered with hydrochloric acid and ethanol

mixture and the residue after filtration, is carboxymethyl cellulose. This is dried at a temperature of around 60 ℃.

3.2.1.3.4 Cellulose nitrate production

This process was adopted from work by (Jamal et al., 2020). Cellulose is added to a concentrated nitric and sulfuric acid nitrating solution and stirred for about an hour. The mixture was quenched by excess de-ionized water to precipitate cellulose nitrate. The cellulose nitrate precipitate is filtered by vacuum then added into boiling water for about 5 minutes. The precipitate is rinsed again with distilled water until a pH of about seven is obtained. It is afterward dried at 60 ℃ to a constant weight.

3.2.2 Environmental Performance Assessment

The environmental performances of the three bioplastics were evaluated with a Life Cycle Assessment study (LCA). LCA basically quantifies the emissions, resources consumed, and environmental and health impacts associated with a good or service. LCA is structured into four phases: goal and scope definition, inventory analysis, impact assessment and results interpretation. The OpenLCA software, version 1.10.3 (GreenDelta, GmbH, Berlin, Germany), was employed to analyze the life cycle assessment of the bioplastic production and compare the results to the activities involved in the disposal of rice husk, specifically combustion.

3.2.2.1 Goal and Scope definition

The overall goal of this study was to determine the environmental implication of producing bioplastics from rice husk relative to combusting an equivalent quantity of the rice husk. Combustion is known to be the conventional way rice husk is managed in most farms hence it is selected as reference for this study. A functional unit of 1 kg bioplastic produced (from 10 kg of rice husk) and 10 kg of RH combusted were selected for the bioplastic process and combustion

respectively for the LCA analysis. The complete process flows are shown in Figure 3.2A. From this chart, a system boundary was developed to mark out the processes that are important for the analysis of each production. Figure 3.2B shows the system boundary for combustion and bioplastic production. As shown, this is a gate-to-gate study, considering rice husk transportation (from milling) to bioplastic production (in the cases of bioplastics), and burning from rice milling (in the case of the combustion process). Apart from the storage process, all other processes discussed for each bioplastic was considered in the LCA phase. The storage process was excluded because an overall impact of zero was assumed for it. Also, this process can be removed from the production line and there will be no net effect.

3.2.2.2 Inventory

A life cycle inventory was created to collect the relevant data required for the impact analysis. The Ecoinvent database, version 3.71, and information from the literature were relied on for all the data needed. These data were used as flows (inputs and outputs) to construct the life cycle analysis. Also, the type of transportation was referred from the Ecoinvent database (freight, truck) and was used for the evaluation. The works of Biswas et al., (2014), Das et al.(2014), Gupta et al. (2019), Jarmkom et al. (2021) and Rashid and Dutta (2021) were referenced and integrated to develop the inventory for the bioplastics in Appendix A.

3.2.2.3 Environmental Impact Assessment

The Life Cycle Impact Assessment (LCIA) phase of an LCA evaluates the potential environmental impacts emanating from the various elementary flows (inventory) (Nieuwlaar, 2013). For this study, the Life Cycle Impact Assessment (LCIA) was computed based on the ReCiPe 2016 version 1.1 midpoint and endpoint methods, Hierarchist version (Huijbregts et al., 2016). The midpoint method presents results on the earlier impacts (emissions) along the cause-

effect chain before the final damages are made (endpoint). The endpoint as a result integrates the different midpoint results and evaluates their effects on the environment, humans, and resources.

3.2.2.4 Environmental Cost Assessment

To better understand and communicate the results of LCA, Environmental Cost Assessment presents a unique metric that complements the overall environmental. Environmental Cost Assessment basically assigns weights to the individual impact categories by translating them into monetary units. For this study, the Ecovalue14 monetization method was used. Table 3.2 below shows the weighting factors used in the EcoValue14 method. The impacts were monetized by multiplying these factors by the impact scores. Some indicators such as particulate matter and fossil fuel scarcity did not have their factors in the corresponding units from the LCIA so were first converted into the units presented in EcoValue14 before the monetization. The results were afterwards converted from Euros (€) into US Dollars ($), with a factor of €1=$1.13 (February 2022) according to Exchange rates, UK (https://www.exchangerates.org.uk/EUR-USD-exchange-rate-history.html).

Table 3.2: EcoValue14 monetary weightings (2017-adjusted) (Malmgren, 2017)

Impact category	**Weighting**
Abiotic resources	€0.0136/ MJ
Global Warming	€0.3315/ kg CO_2-eq
Photochemical oxidation	€2.06/ kg NMVOC-eq
Acidification	€3.76/ kg SO_2-eq
Eutrophication, marine	€11.45/ kg N
Eutrophication, freshwater	€84.7/ kg P
Human toxicity	€0.3555/ kg 1,4 DCB-eq
Marine toxicity	€1.15/ kg 1,4 DCB-eq
Particulate matter	€34.3 /kg PM

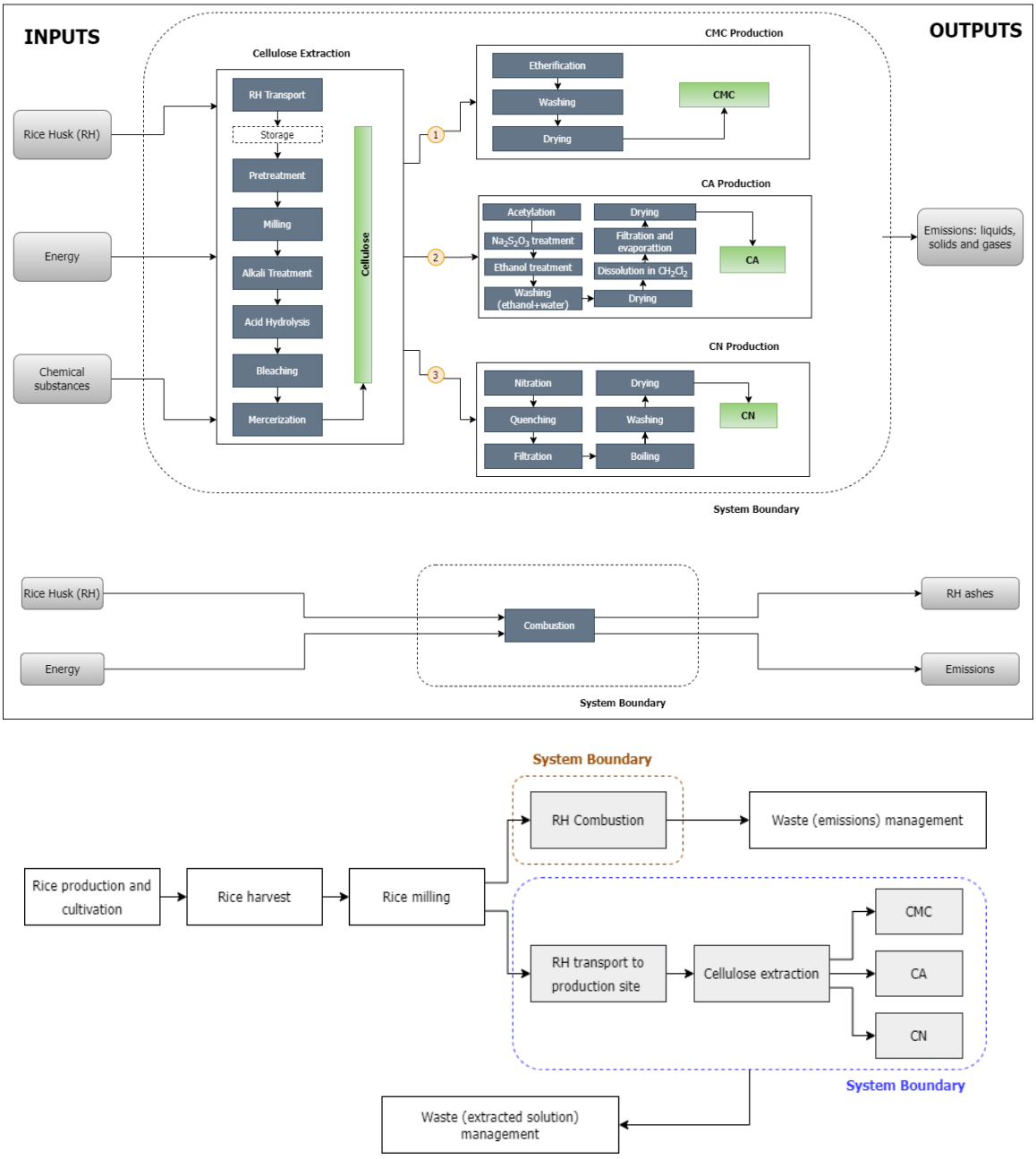

Figure 3.2: (A) Flow diagram for bioplastic production and combustion – 1) CMC, 2) CA, 3) CN. (B) System boundary for rice husk combustion and bioplastic production from rice husk

3.3 Results and Discussion

3.3.1 Process Design Outcome

The flowsheets for different production pathways are shown in Appendix A. The flowsheets show the different input and output streams for each process. The main input for this flowsheet is the rice husk (10 tons). The rice husk goes through series of unit processes, as discussed already to produce cellulose. This cellulose will serve as the main input to each bioplastic production line.

3.3.2 Comparative Environmental Impact Assessment

This section analyzes the life cycle assessment results and compares the impacts of the processes from the bioplastic production and the rice husk combustion. This analysis will guide our decision on the right way to deal with the rice husk (bioplastic production vs. rice husk combustion) and the type of bioplastic (CMC vs. CA vs. CN) we should focus on, if necessary. The overall environmental impacts (normalization) of the bioplastic production and the rice husk combustion are illustrated in Figure 3.3 and Table 3.3. The results show some life cycle midpoint indicators, with global warming, ozone formation (human health), and ozone formation (terrestrial ecosystem) giving the significant impacts contribution for bioplastic production and rice husk combustion. Moreover, freshwater ecotoxicity, fossil resource scarcity, human carcinogenic and non-carcinogenic toxicity, marine ecotoxicity, and terrestrial ecotoxicity also contributed significantly to the impact of bioplastic production. In contrast, fine particulate matter formation and terrestrial acidification contributed to the impacts of rice husk combustion. For CMC, marine ecotoxicity gave the highest impact value of 42%; followed by freshwater ecotoxicity, 27%; human carcinogenic toxicity, 11%; ozone formation (terrestrial ecosystems), 7%; global warming, 4%; ozone formation (human health), 4%; human non-carcinogenic

toxicity, 2%; and finally fossil resource scarcity, and terrestrial ecotoxicity, both with impacts of 1%. A similar trend is observed for CA, with marine ecotoxicity contributing (42%), followed by freshwater ecotoxicity (28%), human carcinogenic toxicity (13%), ozone formation (terrestrial ecosystems) (5%), global warming (3%), ozone formation (human health) (3%), human non-carcinogenic toxicity (3%), terrestrial ecotoxicity (1%) and fossil resource scarcity (1%). However, for CN, the trend was significantly changed. Marine ecotoxicity contributed about 43%, followed by freshwater ecotoxicity (26%), human carcinogenic toxicity (9%), ozone formation (terrestrial ecosystems) (5%), terrestrial ecotoxicity (5%), human non-carcinogenic toxicity (4%), global warming (3%), ozone formation (human health) (3%), and fossil resource scarcity (1%). In rice husk combustion, a complete change in trend and impact category significance was observed. Fine particulate matter formation contributed the most to the impact, with an impact score of 77%. This is followed by global warming (9%), ozone formation (terrestrial ecosystems) (6%), ozone formation (human health) (5%), and terrestrial acidification (4%). These results are typical for combustion as most toxic substances such as CO_2, nitrous oxides, and fine particulates are released into the environment from the process (Caserini et al., 2010). Table 3.4 presents a detailed explanation of these midpoint categories and their impacts.

Table 3.3: Life cycle impacts for bioplastics production and rice husk combustion

Impact category	Reference unit	Impact scores			
		CMC	CA	CN	Combustion
Fine particulate matter formation	kg PM2.5 eq	0.0002	0.0005	0.0003	0.0981
Fossil resource scarcity	kg oil eq	0.0145	0.0156	0.0144	0.0000
Freshwater ecotoxicity	kg 1,4-DCB	0.2795	0.3711	0.3378	0.0000
Freshwater eutrophication	kg P eq	0.0019	0.0031	0.0022	0.0000
Global warming	kg CO2 eq	0.0405	0.0408	0.0404	0.0122
Human carcinogenic toxicity	kg 1,4-DCB	0.1145	0.1719	0.1220	0.0000
Human non-carcinogenic toxicity	kg 1,4-DCB	0.0233	0.0338	0.0563	0.0000
Ionizing radiation	kBq Co-60 eq	0.0005	0.0006	0.0003	0.0000
Land use	m2a crop eq	0.0000	0.0000	0.0000	0.0000
Marine ecotoxicity	kg 1,4-DCB	0.4249	0.5610	0.5578	0.0000
Marine eutrophication	kg N eq	0.0000	0.0001	0.0001	0.0000
Mineral resource scarcity	kg Cu eq	0.0000	0.0000	0.0000	0.0000
Ozone formation, Human health	kg NOx eq	0.0359	0.0363	0.0360	0.0063
Ozone formation, Terrestrial ecosystems	kg NOx eq	0.0668	0.0673	0.0669	0.0073
Stratospheric ozone depletion	kg CFC11 eq	0.0020	0.0016	0.0017	0.0000
Terrestrial acidification	kg SO2 eq	0.0005	0.0008	0.0006	0.0043
Terrestrial ecotoxicity	kg 1,4-DCB	0.0128	0.0184	0.0633	0.0000
Water consumption	m3	0.0004	0.0008	0.0003	0.0000

Table 3.4: Description and implications of some impact categories from the LCA

Impact category	**Description/Implication**
Fine particulate matter formation	Fine particulate matter formation measures the amount of particulate matter in kg PM2.5 or kg PM10 equivalence (PM means particulate matter). This impact category indicates the possible occurrence of diseases, typically respiratory diseases, due to the release of fine particulate matter.
Fossil resource scarcity	This measures the depletion of fossil resources, typically oil. It implies the potential of the resources going scarce (depletion factor).
Freshwater ecotoxicity	This impact category measures the number of toxic substances, such as Dichlorobenzene (DCB) or other comparative toxic units equivalence (ecosystem) (CTUe), that a process releases into a freshwater ecosystem. It implies the distress these substances cause to freshwater organisms.
Freshwater eutrophication	Just like Freshwater ecotoxicity, Freshwater eutrophication measures the number of substances, but in this case, nutritional elements and compounds released into a freshwater ecosystem. It is typically in kg P or kg PO_4 equivalence. This impact category implies the level of enrichment of these elements/compounds and their effect to freshwater organisms.
Global warming	This measures the number of compounds (greenhouse gases) released into the air. It is typically measured in kg CO_2, N_2O, or CH_4 equivalence. It implies the potential of these gases to cause climate change (global warming).
Human carcinogenic toxicity	Human carcinogenic toxicity measures the number of cancer-causing substances released into the environment. It is measured in kg DCB or other comparative toxic units equivalence (human health) (CTUh). They imply the occurrence of cancer in humans.

83

Human non-carcinogenic toxicity	Human carcinogenic toxicity measures the number of non-cancer-causing substances released into the environment. It is measured in kg DCB or other comparative toxic units equivalence (human health) (CTUh). They imply the effects (non-cancerous) of these substances on human health.
Ionizing radiation	Ionization radiation determines the number of radioactive nuclides released into the ecosystem. Typical units include kg Co-60 and kBq U-235 equivalence. It implies the damage of these radionuclides to human health and the ecosystem.
Land use	This measures the changes in soil quality and other land properties. It is typically measured in m^2a crop equivalence.
Marine ecotoxicity	This impact category measures the number of toxic substances, such as Dichlorobenzene (DCB) or other comparative toxic units equivalence (ecosystem) (CTUe), that a process releases into a marine ecosystem. It implies the distress these substances cause to marine organisms.
Marine eutrophication	Marine eutrophication measures the number of nutritional elements and compounds released into a marine ecosystem. It is typically in kg P or kg PO_4 equivalence. This impact category implies the level of enrichment of these elements/compounds and their effect on marine organisms
Mineral resource scarcity	This measures the depletion of mineral resources, typically copper or antimony. It implies the potential of these resources going scarce (depletion factor).
Ozone formation, Human health	This measures ozone formation close to the ground by ozone-forming compounds, typically NO_x, and its effect on human health.
Ozone formation, Terrestrial ecosystems	This measures ozone formation close to the ground by ozone-forming compounds, typically NO_x, and its effect on terrestrial ecosystems.
Stratospheric ozone depletion	It quantifies the ozone depletion potential in Chlorofluorocarbons (CFCs).

84

Terrestrial acidification	Terrestrial acidification measures the acidification potential of the process due to the emission of some acidic substances, typically SO_2. It implies the distress these substances cause to terrestrial organisms (humans, animals, and plants).
Terrestrial ecotoxicity	This impact category measures the number of toxic substances, such as Dichlorobenzene (DCB) or other comparative toxic units equivalence (ecosystem) (CTUe), that a process releases into a terrestrial ecosystem. It implies the distress these substances cause to terrestrial organisms (humans, plants and animals)
Water consumption	Water consumption measures the amount of water used by the process. It indicates the relative scarcity of water per m^3.

85

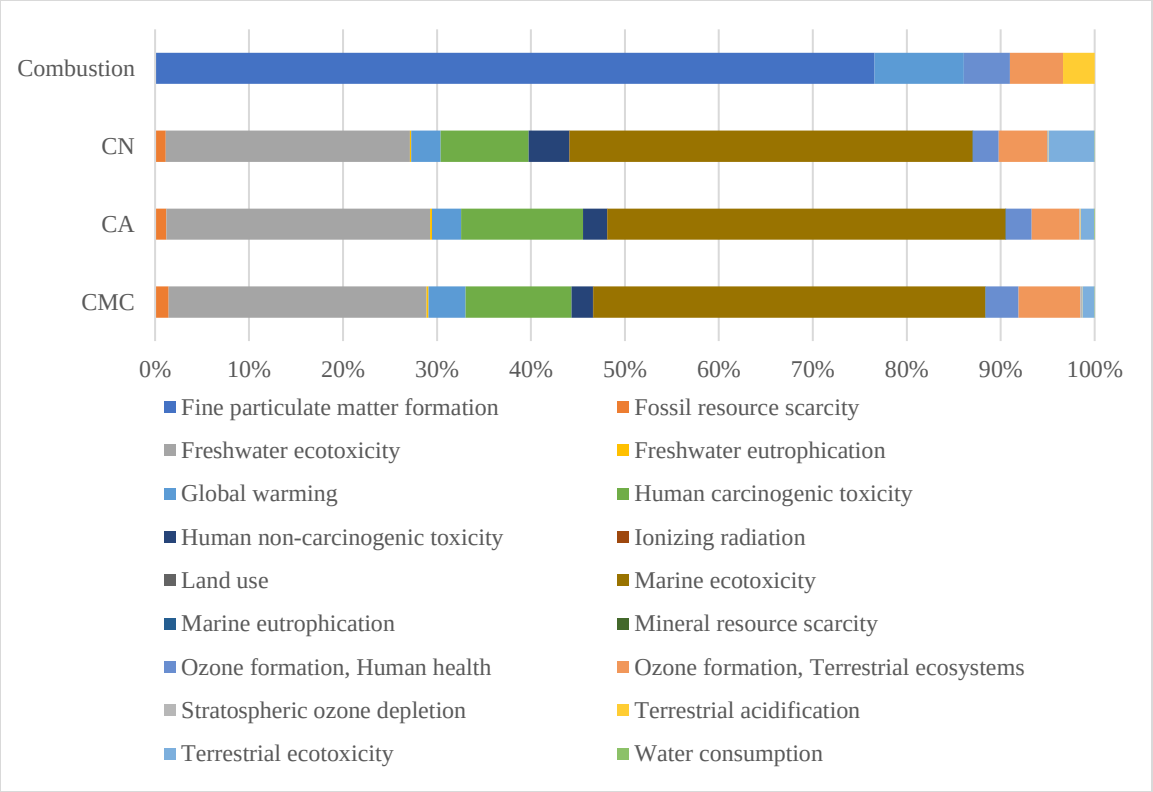

Figure 3.3: Impact Assessment of bioplastics production and combustion

3.3.2.1 Impact Contribution by Process

In every production line, the variation in resource demand, the type of resource (flow), and the activities or reactions involved in a process determine the extent of the impact of that process. This section, therefore, describes the impact contributions by the different processes and provides a further explanation of the impacts in the previous section. The impact contributions by the different processes for CMC, CA, and CN production are shown in Figure 3.4. Because of the initial stage of the production (cellulose extraction), acid hydrolysis, alkali treatment, mercerization, bleaching, drying, washing, grinding, and sieving are typical for all three different bioplastics. For all three bioplastics, acid hydrolysis and mercerization contributed the most to all the various impact categories. In addition to these, etherification, acetylation, and nitration gave significant contributions to CMC, CA, and CN production, respectively. This is typical for

processes that utilize chemicals. However, bleaching and alkali treatment processes contributed little to the different impact categories even though chemicals were used. This observation is nevertheless accurate because the intensity of the impacts associated with a chemical depends on the method of production for that chemical (Khoo et al., 2018). Generally, chemicals produced via biological synthesis or involving some kind of biological process have less impact on the environment (Khoo et al., 2018). In bleaching and alkali treatment, sodium hypochlorite and sodium hydroxide were used, respectively. The synthesis of these chemicals involves biological processes (Bashtan et al., 1999; Du et al., 2018). This explains the results. Also, the amount of chemicals used in the process plays a vital role in the environmental impact. However, this factor did not affect the results as the amount of chemicals used in each process is somewhat equal. Grinding and sieving had significant contributions to the impacts. However, the contributions were higher for only terrestrial ecotoxicity, marine ecotoxicity, and freshwater ecotoxicity, and least for ozone formation (terrestrial ecosystems and human health), global warming, and fossil resource scarcity. Their impacts were mainly because of the electric power generation involved in the process. The impact of washing in the production was insignificant, hence the recorded impact score of approximately 0%. Drying did not give any significant contributions to the overall impacts. This is because the drying process utilizes natural gas. Natural gas releases about 50 to 60% less carbon dioxide than regular fuels, hence, the results.

Figure 3.4: Impact contributions by the different processes in CMC, CA, and CN production

3.3.2.2 Endpoint Indicators

This section translates the results of the impacts for the different midpoint indicators into endpoint indicators. The results are summarized into the three main endpoint areas of protection, namely: Human Health Damage (Disability-Adjusted Life Years, DALY), Ecosystem Damage (species.yr), and Resource Scarcity (USD2013) (Table 3.5). The Human Health Damage category aggregates the results of global warming, ozone formation (human health), human carcinogenic and non-carcinogenic toxicity, and fine particulate matter formation. The results for the Ecosystem Damage account for the impacts from ozone formation (terrestrial ecosystems), freshwater ecotoxicity, marine ecotoxicity, terrestrial ecotoxicity, and terrestrial acidification. Fossil resource scarcity accounts for the entire Resource Scarcity category. From the table, combustion causes the most extensive damage to human health (0.396 DALY). This is mainly due to the extensive formation of particulate matter from the process. Fine particulate matter has a high effect on human health (Joo et al., 2022; Lin et al., 2022; Prinz & Richter, 2022). It causes a lot of defects in humans, with respiratory disorders being the most common among them. CMC, CA, and CN have relatively similar damage to human health. This is mainly due to the impacts of global warming, ozone formation (human health), and human carcinogenic and non-carcinogenic toxicity. The different impacts on the ecosystem and resources for all the bioplastic production and combustion are minimal (approximately zero). This is because the contributing impacts are insignificant.

Table 3.5: Endpoint areas of protection for CMC, CA, CN, and Rice Husk Combustion

Endpoint AoP	Contributing midpoint category	Reference unit	Impact value			
			CMC	CA	CN	Combustion
Human Health Damage	Fine particulate matter formation	DALY	1.18E-03	1.73E-03	1.04E-03	3.75E-01
	Global warming, Human health		7.12E-02	7.18E-02	7.12E-02	2.14E-02
	Human carcinogenic toxicity		2.88E-04	3.75E-04	2.66E-04	0
	Human non-carcinogenic toxicity		2.22E-04	2.73E-04	4.54E-04	0
	Ionizing radiation		4.09E-07	5.40E-07	2.90E-07	0
	Ozone formation, Human health		1.60E-04	1.62E-04	1.60E-04	2.79E-05
	Stratospheric ozone depletion		1.10E-05	1.23E-05	1.29E-05	0
	Water consumption, Human health		5.36E-05	1.13E-04	4.61E-05	0
Total			**7.31E-02**	**7.45E-02**	**7.32E-02**	**3.96E-01**
Ecosystem Damage	Freshwater ecotoxicity	species.yr	1.93E-09	2.26E-09	2.05E-09	0
	Freshwater eutrophication		7.79E-09	9.80E-09	6.71E-09	0
	Global warming, Freshwater ecosystems		1.77E-10	1.78E-10	1.77E-10	5.32E-11
	Global warming, Terrestrial ecosystems		6.49E-06	6.55E-06	6.49E-06	1.95E-06
	Land use		5.65E-09	7.55E-09	5.07E-09	0
	Marine ecotoxicity		3.75E-10	4.36E-10	4.34E-10	0
	Marine eutrophication		2.99E-12	3.24E-12	2.85E-12	0
	Ozone formation, Terrestrial ecosystems		1.10E-06	1.10E-06	1.10E-06	1.19E-07
	Terrestrial acidification		3.55E-08	4.96E-08	3.58E-08	2.67E-07
	Terrestrial ecotoxicity		1.24E-09	1.55E-09	5.36E-09	0
	Water consumption, Aquatic ecosystems		4.40E-13	9.28E-13	3.78E-13	0
	Water consumption, Terrestrial ecosystem		9.83E-09	2.07E-08	8.45E-09	0
Total			**7.65E-06**	**7.74E-06**	**7.65E-06**	**2.33E-06**

Resource Scarcity	Fossil resource scarcity	USD2013	1.40E-12	1.50E-12	1.39E-12	0
	Mineral resource scarcity		1.17E-15	5.65E-14	1.21E-15	0
Total			**1.40E-12**	**1.56E-12**	**1.39E-12**	**0**

3.3.3 Environmental Cost Assessment

The EcoValue14 method of monetizing environmental impact was used to convert the various impacts of rice husk combustion and each bioplastic produced into monetary units. Table 3.6 shows the cost associated with each impact category per 1 kg of rice husk used in dollars. Some impact categories, such as freshwater ecotoxicity, ozone formation, human health, ozone formation, terrestrial ecosystems, and terrestrial ecotoxicity, were not accounted for as Ecovaalue14 does not provide factors for them. However, this will not substantially affect the overall cost results mainly because the impact scores for these categories are small. Fine particulate matter formation gave the highest cost for the combustion process, about $ 2.70/kg rice husk. Marine ecotoxicity gave the highest prices for each bioplastic, $ 0.63 for CMC, $ 0.73 for CA, and $ 0.72 for CN. The cost for fossil resource scarcity was the least for all three bioplastics: $ 0.009 for CMC and CN and $ 0.01 for CA. From the table, the environmental cost associated with rice husk combustion (burning) was significantly reduced by producing the bioplastics. CA reduced the price by about 69%, CN reduced it by 70%, and CMC reduced it by 74%.

Table 3.6: Environmental cost for bioplastic production and rice husk combustion

Impact category	Reference Unit	Amount in Dollars ($)			
		CMC	CA	CN	Combustion
Global warming	kg CO2 eq	0.0154	0.0153	0.0151	0.0046
Fossil resource scarcity	kg oil eq	0.0093	0.0100	0.0092	–
Freshwater ecotoxicity	kg 1,4-DCB	–	–	–	–
Human carcinogenic toxicity	kg 1,4-DCB	0.0529	0.0690	0.0490	–
Human non-carcinogenic toxicity	kg 1,4-DCB	0.0110	0.0136	0.0226	–
Marine ecotoxicity	kg 1,4-DCB	0.6269	0.7289	0.7249	–
Ozone formation, Human health	kg NOx eq	–	–	–	–
Ozone formation, Terrestrial ecosystems	kg NOx eq	–	–	–	–
Terrestrial ecotoxicity	kg 1,4-DCB	–	–	–	–
Fine particulate matter formation	kg PM2.5 eq	–	–	–	2.6991
Terrestrial acidification	kg SO2 eq	–	–	–	0.0182
Total		**0.7153**	**0.8369**	**0.8209**	**2.7219**

3.3.4 Sensitivity Analysis

Sensitivity analysis examines the effects of the different choices made concerning processes and their flows on the outcome of a study (Guo & Murphy, 2012). In this analysis the systematic approach (scenario modelling approach) outlined by the International Organization for Standardization (ISO) was utilized. Cellulose extraction was selected as the base process because it is common for all the bioplastics. From the results presented in section 4, it was observed that acid hydrolysis, mercerization and alkali treatment processes considerably affected the overall impact of the production. The key flows in these processes were hence altered to observe how significantly the overall impacts will change. Also, because of the initial assumption that the site of production is 20 km away from the source of rice husk (farm), the distance is changed as well in the analysis. Thus, five different scenarios (apart from the base scenario) were considered for this analysis. LCA was performed for each scenario.

- **Base scenario:** Same flows discussed in section 3.1.3
- **Scenario 1:** Potassium hydroxide is used as the base for alkali treatment
- **Scenario 2:** The initial transportation of 20 km is changed to 1000 km
- **Scenario 3:** Sulfuric acid (H_2SO_4) is used for the acid hydrolysis
- **Scenario 4:** Sulfuric acid – Nitric acid mixture in a 50-50 ratio is used for the acid hydrolysis
- **Scenario 5:** Potassium hydroxide (KOH) is used in the mercerization process

The results for the sensitivity analysis are presented in Figure 3.5 below, for the top nine midpoint impact categories. Among all the six scenarios, scenario 3 recorded the least environmental impact for all the nine impact categories, with major percentage decrease of 33%, 24%, 24% and 17% for Human carcinogenic toxicity, Human non-carcinogenic toxicity, marine

toxicity and freshwater ecotoxicity respectively. Scenario 1 recorded the most impact for all the impact categories except for fossil resource scarcity and freshwater ecotoxicity. A percentage increase of 10%, 8%, 7% and 6% were recorded for Human carcinogenic toxicity, Human non-carcinogenic toxicity and terrestrial ecotoxicity.

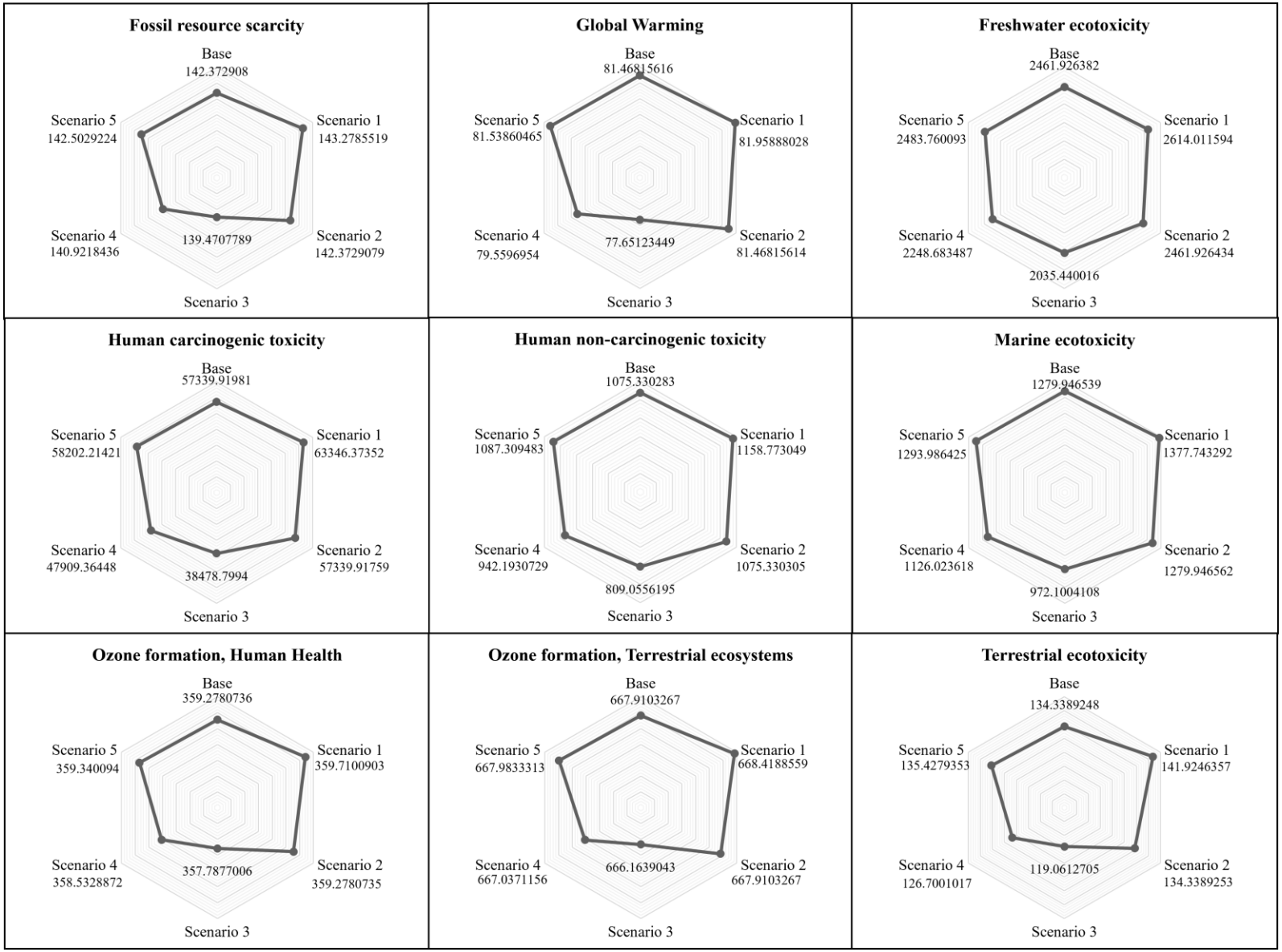

Figure 3.5: Sensitivity analysis – top nine impact categories

3.3.5 Uncertainty Analysis

In decision-making problems, selecting the right variables to use for each model is very crucial. This is because of the large number of possible variables that can work for a model. Uncertainty analysis is one way of solving the issues regarding the selection of these variables. This analysis investigates the insecurity of the relevant variables and hence the kind of results and observations they present for a model. In this section, the uncertainties regarding the LCA impact results for each bioplastic was examined. Monte-Carlo simulation was employed as the calculation type for this analysis. The simulation was run in the openLCA software, with an iteration number of 500 and a log normal distribution for each flow in each bioplastic process. Figure 6 presents the results for the uncertainty analysis. The bar-charts represent the uncertainties in LCIA profiles for the top nine impact categories for each bioplastic: Fossil resource scarcity (FRS), Freshwater ecotoxicity (FWE), Global warming (GWP), Human carcinogenic toxicity (HCT), Human non-carcinogenic toxicity (HNT), Marine ecotoxicity (MET), Ozone formation, Human health (OZH), Ozone formation, Terrestrial ecosystems (OZT), and Terrestrial ecotoxicity (TEC). The error bars represent uncertainty range in terms of the ratio of 5^{th} and 95^{th} percentile to the mean value. The graphs (histogram) represent the probability distribution of Global Warming Potential (GWP) for each bioplastic. The highest degree of uncertainty was observed for human carcinogenic toxicity for CMC. This may be due to the large uncertainties in the major toxic driver, 1,4-dichlorobenzene. Conversely, the variances in the remaining impact categories were minimal. This indicates that the environmental profile of the LCA results for the bioplastics well represented the reality on the impact categories.

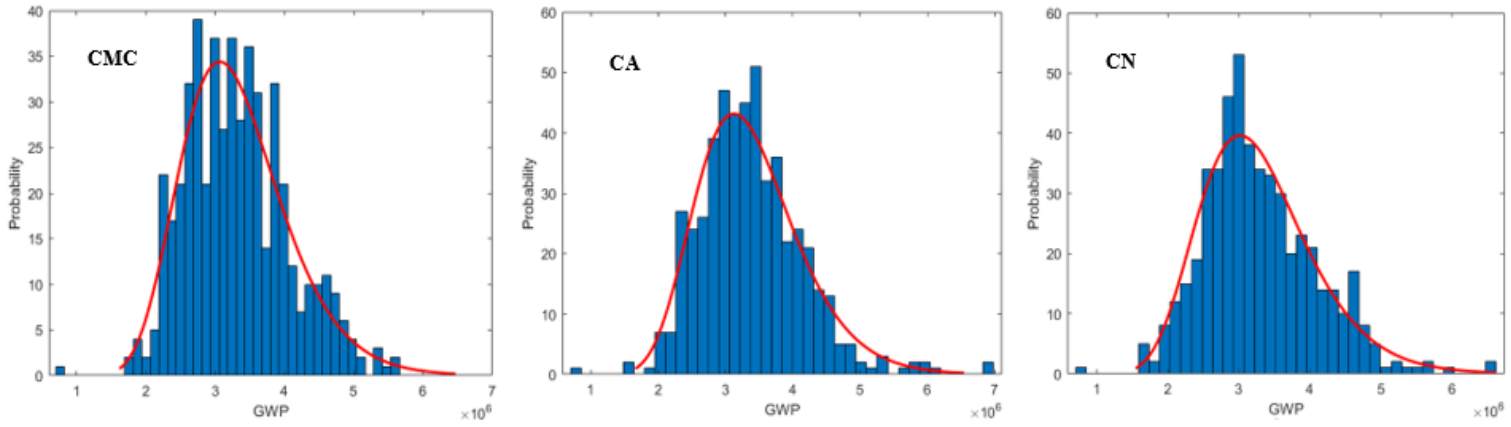

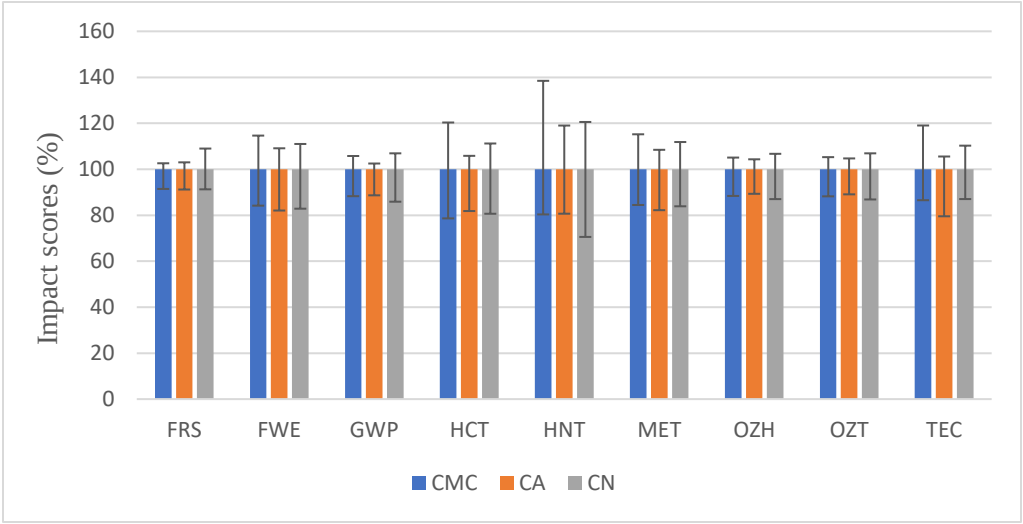

Figure 3.6: Uncertainty analysis for CMC, CN, and CA showing uncertainties in LCIA profiles on the left columns (the error bars represent uncertainty range in terms of the ratio of 5th and 95th percentile to the mean value) and the probability distribution of GWP on the right columns. (*FRS-Fossil Resource Scarcity; FWE-Freshwater Ecotoxicity; GWP-Global Warming Potential; HCT-Human Carcinogenic Toxicity; HNT-Human Non-Carcinogenic Toxicity; MET-Marine Ecotoxicity; OZH-Ozone Formation, Human Health; OZT-Ozone Formation, Terrestrial Ecosystems; TEC-Terrestrial Ecotoxicity*).

3.4 Conclusion

In this study, we evaluated the techno-environmental potential of rice husk as a resource for bioplastic production relative to open-air combustion (current practice). The results suggest that the bioplastics production reduces the overall impact on human health by 81% ± 0.002 and environmental cost from $2.7 to $0.79 ± 0.07 per kilogram of bioplastic. Later sensitivity analysis showed that sulfuric acid could be a good substitute for nitric acid in the acid hydrolysis process. Further research on the cost analysis (Techno-Economic Analysis) is needed to provide a complete view of this upcycling pathway.

References

Aidoo, R., Kwofie, E. M., & Ngadi, M. O. (2022). Circularity of Cashew Apples: Examining the Product-Process Pathways, Techno-Functional, Nutritional/Phytomolecular Qualities for Food Applications. *ACS Food Science & Technology*, *2*(7), 1051–1066. https://doi.org/10.1021/acsfoodscitech.2c00093

Awulu, J. O., Omale, P. A., & Ameh, J. A. (2018). Comparative analysis of calorific values of selected agricultural wastes. *Nigerian Journal of Technology*, *37*(4), 1141. https://doi.org/10.4314/njt.v37i4.38

Bajo Jr, P. O., & Acda, M. N. (2017). Fuel Pellets from a Mixture of Rice Husk and Wood Particles. *BioResources*, *12*(3), 6618–6628. https://doi.org/10.15376/biores.12.3.6618-6628

Bashtan, S. Yu., Goncharuk, V. V., Chebotareva, R. D., Belyakov, V. N., & Linkov, V. M. (1999). Production of sodium hypochlorite in an electrolyser equipped with a ceramic membrane. *Desalination*, *126*(1–3), 77–82. https://doi.org/10.1016/S0011-9164(99)00156-3

Battegazzore, D., Bocchini, S., Alongi, J., & Frache, A. (2014). Rice husk as bio-source of silica: Preparation and characterization of PLA–silica bio-composites. *RSC Adv.*, *4*(97), 54703–54712. https://doi.org/10.1039/C4RA05991C

Biswas, A., Kim, S., Selling, G. W., & Cheng, H. N. (2014). Conversion of agricultural residues to carboxymethylcellulose and carboxymethylcellulose acetate. *Industrial Crops and Products*, *60*, 259–265. https://doi.org/10.1016/j.indcrop.2014.06.004

Cao, Y., Wu, J., Zhang, J., Li, H., Zhang, Y., & He, J. (2009). Room temperature ionic liquids (RTILs): A new and versatile platform for cellulose processing and derivatization. *Chemical Engineering Journal*, *147*(1), 13–21. https://doi.org/10.1016/j.cej.2008.11.011

Caserini, S., Livio, S., Giugliano, M., Grosso, M., & Rigamonti, L. (2010). LCA of domestic and centralized biomass combustion: The case of Lombardy (Italy). *Biomass and Bioenergy*, *34*(4), 474–482. https://doi.org/10.1016/j.biombioe.2009.12.011

Das, A. M., Ali, A. A., & Hazarika, M. P. (2014). Synthesis and characterization of cellulose acetate from rice husk: Eco-friendly condition. *Carbohydrate Polymers*, *112*, 342–349. https://doi.org/10.1016/j.carbpol.2014.06.006

Di Maria, A., Eyckmans, J., & Van Acker, K. (2020). Use of LCA and LCC to help decision-making between downcycling versus recycling of construction and demolition waste. In *Advances in Construction and Demolition Waste Recycling* (pp. 537–558). Elsevier. https://doi.org/10.1016/B978-0-12-819055-5.00026-7

Du, F., Warsinger, D. M., Urmi, T. I., Thiel, G. P., Kumar, A., & Lienhard V, J. H. (2018). Sodium Hydroxide Production from Seawater Desalination Brine: Process Design and Energy Efficiency. *Environmental Science & Technology*, *52*(10), 5949–5958. https://doi.org/10.1021/acs.est.8b01195

Gonçalves de Moura, I., Vasconcelos de Sá, A., Lemos Machado Abreu, A. S., & Alves Machado, A. V. (2017). Bioplastics from agro-wastes for food packaging applications. In *Food Packaging* (pp. 223–263). Elsevier. https://doi.org/10.1016/B978-0-12-804302-8.00007-8

Goodman, B. A. (2020). Utilization of waste straw and husks from rice production: A review. *Journal of Bioresources and Bioproducts*, *5*(3), 143–162. https://doi.org/10.1016/j.jobab.2020.07.001

Gökçe, E. (2018). Rethinking sustainability: A research on starch based bioplastic. *Journal of Sustainable Construction Materials and Technologies*, *3*(3), 249–260. https://doi.org/10.29187/jscmt.2018.28

Guo, M., & Murphy, R. J. (2012). LCA data quality: Sensitivity and uncertainty analysis. *Science of The Total Environment*, *435–436*, 230–243. https://doi.org/10.1016/j.scitotenv.2012.07.006

Gupta, H., Kumar, H., Kumar, M., Gehlaut, A. K., Gaur, A., Sachan, S., & Park, J.-W. (2019). Synthesis of biodegradable films obtained from rice husk and sugarcane bagasse to be used as food packaging material. *Environmental Engineering Research*, *25*(4), 506–514. https://doi.org/10.4491/eer.2019.191

Hafid, H. S., Omar, F. N., Zhu, J., & Wakisaka, M. (2021). Enhanced crystallinity and thermal properties of cellulose from rice husk using acid hydrolysis treatment. *Carbohydrate Polymers*, *260*, 117789. https://doi.org/10.1016/j.carbpol.2021.117789

Hayatun, A., Jannah, M., Ahmad, A., & Taba, P. (2020). Synthetic Bioplastic Film from Rice Husk Cellulose. *Journal of Physics: Conference Series*, *1463*, 012009. https://doi.org/10.1088/1742-6596/1463/1/012009

Heredia-Guerrero, J. A., Caputo, G., Guzman-Puyol, S., Tedeschi, G., Heredia, A., Ceseracciu, L., Benitez, J. J., & Athanassiou, A. (2019). Sustainable polycondensation of multifunctional fatty acids from tomato pomace agro-waste catalyzed by tin (II) 2-ethylhexanoate. *Materials Today Sustainability*, *3–4*, 100004. https://doi.org/10.1016/j.mtsust.2018.12.001

Huijbregts, M. A. J., Steinmann, Z. J. N., Elshout, P. M. F., Stam, G., Verones, F., Vieira, M. D. M., Hollander, A., Zijp, M., & van Zelm, R. (2016). © *RIVM 2017 Parts of this publication may be reproduced, provided acknowledgement*. 201.

Jamal, S. H., Roslan, N. J., Shah, N. A. A., Noor, S. A. M., Ong, K. K., & Yunus, W. M. Z. W. (2020). Preparation and characterization of nitrocellulose from bacterial cellulose for propellant uses. *Materials Today: Proceedings*, *29*, 185–189. https://doi.org/10.1016/j.matpr.2020.05.540

Jannah, M., Ahmad, A., Hayatun, A., Taba, P., & Chadijah, S. (2019). Effect of filler and plastisizer on the mechanical properties of bioplastic cellulose from rice husk. *Journal of Physics: Conference Series*, *1341*, 032019. https://doi.org/10.1088/1742-6596/1341/3/032019

Jarmkom, K., Khobjai, W., Teachaoei, S., & Shuwisitkul, D. (2021). SYNTHESIS OF CARBOXYMETHYL CELLULOSE FROM RICE HUSK. *International Journal of Applied Pharmaceutics*, 50–54. https://doi.org/10.22159/ijap.2021.v13s1.Y0104

Joo, Y. S., Kim, J., Lee, J., & Chung, I.-J. (2022). Fine particulate matter and depressive symptoms in children: A mediation model of physical activity and a moderation model of family poverty. *SSM – Population Health*, *17*, 101015. https://doi.org/10.1016/j.ssmph.2021.101015

Khazaei, N., Esmaiili, M., Djomeh, Z. E., Ghasemlou, M., & Jouki, M. (2014). Characterization of new biodegradable edible film made from basil seed (Ocimum basilicum L.) gum. *Carbohydrate Polymers*, *102*, 199–206. https://doi.org/10.1016/j.carbpol.2013.10.062

Khoo, H. H., Isoni, V., & Sharratt, P. N. (2018). LCI data selection criteria for a multidisciplinary research team: LCA applied to solvents and chemicals. *Sustainable Production and Consumption*, *16*, 68–87. https://doi.org/10.1016/j.spc.2018.06.002

Korotkova, T., Ksandopulo, S., Donenko, A., Bushumov, S., & Danilchenko, A. (2016). Physical Properties and Chemical Composition of the Rice Husk and Dust.

Oriental Journal of Chemistry, *32*(6), 3213–3219. https://doi.org/10.13005/ojc/320644

Lin, K.-C., Yang, J.-W., Ho, P.-Y., Yen, C.-Z., Huang, H.-W., Lin, H.-Y., Chung, J., & Chen, G.-Y. (2022). Development of an alveolar chip model to mimic respiratory conditions due to fine particulate matter exposure. *Applied Materials Today*, *26*, 101281. https://doi.org/10.1016/j.apmt.2021.101281

Mistry, B. (2016). *Properties and Industrial Applications of Rice Husk*. 3.

Moayedi, H., Aghel, B., Abdullahi, M. M., Nguyen, H., & Safuan A Rashid, A. (2019). Applications of rice husk ash as green and sustainable biomass. *Journal of Cleaner Production*, *237*, 117851. https://doi.org/10.1016/j.jclepro.2019.117851

Moraes, C. A., Fernandes, I. J., Calheiro, D., Kieling, A. G., Brehm, F. A., Rigon, M. R., Berwanger Filho, J. A., Schneider, I. A., & Osorio, E. (2014). Review of the rice production cycle: By-products and the main applications focusing on rice husk combustion and ash recycling. *Waste Management & Research: The Journal for a Sustainable Circular Economy*, *32*(11), 1034–1048. https://doi.org/10.1177/0734242X14557379

Nieuwlaar, E. (2013). Life Cycle Assessment and Energy Systems. In *Reference Module in Earth Systems and Environmental Sciences* (p. B9780124095489014000). Elsevier. https://doi.org/10.1016/B978-0-12-409548-9.01334-8

Okunola A, A., Kehinde I, O., Oluwaseun, A., & Olufiropo E, A. (2019). Public and Environmental Health Effects of Plastic Wastes Disposal: A Review. *Journal of Toxicology and Risk Assessment*, *5*(2). https://doi.org/10.23937/2572- 4061.1510021

Prinz, A. L., & Richter, D. J. (2022). Long-term exposure to fine particulate matter air pollution: An ecological study of its effect on COVID-19 cases and fatality in Germany. *Environmental Research*, *204*, 111948. https://doi.org/10.1016/j.envres.2021.111948

Rashid, S., & Dutta, H. (2021). Physicochemical characterization of carboxymethyl cellulose from differently sized rice husks and application as cake additive. *LWT*, 112630. https://doi.org/10.1016/j.lwt.2021.112630

R. G. de Azevedo, A., Amin, M., Hadzima-Nyarko, M., Saad Agwa, I., Zeyad, A. M., Tayeh, B. A., & Adesina, A. (2022). Possibilities for the application of agro-industrial wastes in cementitious materials: A brief review of the Brazilian perspective.

Cleaner Materials, *3*, 100040. https://doi.org/10.1016/j.clema.2021.100040

Singh, B. (2018). Rice husk ash. In *Waste and Supplementary Cementitious Materials in Concrete* (pp. 417–460). Elsevier. https://doi.org/10.1016/B978-0-08-102156-9.00013-4

Tan, B. L., & Norhaizan, M. E. (2020). *Rice By-products: Phytochemicals and Food Products Application*. Springer International Publishing. https://doi.org/10.1007/978-3-030-46153-9

Wang, H., Gong, X., Miao, Y., Guo, X., Liu, C., Fan, Y.-Y., Zhang, J., Niu, B., & Li, W. (2019). Preparation and characterization of multilayer films composed of chitosan, sodium alginate and carboxymethyl chitosan-ZnO nanoparticles. *Food Chemistry*, *283*, 397–403. https://doi.org/10.1016/j.foodchem.2019.01.022

Zou, Y., & Yang, T. (2019). Rice Husk, Rice Husk Ash and Their Applications. In *Rice Bran and Rice Bran Oil* (pp. 207–246). Elsevier. https://doi.org/10.1016/B978-0-12-812828-2.00009-3

4 Chapter Four: Sustainable Production of Xylo-oligosaccharide from Rice Husks: A Techno-economic and Environmental Performance Assessment

Abstract

Producing xylo-oligosaccharides from rice husks has gained research interest owing to the global attention to prebiotics due to the expanding demands for new food products for human welfare and the predicted rise in investment, making it a lucrative business. A thorough evaluation of the costs for production, environmental performance assessment, and objective decision analysis on the production method to justify the entire RH-to-XOS life cycle is lacking. This deprives future research of guidelines to produce xylo-oligosaccharides. Therefore, in this study, we evaluated the techno-economic and environmental possibility of utilizing rice husks to produce xylo-oligosaccharides. We examined the feasibility and environmental implications of two methods of producing xylo-oligosaccharides from rice husks: autohydrolysis and enzymatic hydrolysis. The results revealed that autohydrolysis is the best method to produce xylo-oligosaccharides, considering the damage to the environment and human health, and profitability (net profits of $ 7.1M and $ 42.4M for pilot and large-scale setups) hence, it is viable to thrive in the market.

4.1 Introduction

Xylo-oligosaccharides (XOS) are polymers of the sugar xylose, produced from the degradation of lignocellulosic biomasses typically via enzymatic hydrolysis or autohydrolysis (da Silva Menezes et al., 2018; Hu et al., 2021; Khat-udomkiri et al., 2018; Parajó et al., 2004). These methods are sometimes preceded by chemical treatments of the biomass used (Khat-udomkiri et al., 2018). XOS are primarily used as prebiotics, which serve the purpose of feeding beneficial bacteria within the digestive tract of organisms, specifically humans (Khat-udomkiri et al.,

2018). They can also reduce glycemic indexes and cholesterol in the blood and promote plant growth (Khat-udomkiri et al., 2018; Samanta et al., 2015). Research on xylo-oligosaccharides has grown over the past decade, owing to the global attention on prebiotics due to the expanding demands for new food products for human welfare, especially among the aged (Samanta et al., 2015). Also, they are the only known nutraceutical that can be produced from lignocellulosic biomasses (Samanta et al., 2015). XOS has been predicted to hit a total investment of $130 million in 2023, making it an excellent venture to focus on (Zhu et al., 2021). Different researchers have hence looked at different technologies for the production, usually in terms of processes (methods and production factors) and lignocellulosic biomass source, with the idea of reducing the degree of polymerization (da Silva Menezes et al., 2017). A lower degree of polymerization of XOS promotes better growth of the bacteria. Most of these studies have focused on agricultural by-products such as hazelnut shell, sugarcane bagasse, and rice husk (RH) as the primary substrate for production. This is because of the pursuit to utilize these by-products for value-added products (Hayatun et al., 2020). Another reason is that these by-products have high contents of the base material (lignocellulose) used for production (da Silva Menezes et al., 2017; Samanta et al., 2015). Rice husk has gained attention among these by-products as a material to be exploited for value-added products due to its abundance and low price, even though it was formerly discarded via combustion (Tan and Norhaizan, 2020). RH also has specific mechanical properties such as high bulk density (90 – 150 kg/m^3), packing density (118.2 – 122 kg/m^3), high calorific value (12.3×10^6 – 16.7×10^6 J/kg), and a characteristic dimension of 8-10 mm long, 2-3 mm wide, and 0.2 mm thick that makes it an excellent fit for such explorations (Awulu et al., 2018; Bajo Jr and Acda, 2017). Table 4.1 shows some studies on XOS production from rice husk. These studies have employed the two main

methods of XOS production, with different adjustments, mainly the pretreatment process. However, a thorough evaluation of the costs for production, environmental performance assessment, and objective decision analysis on the production method to justify the entire RH-to-XOS life cycle is lacking. This deprives future research of a guide to produce xylo-oligosaccharides. The aim of this project is, therefore, to analyze the economic and environmental impacts associated with the two main methods of producing xylo-oligosaccharide from rice husks and evaluate the potential of rice husks as a resource for XOS production. The study will include a Techno-economic Assessment (TEA) and an environmental performance assessment by methods of Life Cycle Analysis (LCA) and Life Cycle Cost Analysis (LCCA). This will serve as preliminary data on the techno-eco-environmental analysis of the commercial production of xylo-oligosaccharides from rice husks.

4.2 Methodology

4.2.1 Process Description and Design

This section provides an overview of the production of xylo-oligosaccharide from autohydrolysis and enzymatic hydrolysis. The production in both methods begins with the preparation of the rice husk. This process typically involves the washing and drying of the husks at a suitable temperature to reduce impurities and the water content in the husks. The dried husks are then milled (via grinding and sieving) into finer particles to boost the reaction rate for the subsequent processes. The typical particle size is around 0.6 mm (Khat-udomkiri et al., 2018). The prepared husks then undergo the process of autohydrolysis or enzymatic hydrolysis to produce the xylo-oligosaccharides. Some experimentations pre-treat the rice husk by chemical means, such as dissolving them in an alkali solution or a basal medium before the autohydrolysis or enzymatic hydrolysis process (da Silva Menezes et al., 2017; Khat-udomkiri et al., 2020). In the

autohydrolysis process, the milled RH is cooked in de-ionized water at a suitable temperature to loosen the organic components of the RH to obtain xylan, the main organic substance for XOS synthesis. XOS is produced afterward by spray drying the liquid phase (containing the xylan) from the de-ionization step. In enzymatic hydrolysis, however, xylan is obtained by treating the RH with an enzyme. This process releases the xylan in the RH. Subsequently, XOS is produced via a series of reactions depending on the experimentation process. A detailed production flow of XOS production from RH, indicating the various methods, inputs, and outputs presented by the literature can be found in Table 4.1.

Table 4.1: Review of the methods used for the synthesis of xylo-oligosaccharide from rice husk

Method			Process	
			Xylan formation	**XOS production**
Autohydrolysis	**REFERENCE**	(Nabarlatz et al., 2005, 2007)	**1.**RH is milled and sieved through a 1 mm screen **2.**RH is treated in de-ionized water at 179 ℃ for 23 min in a 10 L stirred batch reactor. The concentration of RH used was 14.3% (833 g of RH per 5 L of water) **3.**The solid hydrolysis residue is separated from the liquid phase (xylan) via filtration **4.**The residue is washed with warm water and dried at room temperature	**1.**The liquid phase is spray-dried to recover the XOS (8 mL/min at an outlet temperature of 85 ℃ and an airflow rate of 670 L/h) **2.**Spray-dried XOS are purified by dialysis
		(Parajó et al., 2004)	**1.**RH is air-dried and milled to the desired size **2.**RH is suspended in water in a bioreactor under specific operational conditions **3.**The solid residue from the reaction is obtained via filtration from the liquid phase and washed with warm water **4.**The solid residue is air-dried	**1.**Filtrate and liquid phase are dried to obtain XOS
Enzymatic hydrolysis		(Khat-udomkiri et al., 2018)	**1.**RH is dried at 50 ℃ for 12 h **2.**Died RH is milled and sieved through a 0.595 mm sieve **3.**RH powder is mixed with an alkali solution (1.91-22.09% NaOH) in a 1:10 ratio	**1.**1 mL of commercial xylanase solution is added to 9 mL of xylan in 50 mM citric acid-disodium phosphate (Na_2HPO_4) buffer at a pH of 6

		4.The mixture is subjected to a steaming process in an autoclave at 121 ℃ and 15 psi for 45 min **5.**The solution is centrifuged at 5000 rpm for 20 min afterward **6.**The supernatant from centrifugation is acidified with glacial acetic acid to a pH of 5 **7.**Three volumes of 95% ice-cold ethanol are added and centrifuged 4480×g at 4 ℃ for 10 min to precipitate xylan **8.**Precipitated xylan is dried at 55-65 ℃	**2.**The solution is incubated at 50 ℃ **3.**The incubation reaction is terminated by putting the solution in boiling water for about 5 min **4.**The XOS mixture is centrifuged at 6000 rpm for 10 min and filtered through a 0.2 µm syringe filter
	(Khat-udomkiri et al., 2020)	**1.**RH is soaked in 12% NaOH solution in a 1:10 ratio for 45 min at 120 ℃ **2.**The supernatant is acidified with glacial acetic acid to a pH of 5 **3.**Three volumes of ice-cold ethanol are added to the acidified supernatant to precipitate xylan **4.**Xylan pellets are dried in hot-oven air	**1.**Xylan is dissolved in 50 mM citric acid citric acid-disodium phosphate (Na_2HPO_4) buffer at a pH of 6 (1% w/v) **2.**The solution is incubated with commercial xylanase at 120 rpm at 50 ℃ for 2 h **3.**The reaction is stopped by boiling the extract in for 5 min in a water bath **4.**XOS slurry is obtained by a filter paper
		1.RH is milled in a knife mill until 1 mm mean particle size	

	(da Silva Menezes et al., 2018)	***Aspergillus brasiliensis BLf1*** **1.**15 mL basal medium is added to 5 g of RH in a 250 mL flask **2.**The flask is autoclaved at 121 ℃ for 20 min (sterilization) **3.**1×10^{8} spores per gram of the substrate is inoculated into *Aspergillus brasiliensis BLf1* by cell counting with a Neubauer chamber **4.**The culture is incubated at 37 ℃ for 5 days **5.**40 mL of 50 mM sodium acetate buffer (pH of 7) is added to the culture **6.**The culture is homogenized in a shaker at 180 rpm for 30 min	***Aspergillus nidulans XynC A773*** **1.**15 mL basal medium is added to 5 g of RH in a 250 mL flask **2.**The flask is autoclaved at 121 ℃ for 20 min (sterilization) **3.**1×10^{5} spores per gram of the substrate is inoculated into *Aspergillus nidulans XynC A773* by cell counting with a Neubauer chamber **4.**The culture is incubated at 37 ℃ for 5 days **5.**40 mL of 50 mM sodium acetate buffer	**1.**The xylanase extract is concentrated with an Amicon membrane (10 KDa, Millipore) **2.**The set-up is centrifuged at 7000 ×g for 5 min **3.**XOS is extracted by reacting the supernatant with 80% 50 mM sodium acetate (pH of 5) at 50 ℃ and enzyme concentration (100 Ug^{-1} xylan) for either 3 h (*Aspergillus brasiliensis BLf1* extract) or 24 h (*Aspergillus nidulans XynC A773* extract)

	7.The homogenized culture is centrifuged at 3000 ×g at 4 ℃ **8.**The supernatant (xylanase extract) is obtained	(pH of 7) is added to the culture **6.**The culture is homogenized in a shaker at 180 rpm for 30 min **7.**The homogenized culture is centrifuged at 3000 ×g at 4 ℃ **8.**The supernatant (xylanase extract) is obtained	

Basal medium			
Composition	**Amount (gL^{-1})**	**Composition**	**Amount (gL^{-1})**
$NaNO_3$	6	H_3BO_3	11
KCL	0.52	$MnCl_2 \cdot 4H_2O$	5
$MgSO_4 \cdot 7H_2O$	0.52	$FeSO_4 \cdot 7H_2O$	5
KH_2PO_4	1.52	$CoCl_2 \cdot 6H_2O$	1.6
1 pyridoxine, 2 mL of salt trace solution	1	$CuSO_4 \cdot 5H_2O$	1.6
$ZnSO_4 \cdot 7H_2O$	22	$(Mn_4)_6Mo_7O_{24}$	1.1
EDTA (Ethylenediaminetetraacetic acid)	5		

4.2.1.1 Process Design Simulations

A comprehensive methodology was developed to produce XOS from RH from both processes of autohydrolysis and enzymatic hydrolysis based on the details from literature. A model for each system was created following this methodology via SuperPro Designer; version 12.02.2300 Build commercial software (Intelligen, Scotch Plains, NJ, United States of America). The model included a process flow design with the various unit processes and their streams (inputs and outputs). These models were set into a simulation with the same software to obtain a mass and energy balance which was used for further techno-economic analysis and environmental impact assessment. A pilot-scale experimental input with a rice processing mill of a distance, 20 km away from the processing plant for each method was assumed. This distance was selected because a higher or lower alternative will have a similar effect (Yeboah et al., 2022). A processing capacity of 3,270 tons RH/annum with an estimated total batch number (annual time for operation) of 990 per year (10 tons RH/batch with 3 batches per day for 330 days) was selected for the techno-economic analysis. The process pathways for the methodologies are illustrated in Figure 4.1A. The detailed processes for autohydrolysis and enzymatic hydrolysis employed for the simulations are described by Nabarlatz et al. (2007) and Khat-udomkiri et al. (2018), respectively.

4.2.2 Techno-economic Assessment

In this section, the technological and commercial feasibility of the two production systems is examined via the method of techno-economic assessment (TEA). TEA provides certain economic parameters that determine whether the system will thrive on a larger scale (Adhikari et al., 2022; Panagopoulos, 2022). The analysis was performed based on the mass-energy principle via SuperPro Designer. The design for each method was created based on the unit procedures

suggested by previous research. From the process description, the autohydrolysis model design included a truck, silo, washing unit, tray dryer, grinding unit, vibrating screen, reactor, microfiltration unit, and spray dryer, with a total production rate of 1,400 tons of XOS per annum as computed from the material balance analysis. The enzymatic hydrolysis model on the other side included a similar truck, silo, washing unit, tray dryer, grinding unit, and vibrating screen as the autohydrolysis process. However, it also included five reactors, each performing different tasks. The production rate for this system was 1,200 tons of XOS per annum. The complete process models are shown in the supplementary document for autohydrolysis and enzymatic hydrolysis. Details of each process unit for both methods are summarized in Table 4.2 below. The flowchart of each system is shown in Appendix B.

Table 4.2: Unit procedures for autohydrolysis and enzymatic hydrolysis systems

Method	Unit Process	Equipment	Process description
Autohydrolysis	Transportation	Truck	Shipment of 10 tons of rice husk (batch) from the farm through 20 km to the production site for a total shipment of 327 per year
	Storage	Silo *(vessel volume of 125 m^3)*	Transported rice husks are temporarily stored in a silo before XOS production
	Washing	Washing unit	Dirt and other inorganic particles are removed by washing rice husks with 1.2 m^3 of water per batch
	Drying	Tray dryer *(tray area of 80 m^2)*	Free water and some percentage of water content in rice husks are removed by drying at an evaporation rate of 0.021 kg/m^2h
	Grinding	Grinding unit *(rated throughput of 1.7 ton/h)*	Dried rice husks are crushed by a grinder at a specific power of 6 kW/(kg/h)
	Sieving	Vibrating screen *(1 mm screen size)*	Ground rice husks are passed through a screen with a mesh size of 1 mm to obtain desired RH particle size for subsequent processes
	De-ionization	Stirred Reactor *(vessel volume of 17 m^3)*	Rice husk particles are dissolved in 60002.4 L of de-ionized water per batch at a temperature of 179 ℃ in a reactor with a 100% set conversion rate to obtain xylan (in liquid phase)
	Filtration	Microfiltration unit *(membrane area of 73 m^2)*	Undissolved solid residues are filtered from the liquid phase with a microfilter at a 5 % product denaturation

	Spray drying	Spray dryer	The liquid phase of the de-ionization reaction is spray dried to precipitate XOS by a spray dyer with a 5 % dried product LOD (loss on drying)
Enzymatic hydrolysis	Transportation	Truck	Shipment of 10 tons of rice husk (batch) from the farm through 20 km to the production site for a total shipment of 327 per year
	Storage	Silo *(vessel volume of 125 m^3)*	Transported rice husks are temporarily stored in a silo prior to XOS production
	Washing	Washing unit	Dirt and other inorganic particles are removed by washing rice husks with 1.2 m^3 of water per batch
	Drying	Tray dryer *(tray area of 80 m^2)*	Free water and some percentage of water content in rice husks are removed by drying at an evaporation rate of 0.021 kg/m^2h
	Grinding	Grinding unit *(rated throughput of 1.7 ton/h)*	Dried rice husks are crushed by a grinder at a specific power of 6 kW/(kg/h)
	Sieving	Vibrating screen *(1 mm screen size)*	Ground rice husks are passed through a screen with a mesh size of 1 mm to obtain desired RH particle size for subsequent processes
	Alkali treatment	Stirred Reactor *(vessel volume of 34.3 m^3)*	Rice husk particles are dissolved in sodium hydroxide solution (22% NaOH) at a temperature of 121 ℃ in a reactor with a 100% set conversion rate
	Acidification	Stirred Reactor *(vessel volume of 18.4 m^3)*	The supernatant is reacted with 8.6 m^3 of glacial acetic acid (99% CH_3COOH) at room temperature with a set conversion rate of 100%

	Ethanol treatment	Stirred Reactor *(vessel volume of 16.7 m^3)*	8.9 m^3 of 95% ice-cold ethanol (4 ℃) is added to the acidified mixture to precipitate xylan at a 100% conversion rate. Glycol was used as a heat transfer agent.
	Enzyme treatment/ Incubation	Bioreactor *(vessel volume of 8.5 m^3)*	Xylan is dissolved in 2 m^3 of McIlvaine buffer at a pH of 6 (0.2 M Na_2HPO_4; 0.1 M $C_6H_8O_7$), and 0.8 m^3 of xylanase solution is added. The solution is incubated at 50 ℃
	Boiling/Centrifugation	Stirred Reactor *(vessel volume of 7.8 m^3)*	4.1 m^3 of boiling water is used to boil the mixture to terminate the incubation reaction and afterward centrifuged at 6000 rpm for 10 min to produce XOS

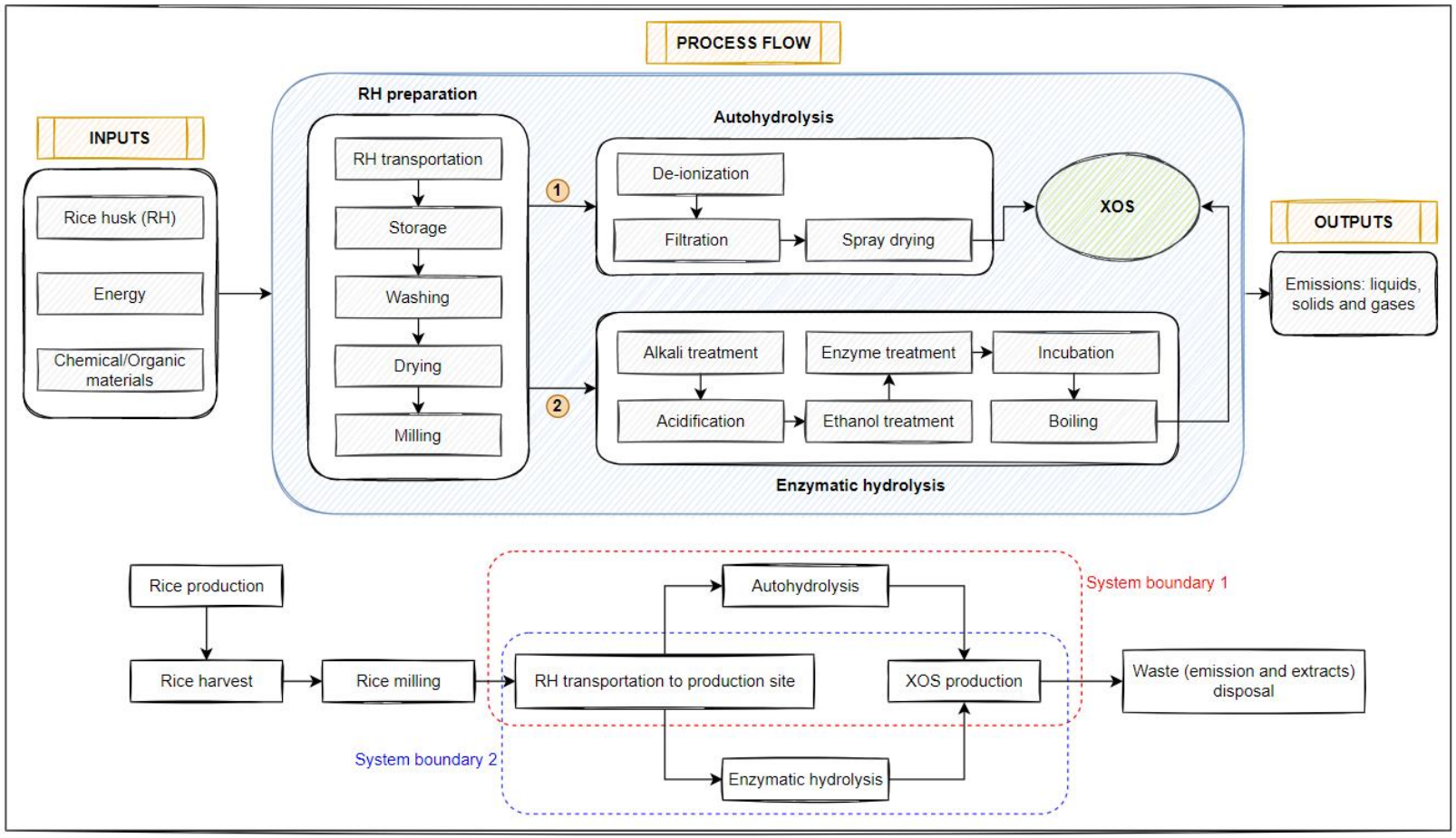

Figure 4.1: (A) Process flowchart for XOS production from RH – (1) Autohydrolysis, (2) Enzymatic hydrolysis; (B) Preferred system boundaries for XOS production from Rice Husks

4.2.3 Environmental Performance Assessment

In this section, the different emissions, resources used, and other environmental and health implications of the production streams are assessed via LCA. LCA can be done in three forms: conceptual, simplified, or detailed (Hoogervorst, 2004). Conceptual LCA relies on qualitative inventory to assess the impacts associated with the elements or materials of the product system. This is the simplest type of LCA, hence the results it presents are not in-depth. The simplified form of LCA on the other hand relies on quantitative data for the analysis, however, these data are generic and basic. Hence, the results it presents, even though are more reliable than those of the conceptual LCA, are not enough for a proper justification of a system. The final type of LCA, detailed LCA, utilizes system-specific quantitative data for the analysis (Hoogervorst, 2004). This type of LCA is the most reliable, considering a review of a specific product such as that in this study. The detailed approach is therefore employed in this research. The OpenLCA software, version 1.10.3 (GreenDelta, GmbH, Berlin, Germany), was used for the assessment per the set system boundaries (Figure 1B). The assessment was performed following the four main phases of detailed LCA, designed by the International Standards Organization (ISO 14040): goal and scope definition, inventory analysis, impact assessment, and results interpretation.

4.2.3.1 Goal and Scope Definition

The goal of this study was to determine the environmental impacts of xylo-oligosaccharide production from rice husk via autohydrolysis and enzymatic hydrolysis. A functional unit of 1 kg XOS produced was selected for the assessment, with preferred system boundaries shown in Figure 4.1B. The system boundary excluded rice production, rice harvest, and the rice milling process of the rice value chain. The analysis is a gate-to-gate study, considering rice husk transportation (from rice milling) to XOS production.

4.2.3.2 Life Cycle Inventory

An inventory in the form of an Excel spreadsheet was created to compile the relevant data required for the analysis. As a detailed LCA, the inventory was specific on the various inputs, outputs, and energy required for each process. The Ecoinvent database, version 3.71, and information from literature were used to compile this inventory. These data were used as flows for the assessment. Other information was compiled from Nabarlatz et al. (2007), Parajó et al. (2004), Khat-udomkiri et al. (2018), (da Silva Menezes et al., 2018). Details of this inventory for both production systems can be found in the Appendix B.

4.2.3.3 Environmental Impact Assessment

This phase evaluates the environmental impacts associated with the various elementary flows (inventory) (Nieuwlaar, 2013). The Life Cycle Impact Assessment (LCIA) was computed based on the ReCiPe 2016 version 1.1, Hierarchist version (Huijbregts et al., 2016). Both the Midpoint and Endpoint functions of this method were used for the assessment, as they present a complete understanding of the life cycle impacts when viewed together. The Midpoint method presents results on the emissions along the cause-effect chain before their implications on the different areas of protection (AoPs) (final damage), whereas the Endpoint method presents the effects on these areas of protection (human health, ecosystem, and resource) from the results of the Midpoint method. Additionally, for the Midpoint assessment, a normalization set (World (2010) H) was selected to standardize the different impact categories because of the different reference units the impact categories are presented in. This creates a base for comparison between these impacts.

4.2.3.4 Environmental Cost Assessment

Environmental Cost Assessment presents a unique metric (money) that complements the overall environmental impact. It assigns weights to the individual impact categories by translating them into monetary units (Yeboah et al., 2022). The Environmental Prices monetization method was used for this assessment. The impacts were monetized by multiplying these factors by the impact scores from the LCA Midpoint results. Factors for some impact categories were missing from this method, hence, were not included in the calculation. Others such as particulate matter formation did not have their factors in the corresponding units from the LCIA so were first converted into the units presented in Environmental Prices before the monetization. The results were afterward converted from Euros (€) into US Dollars ($) with a currency equivalent factor of €1 = $1.02 (November 2022) according to Forbes Advisor (Forbes, 2023). The factors for the Environmental Prices monetization method are presented in Table 3.2.

4.3 Results and Discussion

4.3.1 Techno-economic Assessment

The economic evaluations for the production systems provided by SuperPro Designer, following the mass and energy balance analysis included a total capital investment cost, operation and maintenance cost, energy requirements and costs, and revenues generated (before and after tax) per 2023 prices in US Dollar ($). The total capital investment cost encompassed costs associated with direct fixed capital (equipment purchase cost, installation cost, process piping cost, instrumentation cost, insulation cost, electrical cost, cost of buildings, yard improvements cost, and auxiliary facilities cost), working capital, and startup capital. For the autohydrolysis system, the direct fixed capital cost and working capital were $ 9.2M and $ 2.3M, respectively. The annual operating cost was $ 56.5M, with 29.21% of the cost emanating from raw materials

purchase ($ 16.5M), 28.36% from utilities/energy ($ 16.0M), 11.36% from sales expenses ($ 6.4 M), 11.36% from research and development ($ 6.4M), 6.82% from maintenance ($ 3.9M), 5.24% from operating labor ($ 3.0M), and 2.95% from direct plant overheads ($ 1.6 M). Other costs include administrative expenses ($ 888,264), the cost of supervision ($ 740,220), insurance ($ 641,792), local taxes ($ 256,717), and royalties ($128,358). On the other hand, a direct fixed cost and working capital of $ 16.5M and $ 4.1 M, respectively, were recorded for the enzymatic hydrolysis system. The annual cost of operations was also recorded as $ 54.4M, with raw material purchases contributing about 30.31% of the cost ($ 16.5M). The recorded cost of utilities was $ 19.9M (36.6%), maintenance was $ 6.9M (12.70%), direct plant overhead was $ 1.7M, and operating labor was $ 2.9M (5.41%). For both systems, the cost of rice husk is set at $ 5.00. Table 4.3 shows the executive summary of both pilot scale setups.

4.3.1.1 Annual Profitability and Revenue

Considering a selling price of $ 48.00/ kg of xylo-oligosaccharide (based on 2023 prices), the total revenue generated from the autohydrolysis system can reach up to $ 65.9M, with a gross profit of $ 9.4M. After-tax deduction and other factors such as product value depreciation, however, a yearly net profit of $ 7.1M and internal rate of return (IRR) of 46.89% were recorded. The pilot-scale production of xylo-oligosaccharide by autohydrolysis is economically feasible, with a payback time of about 2 years. For enzymatic hydrolysis, the total revenue can reach up to $ 58.1M, with gross and net profits of $ 3.6M and $ 2.7M, respectively. An IRR and payback time of 10.07% and 8 years were also recorded. Similar research by Otieno and Ahring (2012) states that this low IRR and long payback time is due to the high costs, higher concentrations of monomeric sugars, and low product yields associated with the enzymatic hydrolysis system. The production system is, however, economically feasible.

4.3.1.2 Sensitivity Analysis

The scale of a large system will likely affect the supply and demand of a product, the influence of government, speculation, and expectation, the extent of competition, and other important economic parameters, such as the total capital investment cost, operation and maintenance cost, energy requirements and costs, revenues generated associated with the setup of that system (business). This is because of the variations in operations, material input (quantity), and product output (quantity) of the system. In the present study, the production systems were set to a pilot scale considering a small rice husk input and a corresponding small xylo-oligosaccharide output. This section, however, examines the economic parameters for the case of a large-scale production system. Data on the annual rice husk yield was collected from the United States Department of Agriculture for Arkansas for a 20-year period and this was used to estimate the rice husk input for a large system. A rice husk value of 29,430 tons per year was estimated as system feed. Similar approaches to section 2.2 were followed to compute the technological and commercial feasibilities of the two production systems. Table 4.3 shows the executive summary of both large-scale setups. Considering a similar selling price of $ 48.00/ kg of xylo-oligosaccharide, the total revenue generated from the autohydrolysis system can reach up to $ 593.3M, with a gross and net profit of $ 56.5M and $ 42.4M. An IRR of 71.38% was also recorded. Like the pilot-scale system, the large-scale system for the autohydrolysis process is economically feasible, however, the payback time is about 1 year, 8 months. For the enzymatic process, the total revenue can reach up to only $ 522.7M, with gross and net profits of $ 13.9M and $ 10.4M, respectively. An IRR of 16.74% was recorded, with a payback time of 6 years, indicating that this system is more economical compared to its pilot scale setup.

Table 4.3: Executive summary of pilot- and large-scale autohydrolysis and enzymatic hydrolysis systems

Executive Summary	**Pilot-scale systems**		**Large-scale systems**	
	Autohydrolysis	**Enzymatic hydrolysis**	**Autohydrolysis**	**Enzymatic hydrolysis**
Total Capital Investment	15,100,976 $	27,108,529 $	59,366,506 $	62,361,353 $
Operating Cost	56,482,560 $/yr	54,435,543 $/yr	536,804,277 $/yr	508,760,546 $/yr
Revenues	65,923,200 $/yr	58,075,200 $/yr	593,308,800 $/yr	522,676,800 $/yr
Cost Basis Annual Rate	1,373,400 kg MP/yr	1,209,900 kg MP/yr	12,360,600 kg MP/yr	10,889,100 kg MP/yr
Unit Production Cost	41.13 $/kg MP	44.99 $/kg MP	43.43 $/kg MP	30 $/kg MP
Net Unit Production Cost	41.13 $/kg MP	44.99 $/kg MP	43.43 $/kg MP	30 $/kg MP
Unit Production Revenue	48.00 $/kg MP	48.00 $/kg MP	48.00 $/kg MP	48.00 $/kg MP
Gross Margin	14.32%	6.27%	9.52%	36.81%
Payback Time	2 yr	8 yr	1.7 yr	5 yr
IRR (After Taxes)	46.89%	10.07%	71.38%	16.74
NPV (at 7.0% Interest)	59,702,930.66 $	9,999,706.50 $	376,304,326.02 $	63,483,341.64 $

4.3.2 Environmental Performance Assessment

The ReCiPe 2016 impact assessment method presented eighteen different midpoint impact categories, including ozone formation (human health (OZH) and terrestrial ecosystems (OZT)) in kg NO_x-eq, human carcinogenic toxicity (HCT), human non-carcinogenic toxicity (HNT) in kg 1,4-DCB, marine ecotoxicity (MRE) in kg 1,4-DCB and global warming (GWP) in kg CO_2-eq, and three endpoint impact categories (AoPs) including human health damage in Daily-Adjusted Life Years (DALY), ecosystem damage in species per year (species.yr) and resource scarcity in US dollars (USD). Also, the results of the impact contributions by the different processes are presented in this section.

4.3.2.1 Midpoint Impact Indicators

Figure 4.2 illustrates the results of the midpoint impacts for autohydrolysis and enzymatic hydrolysis production systems. For the autohydrolysis system, marine ecotoxicity gave the highest impact of 41%. This was proceeded by freshwater ecotoxicity (25%), human carcinogenic toxicity (20%), terrestrial ecotoxicity (5%), human non-carcinogenic toxicity (4%), and water consumption (2%). Ozone formation (Terrestrial ecosystems), ozone formation (human health), global warming, and fossil resource scarcity gave a combined impact of about 2%. This same trend was observed for the enzymatic hydrolysis system. For this system however, marine ecotoxicity gave an impact of 42%, followed by freshwater ecotoxicity with 31%, human carcinogenic toxicity (20%), terrestrial ecotoxicity (5%), human non-carcinogenic toxicity (1%), and water consumption, ozone formation (Terrestrial ecosystems), ozone formation (human health), global warming and fossil resource scarcity with a combined impact of about 1%. Overall, the impacts associated with the enzymatic hydrolysis system are significantly different (higher) than those of the autohydrolysis system, as shown in Table 4.4. A

permutation test, with a 95% set confidence interval (CI), was run with R-software to prove this observation. The null hypothesis set was as below (Equation 4.1).

$$\bar{x}_A - \bar{x}_E = 0 \qquad \text{(Equation 4.1)}$$

Where $\bar{x}_A$ is the mean impact of autohydrolysis and $\bar{x}_E$ is the mean impact of enzymatic hydrolysis. The test was completed after 5000 replications. A p-value of 0.00039 (less than 0.05 CI) was obtained, indicating that the null hypothesis is false, implying a difference in the impact results between the two systems. The impacts for both production systems are, however, better than those from rice husk combustion. Research by (Yeboah et al., 2022) proves this, as the study shows burning rice husk gives about 9% GWP (approximately 99% and 66% more than autohydrolysis and enzymatic hydrolysis, respectively).

Table 4.4: LCA midpoint results for autohydrolysis and enzymatic hydrolysis

Impact category	Reference unit	Autohydrolysis	Enzymatic hydrolysis
Fine particulate matter formation	kg PM2.5 eq	1.09E-06	2.58E-03
Fossil resource scarcity	kg oil eq	8.12E-06	1.39E-02
Freshwater ecotoxicity	kg 1,4-DCB	6.25E-04	1.50E+00
Freshwater eutrophication	kg P eq	4.33E-06	2.03E-02
Global warming	kg CO_2 eq	1.14E-05	4.17E-03
Human carcinogenic toxicity	kg 1,4-DCB	5.05E-04	9.71E-01
Human non-carcinogenic toxicity	kg 1,4-DCB	9.29E-05	2.25E-01
Ionizing radiation	kBq Co-60 eq	1.07E-06	3.38E-03
Land use	m^2a crop eq	7.79E-08	1.49E-03
Marine ecotoxicity	kg 1,4-DCB	1.02E-03	2.02E+00
Marine eutrophication	kg N eq	6.15E-08	3.99E-03
Mineral resource scarcity	kg Cu eq	5.12E-10	1.05E-06
Ozone formation, Human health	kg NO_x eq	1.23E-05	4.35E-03
Ozone formation, Terrestrial ecosystems	kg NO_x eq	2.04E-05	5.25E-03
Stratospheric ozone depletion	kg CFC11 eq	1.39E-07	1.15E-03
Terrestrial acidification	kg SO_2 eq	1.60E-06	4.41E-03
Terrestrial ecotoxicity	kg 1,4-DCB	1.22E-04	6.77E-02
Water consumption	m^3	5.09E-05	8.00E-03

4.3.2.2 Process contributions to impacts

Each unit process influences the overall environmental impacts associated with the life cycle of a production system. The impacts by each of these processes amass the total score for each of the different impact categories, however, some of these contributions are insignificant depending on the impact category in question. Figure 4.3 illustrates the implications of the different unit

processes on the impacts categories for autohydrolysis and enzymatic hydrolysis. The analysis centered on the top nine impact categories for each product system.

1.1.1.1 Autohydrolysis

De-ionization, drying, and transportation gave the most significant contributions to almost all the different impact categories (Figure 4.3). For global warming, ozone formation (terrestrial ecosystems), and ozone formation (human health), drying gave the highest impact contributions of 82.8%, 77.8%, and 68.8% respectively, followed by transportation with 11.7%, 19.1%, and 26.8% respectively. This trend was observed due to the release of substances such as CO_2, CO, water vapor, and some associated NO_x compounds from these processes. De-ionization followed in the sequence with 5.2%, 3.0%, and 2.3% respectively, with the remaining processes giving a combined impact of less than 0.5%, 0.1%, and 0.1% to the impact categories respectively. For human non-carcinogenic toxicity, freshwater ecotoxicity, and marine ecotoxicity, de-ionization contributed to 50.0%, 65.3%, and 61.1% respectively. Transportation followed with 47.6%, 28.5%, and 33.1% respectively and then drying with 1.9%, 4.8%, and 4.4% correspondingly. Similarly, the collective impact contributions by the remaining processes were insignificant. Transportation gave the highest contributions of 51.9% and 84.9% to human carcinogenic toxicity and terrestrial ecotoxicity respectively. Following this was de-ionization with 46.6% and 12.9% respectively, and finally drying, with 1.0% and 1.7% contributions respectively. The impact contributions by the remaining processes were insignificant in these impact categories as well, nevertheless, for water consumption, de-ionization and washing had the most contributions of 73.5% and 26.3% respectively. From these results, it is evident that de-ionization was the critical process for the product system.

1.1.1.2 Enzymatic hydrolysis

The major contributions to the impact categories for this product system were recorded by enzyme treatment, ethanol treatment, acidification, and alkali treatment. This was because of the different chemical components present in the execution of the processes. From the illustration (Figure 4.3), acidification put up the highest impact contributions for all the impact categories except for terrestrial ecotoxicity, human non-carcinogenic toxicity and water consumption. The major contributor for these impacts was ethanol treatment with 54.4%, 53.9% and 68.8% respectively. This was followed by acidification (32.1%, 31.4% and 19.1% respectively), alkali treatment (7.8%, 9.7% and 9.4% respectively) and enzyme treatment (5.5%, 4.9% and 2.5% respectively). Considering marine ecotoxicity, acidification contributed 58.2% of the total impact, proceeded by alkali treatment with 16.8%, ethanol treatment (15.4%) and enzyme treatment (9.4%). The rest of the processes gave a collective contribution of less than 1%. Similarly for freshwater ecotoxicity, acidification gave the highest impact of 53.3%, and then ethanol treatment (22.6%), alkali treatment (15.3%) and enzyme treatment (8.5%). For human carcinogenic toxicity, acidification gave 55.1% contribution, followed by enzyme treatment, alkali treatment and ethanol treatment with 16.6%, 15.8% and 12.4% respectively. Lastly, for ozone formation, terrestrial ecotoxicity and fossil resource scarcity, acidification had the highest impact of 48.8%, 44.1% and 75.7% respectively. This affirms that acidification is the most critical process for this product system.

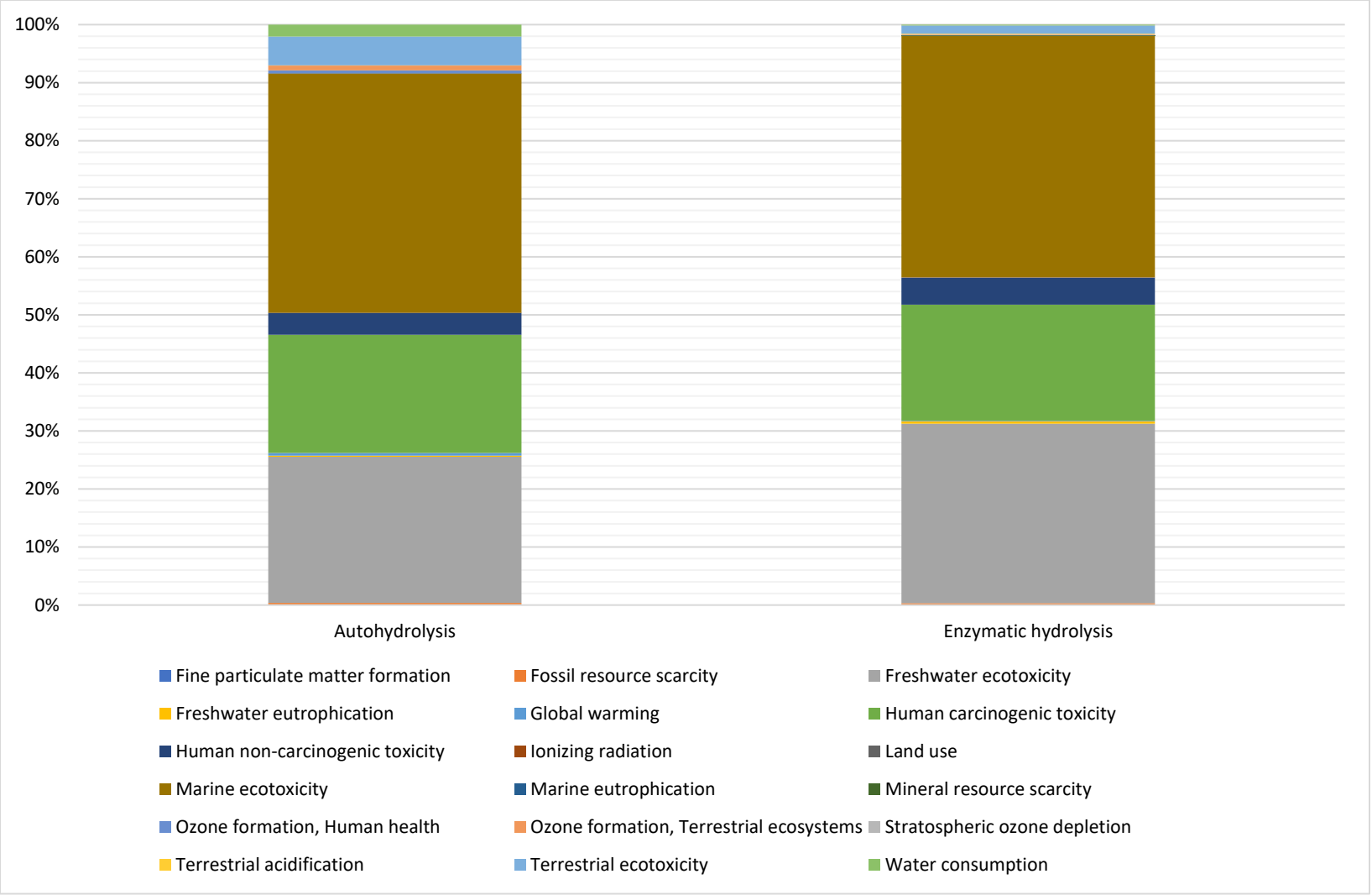

Figure 4.2: Comparative midpoint impacts for autohydrolysis and enzymatic hydrolysis

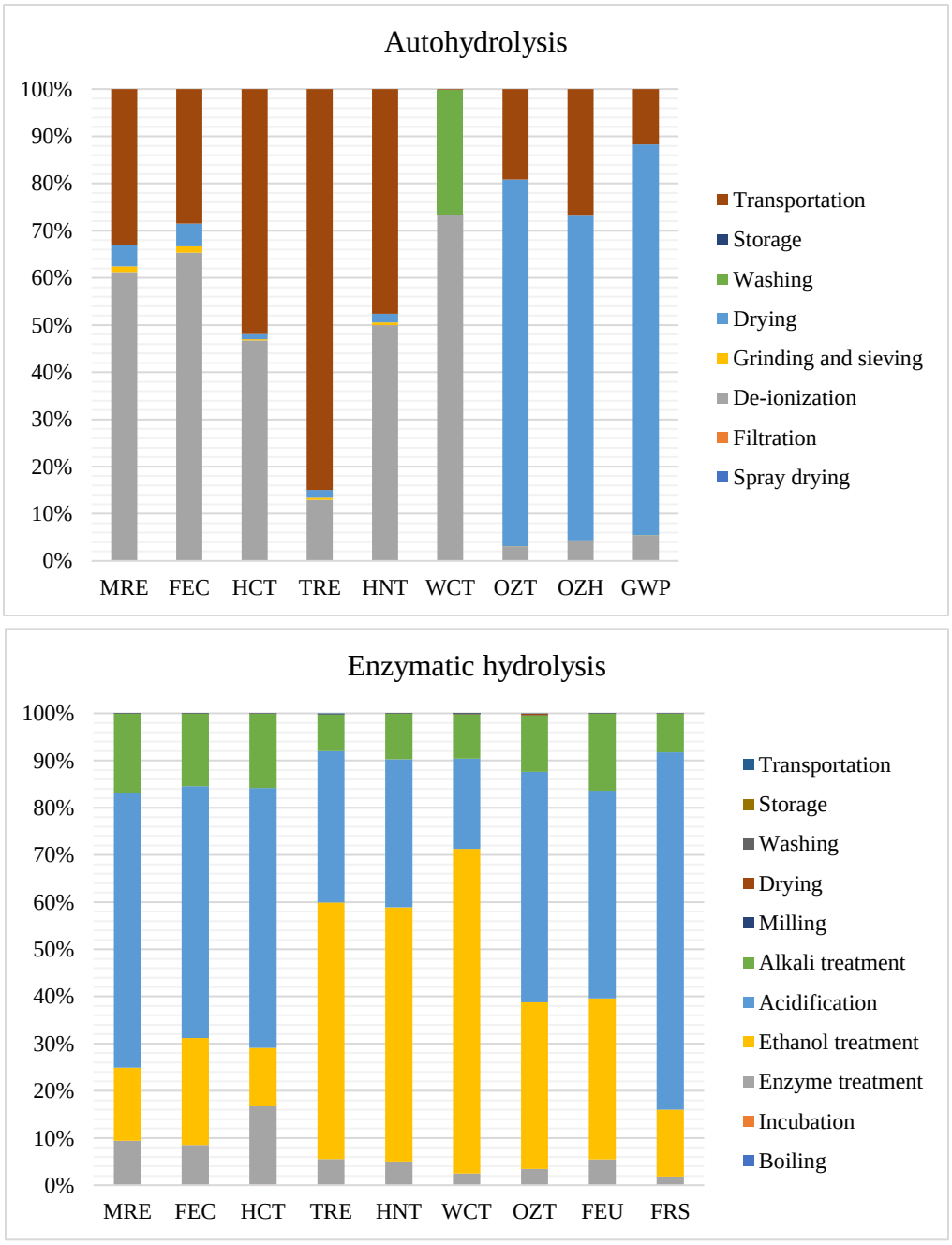

Figure 4.3: Process contribution impacts for autohydrolysis and enzymatic hydrolysis

4.3.2.3 Endpoint Indicators

Table 4.5 summarizes the results for the three main endpoint areas of protection (AoPs) for both production systems, namely: human health damage (in Disability-Adjusted Life Years, DALY),

ecosystem damage (in species.yr), and resource scarcity (in USD2013). These categories are dependent on different midpoint indicators. Human health damage depends on the impacts of global warming, ozone formation (human health), human carcinogenic and non-carcinogenic toxicity, and fine particulate matter formation, ecosystem damage accounts for the impacts from ozone formation (terrestrial ecosystems), freshwater ecotoxicity, marine ecotoxicity, terrestrial ecotoxicity and terrestrial acidification, and finally, the resource scarcity category depends on the impacts of fossil resource scarcity and mineral resource scarcity. The results show that enzymatic hydrolysis had the highest impact on all the three AoPs, with 1.87×10^{-1} DALY damage to human health, 5.30×10^{-4} species.yr damage to ecosystem and 8.9×10^{-3} USD2013 damage to resources, however, the highest of these was the damage to human health. This is because of the high contributions recorded from the formation of fine particulate matter (endpoint) (Kim et al., 2015; Pozzer et al., 2019; Prinz and Richter, 2022). Autohydrolysis on the other hand recorded 5.89×10^{-4} DALY damage to human health, 2.13×10^{-6} species.yr damage to ecosystems and 1.88×10^{-3} USD2013 damage to resources. Resources were the most affected AoPs in this scenario, and it is due to the high utilization of fossil resources from sub-unit processes in the product system.

Table 4.5: Endpoint AoPs for autohydrolysis and enzymatic hydrolysis

Endpoint AoP	Contributing midpoint category	Reference unit	Impact value	
			Autohydrolysis	Enzymatic hydrolysis
Human health damage	Fine particulate matter formation	DALY	7.33E-05	8.30E-02
	Global warming, Human health		3.55E-04	6.19E-02
	Human carcinogenic toxicity		1.95E-05	1.79E-02
	Human non-carcinogenic toxicity		1.33E-05	1.53E-02
	Ionizing radiation		1.83E-08	2.76E-05
	Ozone formation, Human health		9.71E-07	1.63E-04
	Stratospheric ozone depletion		1.86E-08	7.34E-05
	Water consumption, Human health		1.27E-04	9.48E-03
	Total		**5.89E-04**	**1.88E-01**
Ecosystem damage	Freshwater ecotoxicity	species.yr	2.23E-09	2.55E-06
	Freshwater eutrophication		7.91E-09	1.76E-05
	Global warming, Freshwater ecosystems		2.92E-11	5.10E-09
	Global warming, Terrestrial ecosystems		1.07E-06	1.87E-04
	Land use		1.79E-08	1.63E-04
	Marine ecotoxicity		4.66E-10	4.38E-07
	Marine eutrophication		2.02E-12	6.24E-08
	Ozone formation, Terrestrial ecosystems		1.96E-07	2.41E-05
	Terrestrial acidification		5.84E-08	7.66E-05
	Terrestrial ecotoxicity		6.08E-09	1.60E-06
	Water consumption, Aquatic ecosystems		3.44E-11	2.58E-09
	Water consumption, Terrestrial ecosystem		7.70E-07	5.76E-05
	Total		**2.13E-06**	**5.30E-04**
Resource scarcity	Fossil resource scarcity	USD2013	1.80E-03	8.87E-03
	Mineral resource scarcity		8.00E-05	5.80E-05
	Total		**1.88E-03**	**8.93E-03**

4.3.3 Comparative Environmental Impact Cost Assessment

The factors provided by the Environmental Prices monetization method were used to normalize (monetize) the different midpoint impacts, however, some factors were not provided for some of the impact categories. Nevertheless, this will not compromise the comparison of the overall cost values between the production systems, as the environmental implications of these impacts are minimal. The costs associated with the environmental impacts of both product systems are illustrated in Table 4.6 below. For both systems, terrestrial ecotoxicity had the highest cost of implication, $ 1.12 and $ 1.66 for autohydrolysis and enzymatic hydrolysis, respectively. On the other hand, marine eutrophication and land use recorded the least cost of implication for autohydrolysis and enzymatic hydrolysis, respectively. Overall, the costs associated with the environmental impacts of enzymatic hydrolysis were higher than those of autohydrolysis, giving a total cost of $ 2.17 against $ 1.13. These values are nevertheless acceptable, as a recent study by (Yeboah et al., 2022) indicates that burning an equivalent amount of rice husk will give an environmental impact cost of $ 2.72. This means the cost of combusting rice husk is reduced by 20.2% and 57.7% by producing xylo-oligosaccharide via autohydrolysis and enzymatic hydrolysis, respectively.

Table 4.6: Environmental cost for autohydrolysis and enzymatic hydrolysis product systems

Impact categories	Reference unit	Cost in dollars ($)	
		Autohydrolysis	Enzymatic hydrolysis
Marine ecotoxicity	kg 1,4-DCB	0.00001	0.01523
Freshwater ecotoxicity	kg 1,4-DCB	0.00003	0.05531
Human carcinogenic toxicity	kg 1,4-DCB	0.00013	0.08853
Terrestrial ecotoxicity	kg 1,4-DCB	1.12469	1.66401
Human non-carcinogenic toxicity	kg 1,4-DCB	0.00126	0.02053
Water consumption	m3	–	–
Ozone formation, Terrestrial ecosystems	kg NOx eq	–	–
Ozone formation, Human health	kg NOx eq	–	–
Global warming	kg CO2 eq	0.00529	0.02427
Fossil resource scarcity	kg oil eq	–	–
Freshwater eutrophication	kg P eq	0.00001	0.03843
Terrestrial acidification	kg SO2 eq	0.00050	0.03364
Fine particulate matter formation	kg PM2.5 eq	0.00080	0.07430
Ionizing radiation	kBq Co-60 eq	–	–
Stratospheric ozone depletion	kg CFC11 eq	0.00000	0.14488
Land use	m2a crop eq	0.00006	0.00019
Marine eutrophication	kg N eq	0.00000	0.01264
Mineral resource scarcity	kg Cu eq	–	–
Total		**1.13278**	**2.17196**

4.3.4 Uncertainty Analysis

Selecting the correct variables for a model is critical in decision-making problems due to the vast number of possibilities (Yeboah et al., 2022). There is therefore the need to evaluate any uncertainties within any selected variable of the model to ensure credibility in the results from any simulation on the model. This section investigates the uncertainties associated with the Life Cycle Impact Assessment results for each product system. The openLCA was used to run a Monte-Carlo simulation with 1000 iterations and the results were used to graph a bar chart (with error ranges) (Figures 4A and 4C) and a hypothesized probability distribution (lognormal)

(Figures 4B and 4D). The error bars represent the uncertainties (range) in LCIA profiles for the different midpoint impact categories in terms of the ratio of the 5^{th} and 95^{th} percentile to their mean value. The average range of uncertainty was 10.2% to 11.1% for autohydrolysis and 11.2% to 13.4% for enzymatic hydrolysis, however, stratospheric ozone depletion LCIA profile recorded the highest uncertainty for autohydrolysis whereas that for enzymatic hydrolysis was the marine ecotoxicity LCIA profile. These may be due to the large uncertainties in the major toxic drivers, trichlorofluoromethane for stratospheric ozone depletion and 1,4-dichlorobenzene for marine ecotoxicity. The variances in the remaining impact categories were minimal. The lognormal probability distribution was based on the water consumption impacts of the product systems. The results indicate a good representation (credibility) of the LCIA profiles – *FPM-fine particulate matter formation, FRS-fossil resource scarcity; FEC-freshwater ecotoxicity; FEU-freshwater eutrophication; GWP-global warming (GWP); HCT-human carcinogenic toxicity; HNT-human non-carcinogenic toxicity; INR-ionization radiation; LDU-land use; MEU-marine eutrophication; MEC- marine ecotoxicity; MRS-mineral resource scarcity; OZH-ozone formation, human health; OZT-ozone formation, terrestrial ecosystems; SZD-stratospheric ozone depletion; TRA-terrestrial acidification; TEC-terrestrial ecotoxicity; WCT-water consumption.*

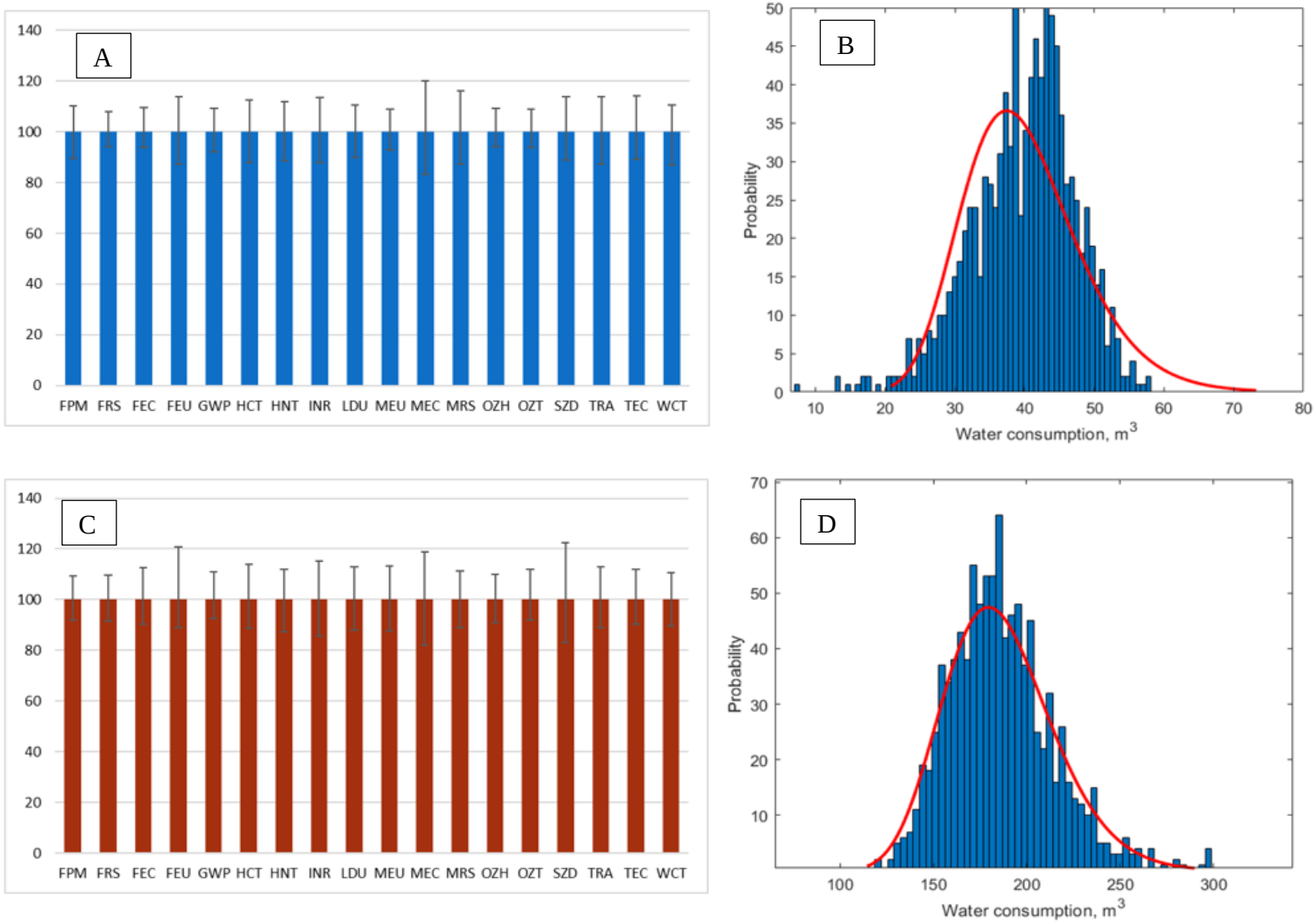

Figure 4.4: Uncertainty analysis: (A) and (C): Uncertainty in LCIA profiles for autohydrolysis and enzymatic hydrolysis respectively; (B) and (D): Probability distribution of water consumption for autohydrolysis and enzymatic hydrolysis respectively.

4.4 Conclusion

This study evaluates the techno-economic assessment and environmental performance assessment of utilizing rice husks to produce xylo-oligosaccharides by the method of autohydrolysis and enzymatic hydrolysis. Results from the Life Cycle Impact Assessment show that autohydrolysis is more environmentally sound than enzymatic hydrolysis, as reduced human health damage, ecosystem damage, and resource scarcity of 99.7%, 99.6%, and 78.9% were recorded respectively. The techno-economic assessment also indicates that producing xylo-oligosaccharide is economically feasible for both autohydrolysis and enzymatic hydrolysis production systems on either a pilot or large scale, however, the payback time is lower for the former on both scales.

References

Awulu, J. O., Omale, P. A., Ameh, J. A. (2018). Comparative analysis of calorific values of selected agricultural wastes. *Nigerian Journal of Technology*, *37*(4), 1141. https://doi.org/10.4314/njt.v37i4.38

Bajo Jr, P. O., Acda, M. N. (2017). Fuel Pellets from a Mixture of Rice Husk and Wood Particles. *BioResources*, *12*(3), 6618–6628. https://doi.org/10.15376/biores.12.3.6618-6628

Bijleveld, M., L. de Graaff, Schep, E., Schroten, A., Vergeer, R., Ahdour, S. (2018). Environmental prices handbook EU28 Version1 methods and numbers for valuation of environmental impacts. https://cedelft.eu/wp-content/uploads/sites/2/2021/04/CE_Delft_7N54_Environmental_Prices_Handbook_EU28_version_Def_VS2020.pdf

da Silva Menezes, B., Rossi, D. M., Ayub, M. A. Z. (2017). Screening of filamentous fungi to produce xylanase and xylooligosaccharides in submerged and solid-state cultivations on rice husk, soybean hull, and spent malt as substrates. *World Journal of Microbiology and Biotechnology*, *33*(3), 58. https://doi.org/10.1007/s11274-017-2226-5

da Silva Menezes, B., Rossi, D. M., Squina, F., Ayub, M. A. Z. (2018). Xylooligosaccharides production by fungi cultivations in rice husk and their application as substrate for lactic acid bacteria growth. *Bioresource Technology Reports*, *2*, 100–106. https://doi.org/10.1016/j.biteb.2018.05.004

Forbes (2023). *Currency converter: Live currency exchange rates calculator*. Forbes Advisor. Retrieved February 12, 2023, from https://www.forbes.com/advisor/money-transfer/currency-converter/eur-usd/?amount=1

Hayatun, A., Jannah, M., Ahmad, A., Taba, P. (2020). Synthetic Bioplastic Film from Rice Husk Cellulose. *Journal of Physics: Conference Series*, *1463*, 012009. https://doi.org/10.1088/1742-6596/1463/1/012009

Hoogervorst, A. (2004). *Life cycle assessment*. Pretoria: Dept. of Environmental Affairs and Tourism.

Hu, Y., Shi, C.-Y., Xun, X.-M., Huang, B.-R., You, S., Wu, F.-A., Wang, J. (2021). Xylanase-polymer conjugates as new catalysts for xylooligosaccharides production from lignocellulose. *Biochemical Engineering Journal*, *171*, 108025. https://doi.org/10.1016/j.bej.2021.108025

Huijbregts, M. A. J., Steinmann, Z. J. N., Elshout, P. M. F., Stam, G., Verones, F., Vieira, M. D. M., … van Zelm, R. (2016). © RIVM 2017 Parts of this publication may be reproduced, provided acknowledgement, 201.

Khat-udomkiri, N., Sivamaruthi, B. S., Sirilun, S., Lailerd, N., Peerajan, S., Chaiyasut, C. (2018). Optimization of alkaline pretreatment and enzymatic hydrolysis for the extraction of xylooligosaccharide from rice husk. *AMB Express*, *8*(1), 115. https://doi.org/10.1186/s13568-018-0645-9

Khat-udomkiri, N., Toejing, P., Sirilun, S., Chaiyasut, C., Lailerd, N. (2020). Antihyperglycemic effect of rice husk derived xylooligosaccharides in high-fat diet and low-dose streptozotocin-induced type 2 diabetic rat model. *Food Science & Nutrition*, *8*(1), 428–444. https://doi.org/10.1002/fsn3.1327

Kim, K.-H., Kabir, E., Kabir, S. (2015). A review on the human health impact of airborne particulate matter. *Environment International*, *74*, 136–143. https://doi.org/10.1016/j.envint.2014.10.005

Malmgren, E. (2017). Monetary estimates of human health impacts in weighting sets, 69.

Nabarlatz, D., Ebringerová, A., Montané, D. (2007). Autohydrolysis of agricultural by-products for the production of xylo-oligosaccharides. *Carbohydrate Polymers*, *69*(1), 20–28. https://doi.org/10.1016/j.carbpol.2006.08.020

Nabarlatz, D., Farriol, X., Montané, D. (2005). Autohydrolysis of Almond Shells for the Production of Xylo-oligosaccharides: Product Characteristics and Reaction Kinetics. *Industrial & Engineering Chemistry Research*, *44*(20), 7746–7755. https://doi.org/10.1021/ie050664n

Nieuwlaar, E. (2013). Life Cycle Assessment and Energy Systems. In *Reference Module in Earth Systems and Environmental Sciences* (p. B9780124095489014000). Elsevier. https://doi.org/10.1016/B978-0-12-409548-9.01334-8

Parajó, J. C., Garrote, G., Cruz, J. M., Dominguez, H. (2004). Production of xylooligosaccharides by autohydrolysis of lignocellulosic materials. *Trends in Food Science & Technology*, *15*(3–4), 115–120. https://doi.org/10.1016/j.tifs.2003.09.009

Pozzer, A., Bacer, S., Sappadina, S. D. Z., Predicatori, F., Caleffi, A. (2019). Long-term concentrations of fine particulate matter and impact on human health in Verona, Italy. *Atmospheric Pollution Research*, *10*(3), 731–738. https://doi.org/10.1016/j.apr.2018.11.012

Prinz, A. L., Richter, D. J. (2022). Long-term exposure to fine particulate matter air pollution: An ecological study of its effect on COVID-19 cases and fatality in Germany. *Environmental Research, 204,* 111948. https://doi.org/10.1016/j.envres.2021.111948

Samanta, A. K., Jayapal, N., Kolte, A. P., Senani, S., Sridhar, M., Dhali, A., … Prasad, C. S. (2015). Process for Enzymatic Production of Xylooligosaccharides from the Xylan of Corn Cobs: Xylooligosaccharides from Corn Cobs. *Journal of Food Processing and Preservation*, *39*(6), 729–736. https://doi.org/10.1111/jfpp.12282

Tan, B. L., Norhaizan, M. E. (2020). *Rice By-products: Phytochemicals and Food Products Application*. Cham: Springer International Publishing. https://doi.org/10.1007/978-3-030-46153-9

Yeboah, W. O., Kwofie, E. M., Wang, D. (2022). Circular bioeconomy potential of rice husk as a bioplastic resource: Techno-environmental assessment. *Bioresource Technology Reports, 20,* 101248. https://doi.org/10.1016/j.biteb.2022.101248

Zhu, J., Zhang, H., Jiao, N., Xiao, Y., Shi, D., Xu, Y. (2021). A green process for producing xylooligosaccharides from poplar: Endoxylanase assisted autohydrolysis, activated carbon separation, and spent liquor for rice growth. *Industrial Crops and Products*, *174*, 114187. https://doi.org/10.1016/j.indcrop.2021.114187

Adhikari, B., Lister, T. E., Reddy, R. G. (2022). Techno-economic and life cycle assessment of aluminum electrorefining from mixed scraps using ionic liquid. *Sustainable Production and Consumption*, *33*, 932–941. https://doi.org/10.1016/j.spc.2022.08.020

Otieno, D. O., Ahring, B. K. (2012). The potential for oligosaccharide production from the hemicellulose fraction of biomasses through pretreatment processes: xylooligosaccharides (XOS), arabinooligosaccharides (AOS), and mannooligosaccharides (MOS). *Carbohydrate Research*, *360*, 84–92. https://doi.org/10.1016/j.carres.2012.07.017

Panagopoulos, A. (2022). Techno-economic assessment and feasibility study of a zero liquid discharge (ZLD) desalination hybrid system in the Eastern Mediterranean. *Chemical Engineering and Processing - Process Intensification*, *178*, 109029. https://doi.org/10.1016/j.cep.2022.109029

Yeboah, W. O., Kwofie, E. M., Wang, D. (2022). Circular bioeconomy potential of rice husk as a bioplastic resource: Techno-environmental assessment. *Bioresource Technology Reports, 20,* 101248. https://doi.org/10.1016/j.biteb.2022.101248

5 Conclusion

This thesis promotes rice systems' circularity by providing techno-eco-environmental evidence of non-energy utilization pathways of rice husks. The study was organized into three objectives; the first objective provided a review of the different non-energy utilization pathways over a 5-year period to understand what has been done and how they could be improved, and the second and third objectives explored the overall circularity potential of using husks as a resource to produce bioplastics and xylo-oligosaccharides respectively. The studies revealed that rice husks have a high potential to be utilized for different purposes, such as biopolymers, secondary cementitious materials, xylo-oligosaccharides, carbon, biocatalysts, molecular sieves, and bioactive peptides. A thorough environmental impact assessment of rice husks-to-biopolymer and rice husks-to-xylo-oligosaccharides shows that these pathways are environmentally friendly. The rice husks-to-xylo-oligosaccharides pathway was also proven to be commercially feasible and profitable both on pilot and large scales via a techno-economic assessment.

5.1 Future Outlook

This research successfully examined the non-energy utilization pathways of rice husks and provided metrices via life cycle assessment, life cycle impact cost assessment, and techno-economic assessment of two of these pathways: bioplastics and xylo-oligosaccharides. However, paying attention to some limitations will help enhance the overall goal and help future research on this topic.

1. Design a website for the decision support system for rice circularity. In the first objective of the research, data was collected on the various non-energy utilization pathways of rice husks. This data could be put together as a database (on a website) accessible to the

general public, researchers, and any other stakeholders, such as farmers and government. This would guide decision making regarding rice husk circularity.

2. Perform a techno-economic assessment of the rice husks-to-bioplastics system. Just like the third objective, a comprehensive TEA on the production of bioplastics (CMC, CA, and CA) from rice husks will be necessary to give insight on the commercial feasibility and profitability of this system.
3. Perform social life cycle assessment for both second and third objectives. A comprehensive evaluation of the sociological impacts of rice husks-to-bioplastics and rice husks-to-xylo-oligosaccharides will not only provide additional justifications on the sustainability of these systems but will also provide some sort of leverage for parties that decide to commercialize these systems.
4. Perform all analysis for other non-energy pathways. Performing all the sustainability assessments for all the various pathways revealed in the first objective would provide more insight on their sustainability which could guide future researchers and companies who want to pursue those systems.
5. Look at the potential of the other rice by-products. There are other rice by-products that possess good characteristics and could be harnessed for other important valorization pathways. A look at these other by-products would even provide a more comprehensive rice circularity.

Appendix A – Supplementary material for Chapter 3

Table A.1: Harmful compounds produced from the incineration of a synthetic plastic (polyvinyl chloride) and their effects on the human body (Gilpin et al., 2005; Okunola A et al., 2019)

Compound	Effect	Part of body affected
Acetaldehyde	Lesion	Nervous system
Acetone	Irritations in the form of inflammation	Eyes; respiratory tract
Benzaldehyde	Irritations in the form of inflammation; dysfunctions	Eyes; skin; respiratory system; brain
Benzole	Cancer	Bone marrow; liver; immune system
Formaldehyde	Irritations; edema; cancer	Eye; lungs
Hydrochloric acid	Corrosion	Eyes; skin; respiratory tract
Phosgene	Corrosion	Eye; skin; respiratory organs
Polychlorinated dibenzo-dioxin	Cancer; irritations	Eye; skin; respiratory system; circulatory system, digestive system, liver; bone marrow
Polychlorinated dibenzofuran	Irritations; asthma	Eyes; respiratory system
Salicyl-aldehyde	Irritations	Eyes; skin; respiratory tract; central nervous system
Propylene	Lowering of consciousness	Central nervous system
Toluene	Irritations; depression	Eyes; respiratory tract
Vinyl chloride	Cancer; irritations	Eyes; skin; respiratory systems; central nervous system; liver; spleen; blood-forming organs
Xylene	Irritations; lowering of consciousness	Eyes; central nervous system

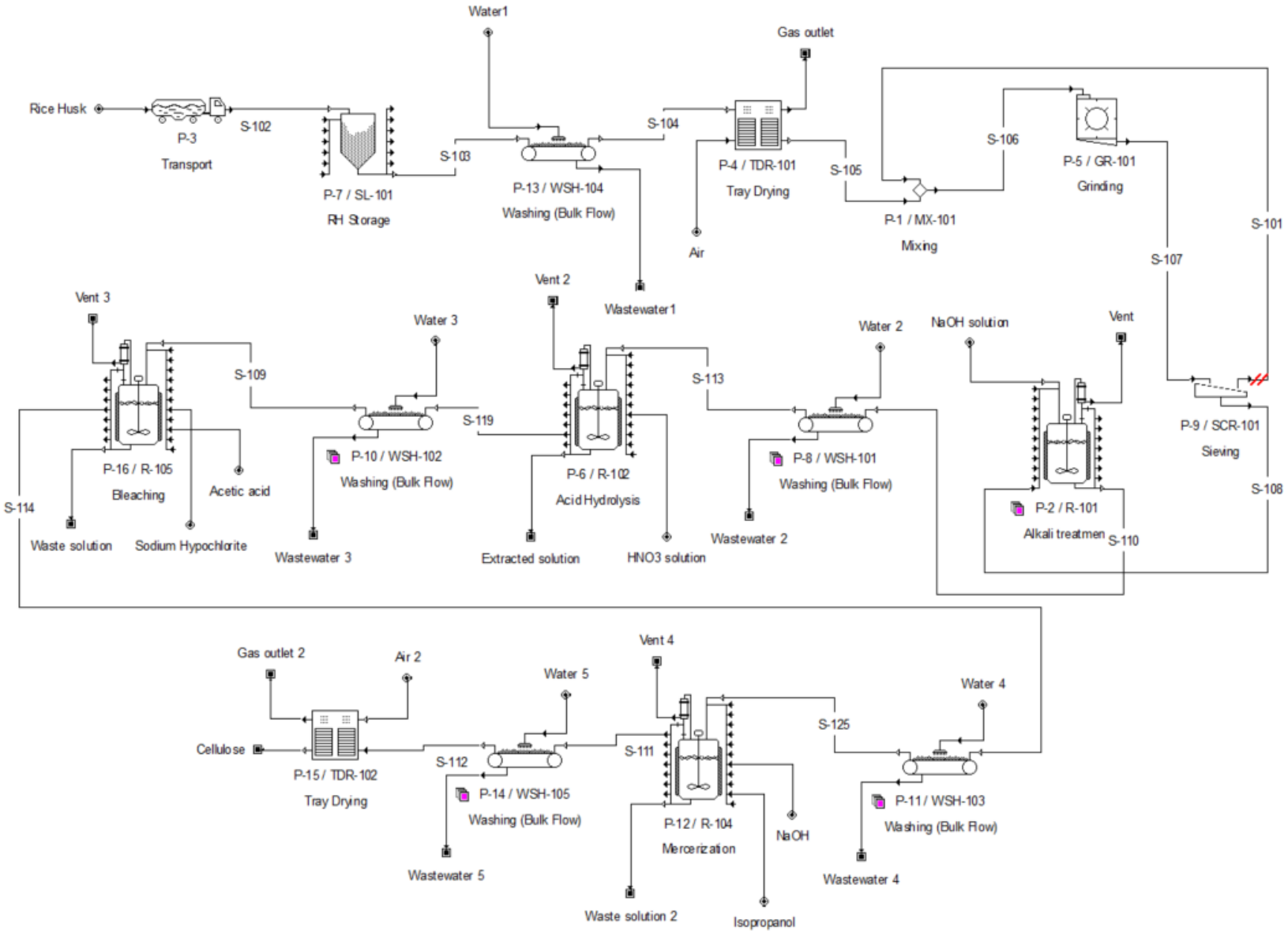

Figure A.1: Flowchart showing Cellulose extraction process

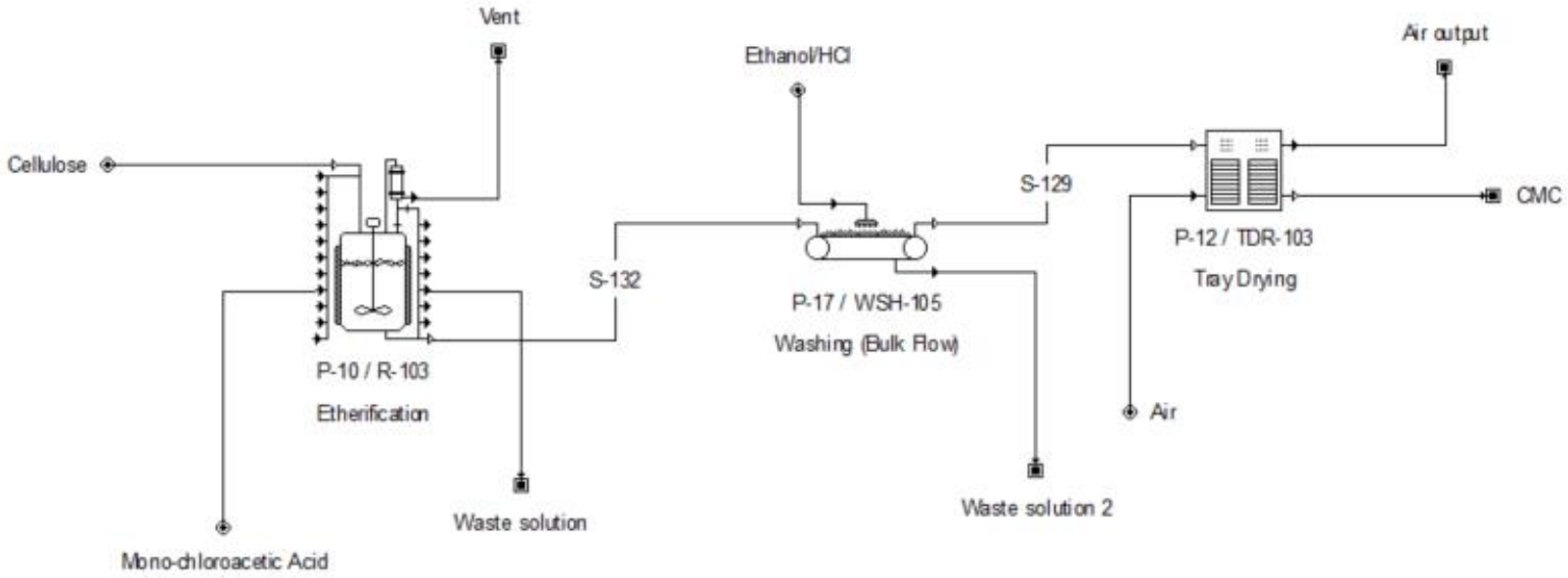

Figure A.2: Flowchart showing carboxymethyl cellulose production

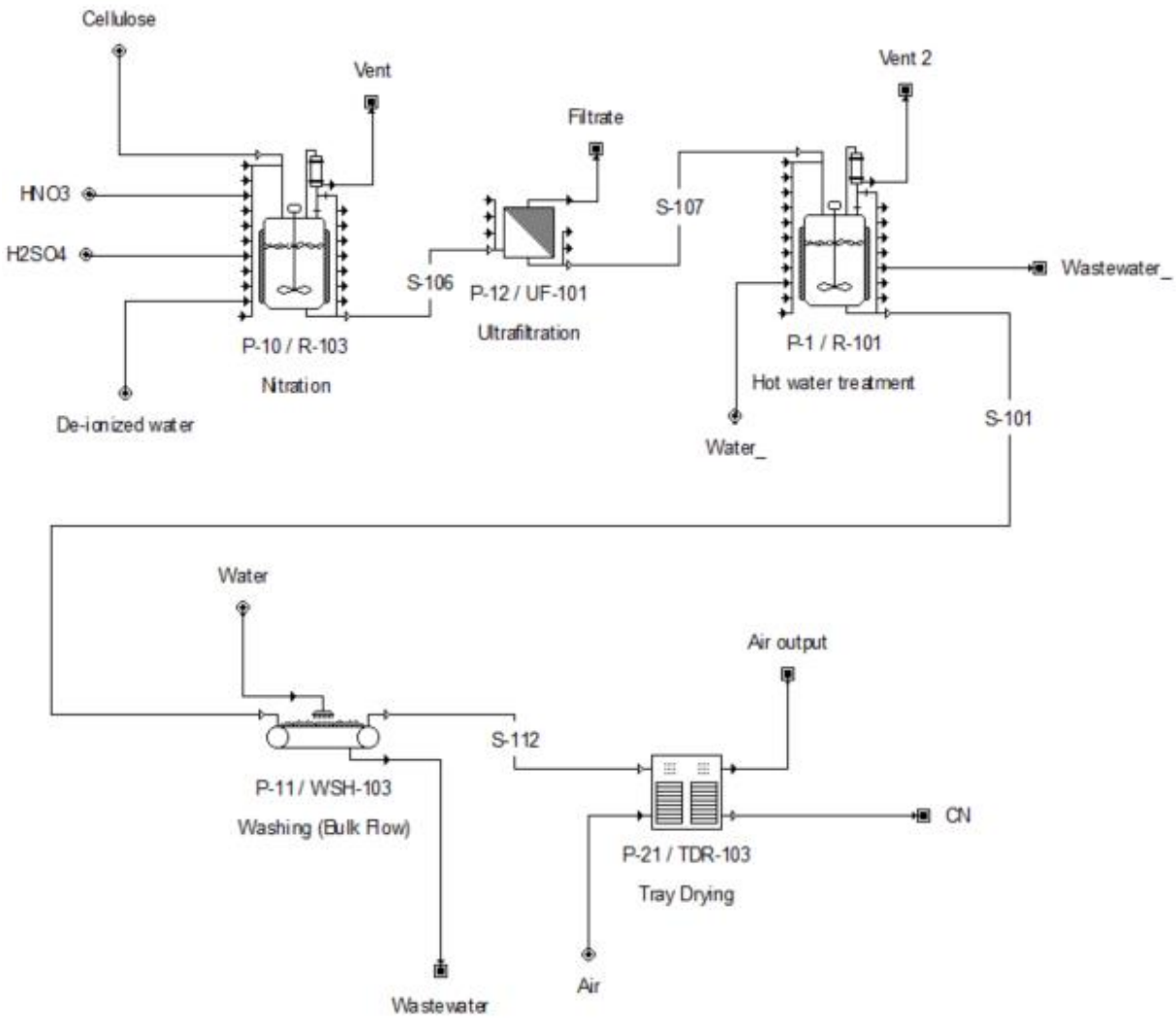

Figure A.3: Flowchart showing cellulose nitrate production

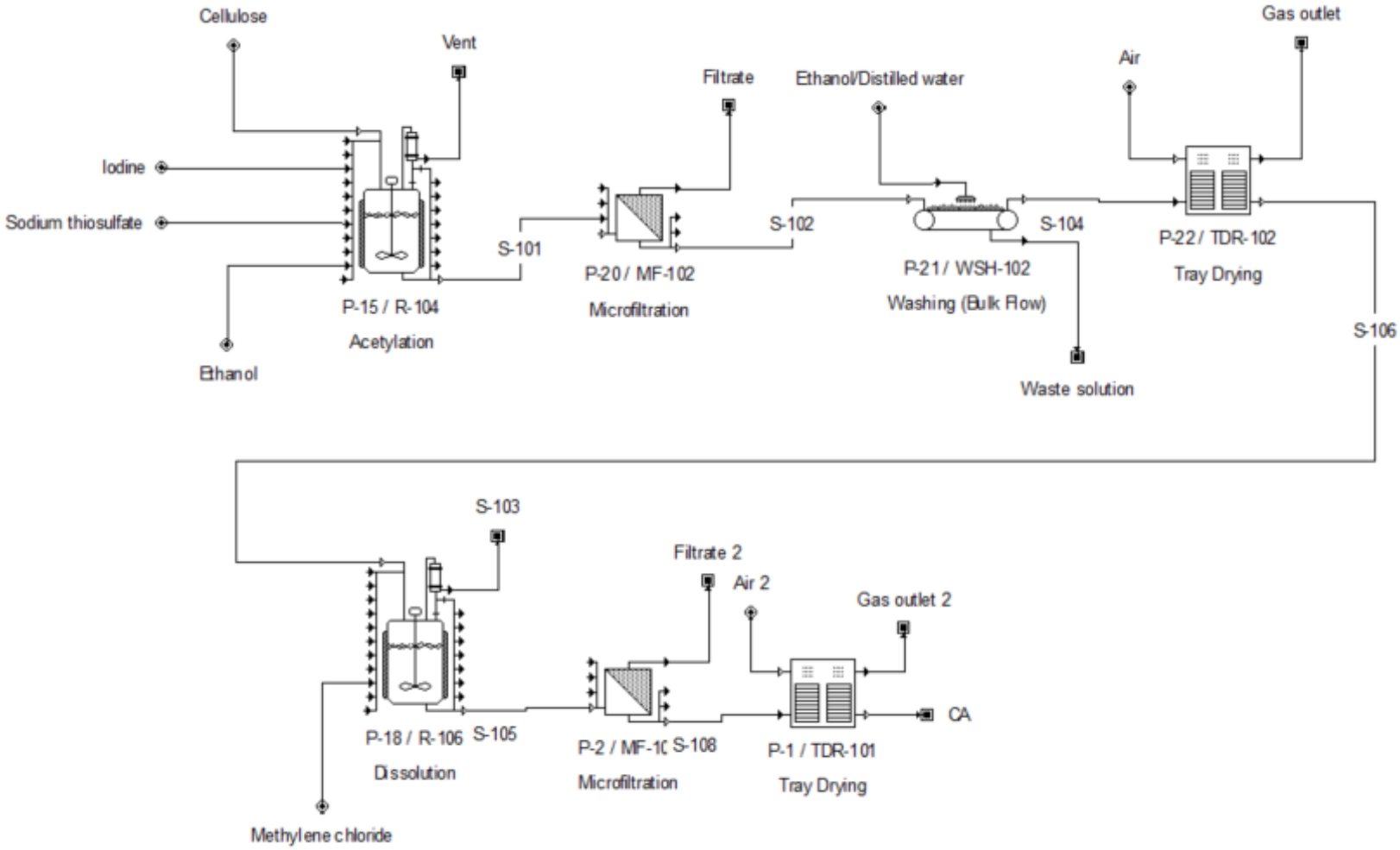

Figure A.4: Flowchart showing cellulose acetate production

Table A.2: Inventory for cellulose extraction process

No.	Process	Input			Output		
		Flow	**Amount**	**Unit**	**Flow**	**Amount**	**Unit**
1.	RH transportation	RH	10	kg	RH	10	kg
		Transport	0.2	tkm			
2.	Washing	RH	10	kg	RH	9.99	kg
		Water	0.015	m^3	Wastewater	12	m^3
					Free water	0.003	m^3
3.	Drying	RH	9.99	kg	RH	9.99	kg
		Free water	0.003	m^3	Water vapor	0.003	m^3
		Air	15	kg	Air	15	kg
		Electrical energy	18	kJ			
4.	Grinding and sieving	RH	9.99	kg	Sized RH	9.99	kg
		Electrical energy	5	kJ			
5.	Alkali treatment	Sized RH	9.99	kg	Delignified RH	3.996	kg
		5% w/v NaOH solution	50	kg	Black liquor	5.5994	kg
		Heat	5	kW			
6.	Washing	Delignified RH	3.996	kg	Delignified RH	3.996	kg
		Water	5	kg	Wastewater	5	kg
7.	Acid hydrolysis	Delignified RH	3.996	kg	HNO_3-treated RH (cellulose)	1.1976	kg
		10% w/v HNO_3	19.96	kg	Extracted solution	22.754	kg
		Heat	5	kW			
8.	Washing	HNO_3-treated RH (cellulose)	1.1976	kg	Cellulose	1.1964	kg
		Water	1.6976	kg	Wastewater	1.6989	kg
9.	Bleaching	Cellulose	1.1964	kg	Cellulose	1.18444	kg
		Sodium hypochlorite, NaClO	0.2393	kg	Extracted chlorite solution	19.5014	kg
		Acetic acid, CH_3COOH	0.1196	kg			
		Water	19.1425	kg			
10.	Washing	Cellulose	1.18444	kg	Cellulose	1.18444	kg
		Water	1.5	kg	Wastewater	1.5	kg
11.	Mercerization	Cellulose	1.18444	kg	Cellulose	1.18444	kg

		Isopropanol + 20% w/v NaOH	5.9820	kg	Extracted solution	5.9820	kg
		Heat	5	kW			
12.	Washing	Cellulose	1.18444	kg	Cellulose	1.18444	kg
		Water	1.5	kg	Wastewater	1.5	kg

Table A.3: Inventory for CMC production

No.	**Process**	**Input**			**Output**		
		Flow	**Amount**	**Unit**	**Flow**	**Amount**	**Unit**
1.	Etherification	Cellulose	1.01	kg	CMC	1	kg
		Monochloroacetic acid	2.0405	kg	Extracted solution	2.0505	kg
		Heat	5	kW			
2.	Washing	CMC	1	kg	CMC	1	kg
		Water	1.3	kg	Wastewater	1.2	kg
					Free water	0.1	kg
3.	Drying	CMC	1	kg	CMC	1	kg
		Free water	0.1	kg	Water vapor	0.1	kg
		Air	1.2	kg	Air	1.2	kg
		Electrical energy	18	kJ			

Table A.4: Inventory for CN production

No.	Process	Input			Output		
		Flow	**Amount**	**Unit**	**Flow**	**Amount**	**Unit**
1.	Nitration	Cellulose	1.06	kg	Nitrated cellulose	1	kg
		Nitric acid, HNO_3	3	kg	Extracted acid solution	8.06	kg
		Sulfuric acid, H_2SO_4	5	kg			
2.	Quenching	Nitrated cellulose	1	kg	Cellulose nitrate precipitates	1	kg
		Water	1.3	kg	Water	1.3	kg
3.	Hot water treatment	Cellulose nitrate precipitates	1	kg	CN	1	kg
		Water	1.3	kg	Water	1.3	kg
		Electrical energy	18	kJ			
4.	Washing	CN	1	kg	CN	1	kg
		Water	1.3	kg	Wastewater	1.3	kg
5.	Drying	CN	1	kg	CN	1	kg
		Air	1.013	kg	Air	1.013	kg
		Electrical energy	18	kJ			

Table A.5: Inventory for CA production

No.	Process	Input			Output		
		Flow	**Amount**	**Unit**	**Flow**	**Amount**	**Unit**
1.	Acetylation	Cellulose	1	kg	Acetylated cellulose	1	kg
		Acetic anhydride	5.4	kg	Extracted solution	6.413	kg
		Iodine	1.013	kg			
		Heat	5	kW			
2.	Sodium thiosulphate (ST) treatment	Acetylated cellulose	1	kg	ST-treated cellulose	1	kg
		Sodium thiosulphate	2.7	kg	Extracted solution	2.7	kg
		Heat	5	kW			
3.	Ethanol treatment (ET)	ST-treated cellulose	1	kg	ET-treated cellulose	1	kg
		Ethanol	2.53	kg	Extracted ethanol solution	2.53	kg
4.	Washing	ET-treated cellulose	1	kg	Washed cellulose	1	kg
		Ethanol	0.38	kg	Wastewater	1.266	kg

		Water	0.886	kg			
5.	Drying	Washed cellulose	1	kg	Dried cellulose	1	kg
		Air	1.013	kg	Air	1.013	kg
		Electrical energy	18	kJ			
6.	Dissolution	Dried cellulose	1	kg	MC-dissolved cellulose	1	kg
		Methylene chloride (MC)	1.266	kg	Extracted MC solution	0.253	kg
7.	Drying	MC-dissolved cellulose	1	kg	CA	1	kg
		Air	1.013	kg	Air	1.013	kg
		Electrical energy	18	kJ			

Appendix B – Supplementary material for Chapter 4

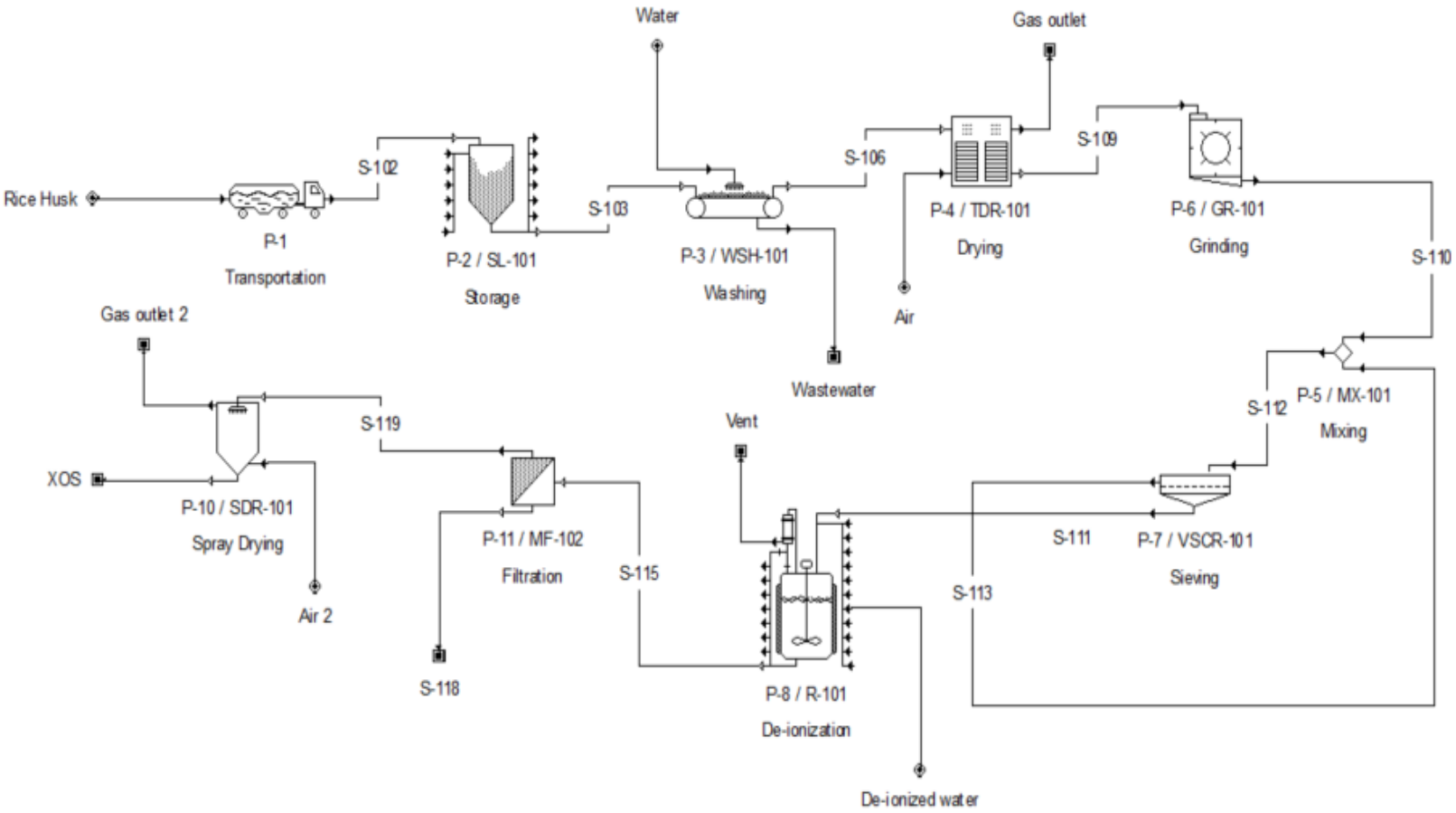

Figure B.1: Autohydrolysis production system flowchart

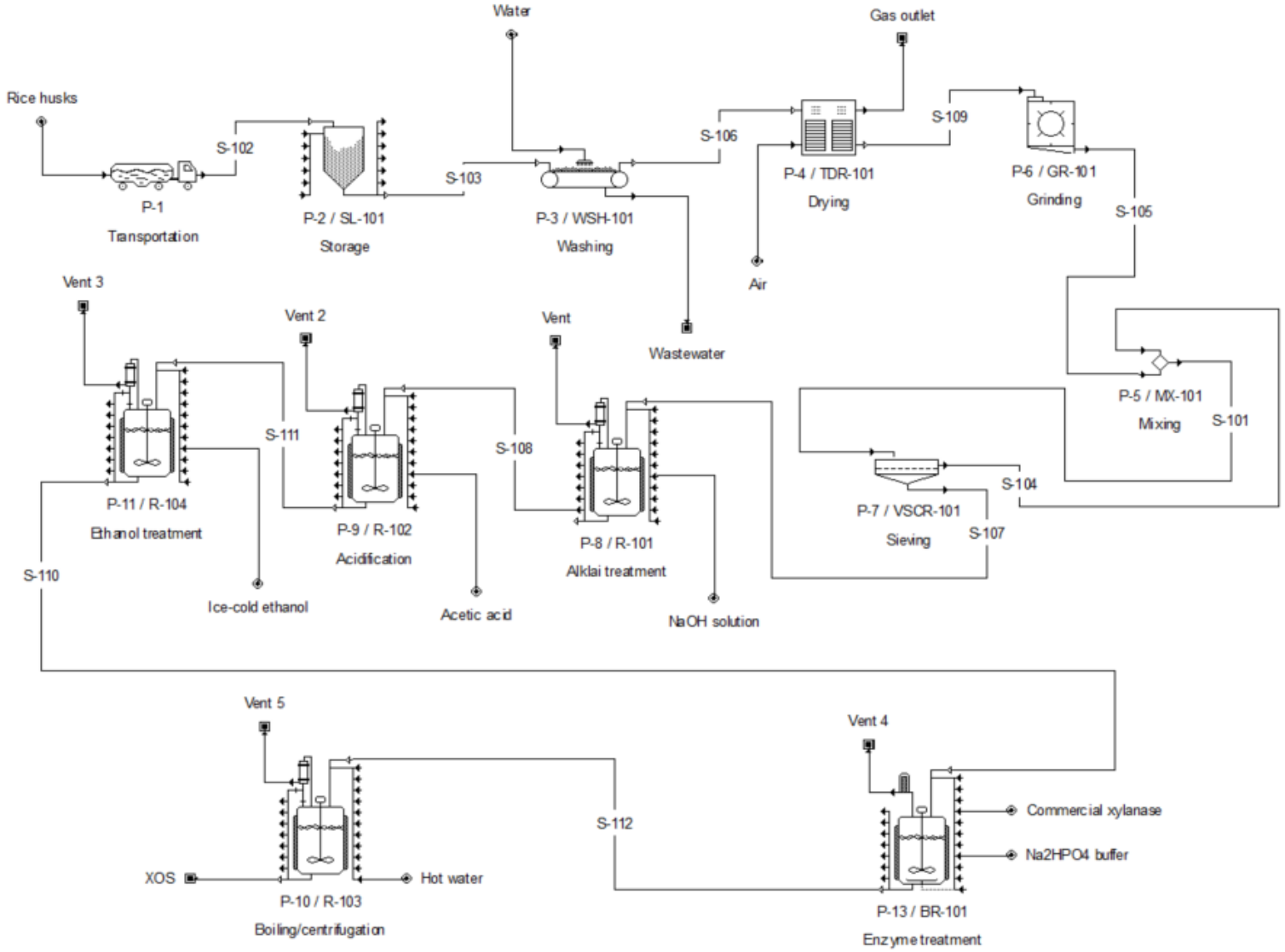

Figure B.2: Enzymatic hydrolysis production system flowchart

Table B.1: Inventory for autohydrolysis process

No.	Process	Input			Output		
		Flow	**Amount**	**Unit**	**Flow**	**Amount**	**Unit**
1.	RH transportation	RH	10	kg	RH	10	kg
		Transport	0.2	tkm			
2.	Washing	RH	10	kg	RH	9.99	kg
		Water	0.015	m^3	Wastewater	12	m^3
					Free water	0.003	m^3
3.	Drying	RH	9.99	kg	RH	9.99	kg
		Free water	0.003	m^3	Water vapor	0.003	m^3
		Air	15	kg	Air	15	kg
		Electrical energy	18	kJ			
4.	Grinding and sieving	RH	9.99	kg	Sized RH	9.99	kg
		Electrical energy	5	kJ			
5.	De-ionization	Sized RH	9.99	kg	Xylan (in liquid phase)	4.25	kg
		De-ionized water	50	kg	Solid residues	5.74	kg
		Heat	5	kW	Liquid solvent	50	kg
6.	Filtration	Xylan (in liquid phase)	4.25	kg	Xylan (in liquid phase)	4.25	kg
		Solid residue	5.74	kg	Liquid solvent	50	kg
		Liquid solvent	50	kg	Solid residues	5.74	kg
7.	Spray drying	Xylan (in liquid phase)	4.25	kg	XOS	4.2	kg
		Liquid solvent	50	kg	Vapor	50	kg
		Heat	5	kW			

Table B.2: Inventory for enzymatic hydrolysis method

No.	Process	Input			Output		
		Flow	**Amount**	**Unit**	**Flow**	**Amount**	**Unit**
1.	RH transportation	RH	10	kg	RH	10	kg
		Transport	0.2	tkm			
2.	Washing	RH	10	kg	RH	9.99	kg
		Water	0.015	m^3	Wastewater	12	m^3
					Free water	0.003	m^3
3.	Drying	RH	9.99	kg	RH	9.99	kg
		Free water	0.003	m^3	Water vapor	0.003	m^3
		Air	15	kg	Air	15	kg
		Electrical energy	18	kJ			
4.	Grinding and sieving	RH	9.99	kg	Sized RH	9.99	kg
		Electrical energy	5	kJ			
5.	Alkali treatment	Sized RH	9.99	kg	Delignified RH	3.996	kg
		22% NaOH solution	50	kg	Black liquor	55.994	kg
		Heat	5	kW			
6.	Acidification	Delignified RH	3.996	kg	HNO_3-treated RH	3.299	kg
		99% Glacial acetic acid	19.96	kg	Extracted solution	20.657	kg
		Heat	2.9	kW			
7.	Ethanol treatment	HNO_3-treated RH	3.996	kg	Xylan	3.2	kg
		95% ice-cold ethanol	8.9×10^{-4}	m^3			kg
		Heat	5	kW			
8.	Enzyme treatment	Xylan	3.2	kg	XOS solution	4.6	kg
		McIlvaine buffer	2.0×10^{-4}	m^3			
		Xylanase solution	8.0×10^{-5}	m^3			
		Heat	2.3	kW			
9.	Boiling/Centrifugation	Boiling water	4.1×10^{-4}	m^3	XOS	3.1	kg
		Electrical energy	18	kJ	Organic mixture	3.5	kg